EFFECT OF AXIAL STRAIN ON POSTBUCKLING BEHAVIOR OF SLANTED ELASTIC COLUMNS

by

Eduardo Ugarte

Submitted in Partial Fulfillment of the Requirements
for the Degree of
Master of Science in Engineering
in the
Civil Engineering
Program

Paul X. Belinis — 19 AUG. '80
Adviser — Date

Dean of the Graduate School — 8/20/80
Date

YOUNGSTOWN STATE UNIVERSITY

August, 1980

ABSTRACT

EFFECT OF AXIAL STRAIN ON POSTBUCKLING BEHAVIOR OF SLANTED ELASTIC COLUMNS

Eduardo Ugarte
Master of Science in Engineering
Youngstown State University, 1980

The purpose of this thesis is to investigate the load-displacement characteristics of a pinned-end axially-loaded column including the effect of axial strain.

The buckling and post-buckling behavior of the column is investigated utilizing a nonlinear theory of large deflections analogous to the "elastica problem" of classical nonlinear elasticity.

The minimum potential theorem of variational calculus is utilized to obtain the nonlinear differential equations of equilibrium. Numerical solutions of the problem are obtained using an "Intermediate Theory" which combines the potential energy function together with the Rayleigh-Ritz method to produce a set of nonlinear algebraic equations which are solved by numerical iterative techniques.

The results of the "Intermediate Theory" are compared with the classical nonlinear differential equation solutions in order to justify the adequacy of the approximate procedure.

The problem of the vertical column is examined as a first step to justify the latter considerations. The entire mathematical process is then used to investigate the behavior of a slanted column where the axial force does not align with the column axis.

ACKNOWLEDGEMENTS

The author thanks his advisor, Dr. Paul X. Bellini, who took a personal interest in guiding and encouraging him in the completion of this work.

He also wishes to thank Dr. Jack D. Bakos for his valuable time and energy toward the completion of the requirement of this thesis.

He is deeply grateful to his wife Maria Teresa and his children for their constant support and patience enabling him to complete this very important step in improving his education.

TABLE OF CONTENTS

LIST OF SYMBOLS

SYMBOL	DESCRIPTION
A	Cross-sectional area of column
a	Parameter related to the maximum deflection of the column a = (Ymax/L)
B	Constant of the Eingenfunction $Y = B\sin\frac{\pi s}{L}$
b	Cross-sectional width
C	Constant of Integration
E	Young's modulus
H	Horizontal reaction (Slanted Column)
h	Cross-sectional depth
I	Moment of inertia of cross-section
k	Curvature
L	Length of column
M	Bending moment
P	Applied Force
P_E	Euler load for a simple prismatic column
Q	Applied Force
R	Compressibility parameter = I/AL^2
s	Distance along deformed center line
U	Strain Energy
u	X-Displacement (Slanted Column)
V	Potential energy
v	Vertical Displacement (Slanted Column)
w	Y-Displacement (Slanted Column)
x,y	Coordinates for undeformed state
Ymax	Maximum midpoint deflection of the column.

α' Value of θ at A,B (Axially Loaded Column)

α Angle of inclination for the Slanted Column

Δ X-Displacement at B (Axially Loaded Column)

δ Delta operator for variational operations

ϵ Strain

ϵ_o Strain at center line

$\hat{\lambda}$ Langrange multiplier

λ Angle Lambda defined in Figure 10

π Total energy function = U - V

ρ Instantaneous radius of curvature for the incompressible column

ρ^* Instantaneous radius of curvature for the compressible column

σ Stress

θ Instantaneous Inclination

θ_A Value of θ at A (Slanted Column)

θ_B Value of θ at B (Slanted Column)

θ_o End rotation

LIST OF FIGURES

LIST OF TABLES

TABLE PAGE

TABLE PAGE

TABLE PAGE

CHAPTER I

INTRODUCTION

1.1 Historical Review

In the theory of elastic stability of an elastic column, certain traditional assumptions have become standard. Examples are incompressibility, or zero center line strain, zero shear deformability, unchanging cross section during buckling. This is by no means true. There is much that is still unknown about the true behavior of the elastic column.

On of the earliest nonlinear problems to arise in the field of applied mechanics is the problem of the "elastica", in which a slender elastic column initially straight, is held in a bent position by end forces and moments.

As Koiter[1]* says, "the problem of elastic stability belongs inherently to the domain of the nonlinear theory of Elasticity", although satisfactory results may be obtained from a linearized analysis in many important practical cases. Kirchhoff's uniqueness theorem[2] which has a central role in the classical linear theory of elasticity is no longer valid. In fact, the simplest form of a loss of stability manifests itself in the appearance of more than one solution. In other words, a structural element which has a particular

* Number in parenthesis refers to literature cited in the Bibliography

dimension much smaller than the remaining dimensions--such as bars, thin plates and shells--is liable to exhibit more than one equilibrium configuration under a given external loading, thus evading Kirchhoff's Law.

In the interval between the discovery of Hooke's Law and that of the general differential equations of Elasticity by Navier, the attention of those mathematicians who occupied themselves with our science was chiefly directed to the solution and extension of Galileo's problem, and the related theories of the vibrations of bars and plates, and the stability of columns. The Galileo problem attempted to determine the resistance of cantilever beam, when the tendency to break it arises from its own or an applied weight. He concluded that the beam tends to turn about an axis perpendicular to its length, and in the plane of its support. The first investigation of any importance is that of the elastic line or elastica by James Bernoulli[3] in 1705, in which the resistance of a bent rod is assumed to arise from the extension and contraction of its longitudinal filaments, and the equation of the curve assumed by the axis is formed. This equation practically involves the result that the resistance to bending is a couple proportional to the curvature of the rod when bent, a result which was assumed by Euler[4] in his later treatment of the problems of the elastica, and of the vibrations of thin rods. As soon as the notion of a flexural couple proportional to the curvature was established, it could be noted that the work done in bending a rod is proportional to the square of the curvature. Daniel Bernoulli[5]

suggested to Euler that the differential equation of the elastica could be found by making the integral of the square of the curvature taken along the rod a minimum; and Euler, acting on this suggestion, was able to obtain the differential equation of the curve and to classify the various forms of it. One form is a curve of sine functions of small amplitude, and Euler pointed out that in this case the line of thrust coincides with the unstrained axis of the rod, so that the rod, if of sufficient length and if vertical when unstrained, may be bent by a weight attached to its upper end. Further investigations led him to assign the least length of a column in order that it may bend under its own or an applied weight. Lagrange [6] followed and used his theory to determine the strongest form of column. These two writers found a certain length which a column must attain to be bent by its own or an applied weight, and they concluded that for shorter lengths it will be simply compressed,while for greater lengths it will be bent. These researchers are the earliest researchers in the field of elastic stability. In Euler's work on the elastica, the rod is thought of as a line of particles which resists bending.

The foundations of the general theory of elastic stability were laid by Poincare[7] (1885) in his classical paper on the stability of rotating liquid masses. Using the concept of generalized coordinates, he studied the equilibrium path configurations in the vicinity of a critical equilibrium state and indicated the possibility of limit points, having devoted most of his nonlinear analysis, however, to

branching conditions. He showed that a loss of stability is normally associated either with a limit point, which represents a local extremum on an initially stable path, or with a point of bifurcation at which the fundamental equilibrium path intersects a second distinct path, and an exchange of stabilities occurs. Poincare's theory provided a valuable insight into the nature of the loss of stability, and although it was developed in terms of generalized coordinates for mechanical systems, it describes the overall buckling characteristics of a continuous body as well.

The elastic stability of bars considering the effect of axial compressibility was studied when the buckling of helical springs was investigated, first by R. Grammel[8] in 1924, later improved by C.B. Biezeno and J.J. Koch[9] in 1925, and later more by J.A. Haringx[10] who introduced a rational approach to consider the shear effects. Timoshenko and Gere[11] made a brief introduction to these methods.

In 1958, John V. Huddleston[12] used a modified Bernoulli-Euler formula that allows for the consideration of the effect of axial strain for predicting the buckling loads. A similar approach which included the effects of axial strain was done by J.J. Stoker[13], 1968 in his text Nonlinear Elasticity, by using the minimum energy principle to obtain a variational problem. The investigations of these authors consider the case when the column is subject to an axial compressive load applied at the ends.

The stability of a slanted column was investigated by R.von Mises[14] in 1923 when he developed a theory which

was applied later by him and J. Ratzersdorfer[15] in 1925, 1926 to various cases of laced columns. In recent years, Chin-Hao Chang[16], using the variational method studied the buckling behavior of a slanted column. An intermediate deflection theory, was used with an approximated expression of the axial strain to include the effect of it in the buckling behavior.

1.2 Thesis Purpose

The purpose of this thesis is to investigate the effect of axial strain on the postbuckling behavior of end-loaded columns subject to large deflections, the problem is defined as "elastica" for the case where axial strain is neglected.

A nonlinear elasticity with small strains is used to define the "true" strain function from which a column subject to an axial compressive load applied at the ends and later in the case of a slanted column. A strain energy expression is formulated. The minimum potential energy theorem is utilized to obtain the required conditions of equilibrium. A special "Intermediate Theory" of large deflections as presented by Dym and Shames[17] is utilized to solve the equilibrium equations.

A column subject to an axial compressive load applied at the ends is first investigated. The mathematical results are compared to the numerical solution of the "exact" numerical differential equations given by Huddleston[12] to justify the acceptability of the "Intermediate Theory" procedures.

Finally, the entire mathematical process is used to investigate the effect of axial strain on the postbuckling behavior of slanted columns where the end compressive force is not aligned with the longitudinal axis of the column.

1.3 Process of Development

This thesis is divided into four main parts

1) Chapter II presents a historical background of the Elastica problem. In addition, the definition of a "true" strain function formulated from a Nonlinear Elasticity with Small Strains Theory.

2) Chapter III includes the development of the total Potential energy for the nonlinear system utilizing the strain functions defined in Chapter II. The Minimum potential energy method of Variational Calculus is used to obtain the nonlinear differential equations required for equilibrium conditions for the case of the vertical compressible column.

3) Chapter IV develops the Intermediate Theory of analysis for the vertical column and includes an iterative numerical solution technique to determine load versus deflections for the element.

4) Chapter V presents a solution of the slanted, elastic, axially-compressible column postulated on the concepts, definitions, and techniques developed in Chapters II, III, and IV.

CHAPTER II

DEFINITION OF STRAIN

2.1 Nonlinear Elasticity with Small Strains - Background

The classical theory of infinitesimal strain or linear elasticity defines the buckling behavior of columns assuming "small" end rotations. In Figure 1 the angle θ_o (End Rotations) is treated as a "small" angle, that is, sin $\theta_o \approx \theta_o$ and and cos $\theta_o \approx 1$. In other words, the linearization of the problem is performed. In addition, the following assumptions are made: The column is infinity stiff in axial and shear deformation, and changes in the cross section geometry due to the Poisson's effect in the deformed state is neglected.

To attempt the solution of the effect of the axial strain on the true behavior of columns under buckling loads and postbuckling loads, the present work establishes the following assumptions:

Strains are small, when the components of the strain are small compared to unity (see p. 3[13]; p. 431[17]; Sokolnikoff, p. 33[18]; A.E.H. Love, p. 59[19]).

Planes normal to the center line in the undeformed state remain plane and normal to the deformed center line.

No conditions are imposed on the strain of the center line other than smallness (as is usually done for large

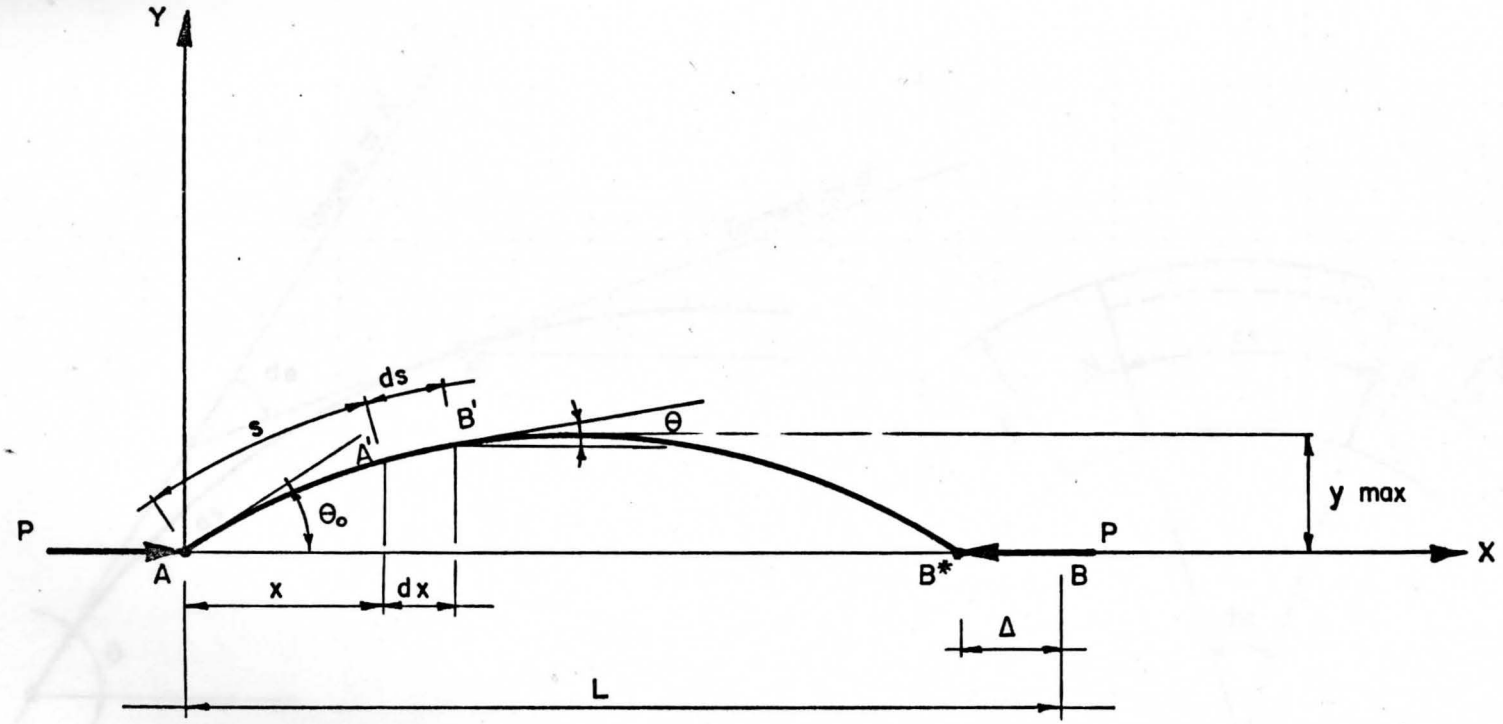

Deformed Shape

Figure 1. Compressible Column in Postbuckled State

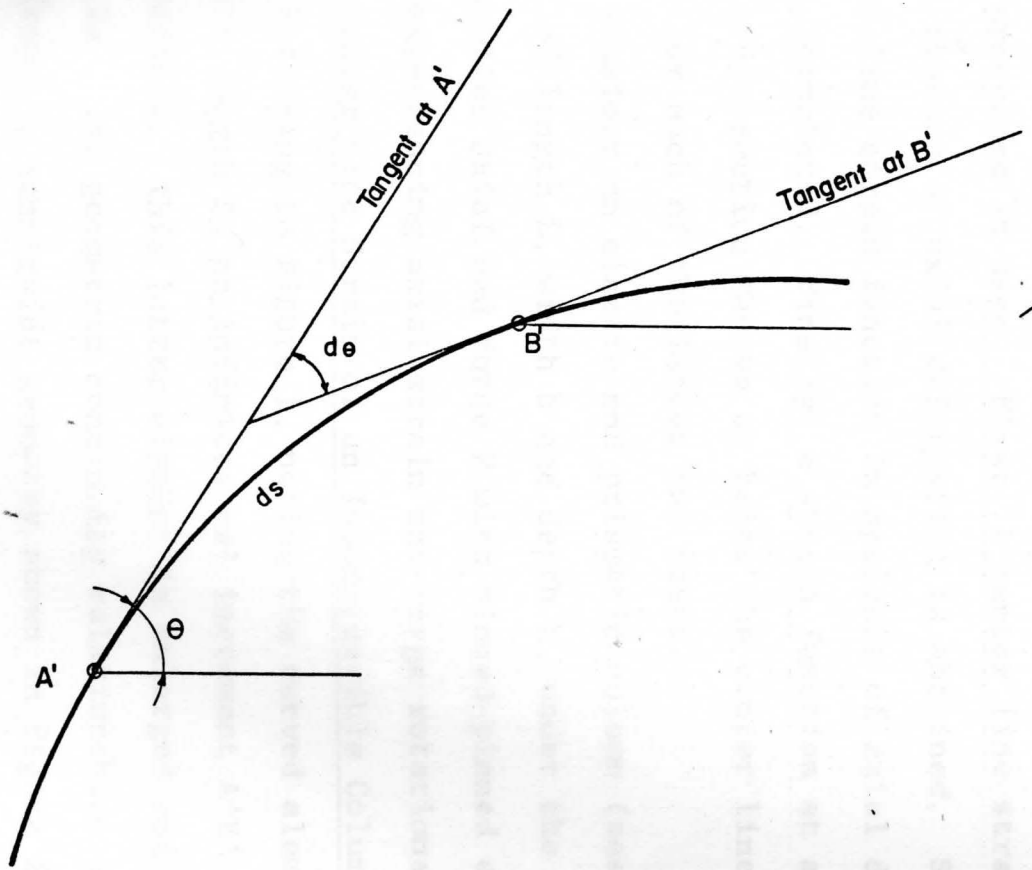

Figure 2a. Geometry of a Finite Increment of Length of Curved Element

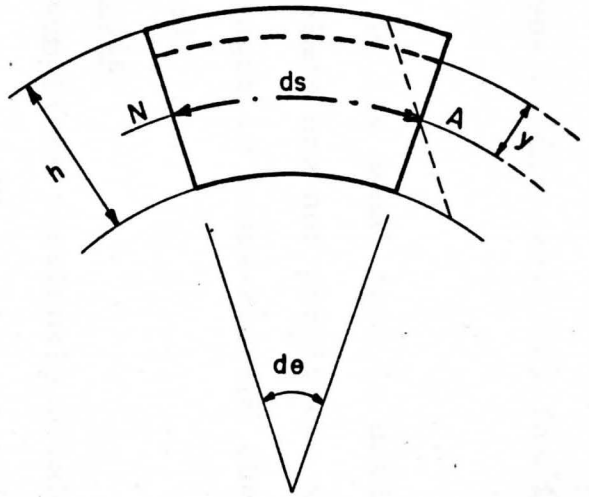

Figure 2b. Geometry of a Infinitesimal Increment of Length of Curved Element

displacements).

No assumptions are made on the order of relative magnitude of derivatives of displacements (as is done for small displacements).

Hooke's Law in its usual form is used, however, displacements out of plane are not permitted, as well as, shear deformation and changes in cross-section due to Poisson's effect are neglected.

2.2 Strain Analysis

With the assumptions previously established, the following procedure is used. First, a center line strain function is absence of axial deformation is obtained. Secondly, a center line strain function in presence of axial deformation is formulated. Finally, a strain function at any point on the cross-section (above or below the center line) is defined for each of the latter two cases.

Consider an elastic and prismatic column (see Figure 1), AB, of length L, width b and depth h, under the action of an applied axial end force P with pinned-pinned end supports, experiencing axial strain and large rotations.

2.2.1 Center Line Strain of an Incompressible Column

Referring to Figure 1, noting the curved element AA' of finite length S, an infinitesimal increment A'B' of length ds is defined. This latter element is enlarged and shown in Figure 2a. The geometric continuity relationships are determined from the constraint geometry shown in Figure 2b, where

displacements).

No assumptions are made on the order of relative magnitude of derivatives of displacements (as is done for small displacements).

Hooke's Law in its usual form is used, however, displacements out of plane are not permitted, as well as, shear deformation and changes in cross-section due to Poisson's effect are neglected.

2.2 Strain Analysis

With the assumptions previously established, the following procedure is used. First, a center line strain function in absence of axial deformation is obtained. Secondly, a center line strain function in presence of axial deformation is formulated. Finally, a strain function at any point on the cross-section (above or below the center line) is defined for each of the latter two cases.

We consider an elastic and prismatic column (see Figure-1), AB, of length L, width b and depth h, under the action of an applied axial end force P with pinned-pinned end supports, experiencing axial strain and large rotations.

2.2.1 Center Line Strain of an Incompressible Column

Referring to Figure 1, noting the curved element AA' of finite length S, an infinitesimal increment A'B' of length ds is defined. This latter element is enlarged and shown in Figure 2a. The geometric continuity relationships are determined from the constraint geometry shown in Figure 2b, where

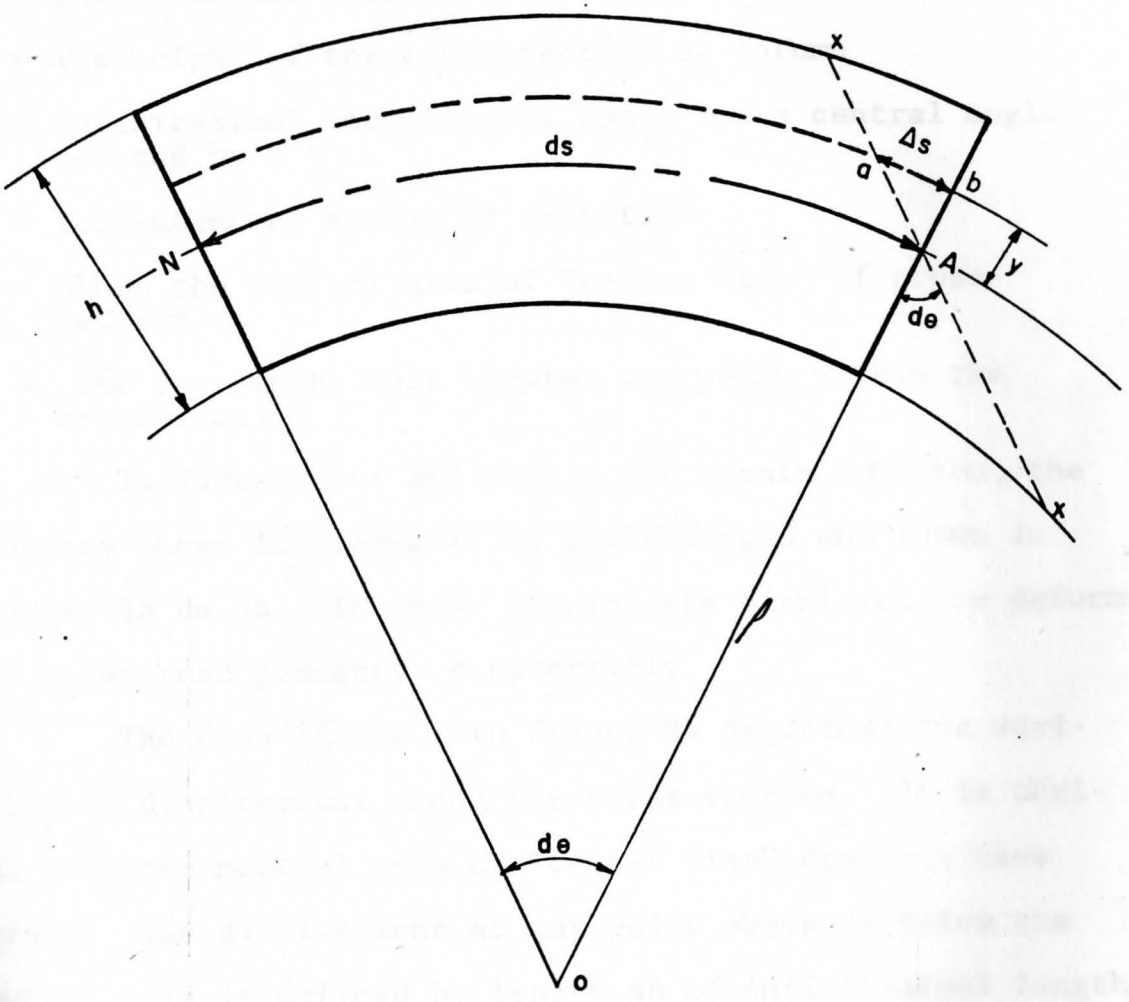

Figure 3a. Deformed Element Geometry-Incompressible Column

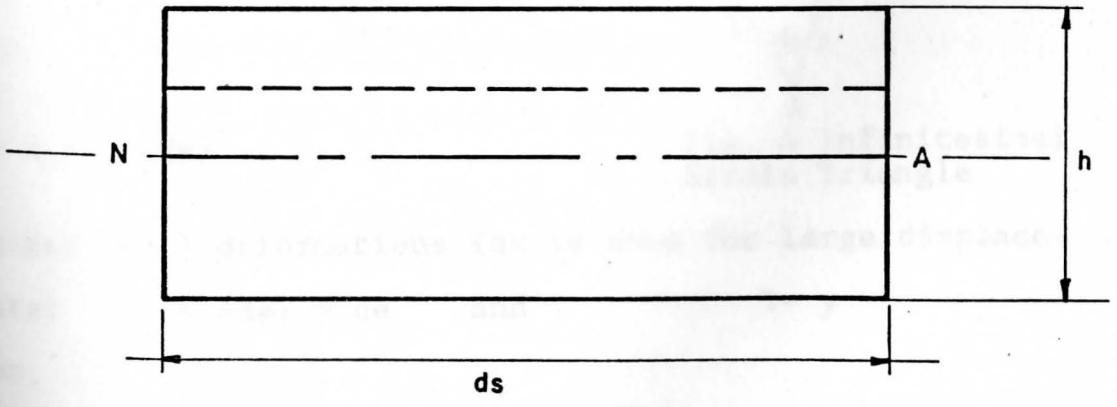

Figure 3b. Undeformed Element Geometry

ds = Infinitesimal increment of length

h = The height of the cross-section of column

dθ = Infinitesimal increment of angle and a central angle subtend by A'B'

ρ = Instantaneous radius of curvature

N-A = Shows the neutral axis of "center line" of cross-section

Y = The coordinate that locates any point within the cross-section

To investigate and obtain the strain function, the geometry shown in Figure 2b is now enlarged and shown in Figures 3a dn 3b. In these Figures are displayed the deformed and undeformed geometry, respectively.

The dash line x-x in Figure 3a describes the variation in displacement along the cross-section. It is obvious that the neutral axis or "center line" does not have strain. The displacement at any point above or below the neutral axis is defined by length ab of infinitesimal length S.

From Figure 3b on the triangle aAb, it follows that

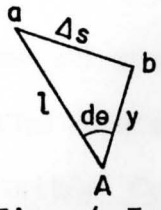

Fig.-4 Infinitesimal Strain Triangle

$\Delta s = l \sin(d\theta)$

But for small deformations (as is done for large displacements) $\sin(d\theta) \cong d\theta$ and $l = y$

Then,

$\Delta s \cong l(d\theta)$ or $\Delta s \cong y(d\theta)$

From similar triangles NOA and aAb (see Figure 3a and Figure 4), one obtains

$$\frac{\Delta s}{ds} = \frac{y}{\rho} = \epsilon \qquad (2\text{-}1)$$

which is the strain function, where ϵ is the strain at any point on the cross-section, and as described previously the neutral axis or center line has zero strain. (i.e. $\epsilon = 0$ for $y = 0$). The curvature function is now computed by noting

$$\frac{\Delta s}{l} \cong \frac{\Delta s}{y} \qquad \text{and} \qquad \sin(d\theta) \cong d\theta \cong \frac{\Delta s}{y}.$$

From Equation (2-1), it follows that

$$d\theta = \frac{ds}{\rho}$$

taking the differential of both sides of the latter equation with respect to s gives

$$\frac{d}{ds}\left[d\theta\right] = \frac{1}{\rho}\frac{d}{ds}\left[ds\right]$$

or

$$\frac{d\theta}{ds} = \frac{1}{\rho} \qquad (2\text{-}2)$$

Combining Equations (2-1) and (2-2) yields

$$\epsilon = y\frac{d\theta}{ds} \qquad (2\text{-}3)$$

which is the strain ϵ expressed in terms of angular coordinates, arc length, and distance above the neutral line.

2.2.2 Center Line Strain of a Compressible Column

In a manner similar to that used in Section 2.2.1, an enlarged view of the deformed column illustrating angular coordinates is shown clearly in Figure 5. Examination the element of arc length ds bounded by two adjacent cross-sections of the column is made. Prior to loading,

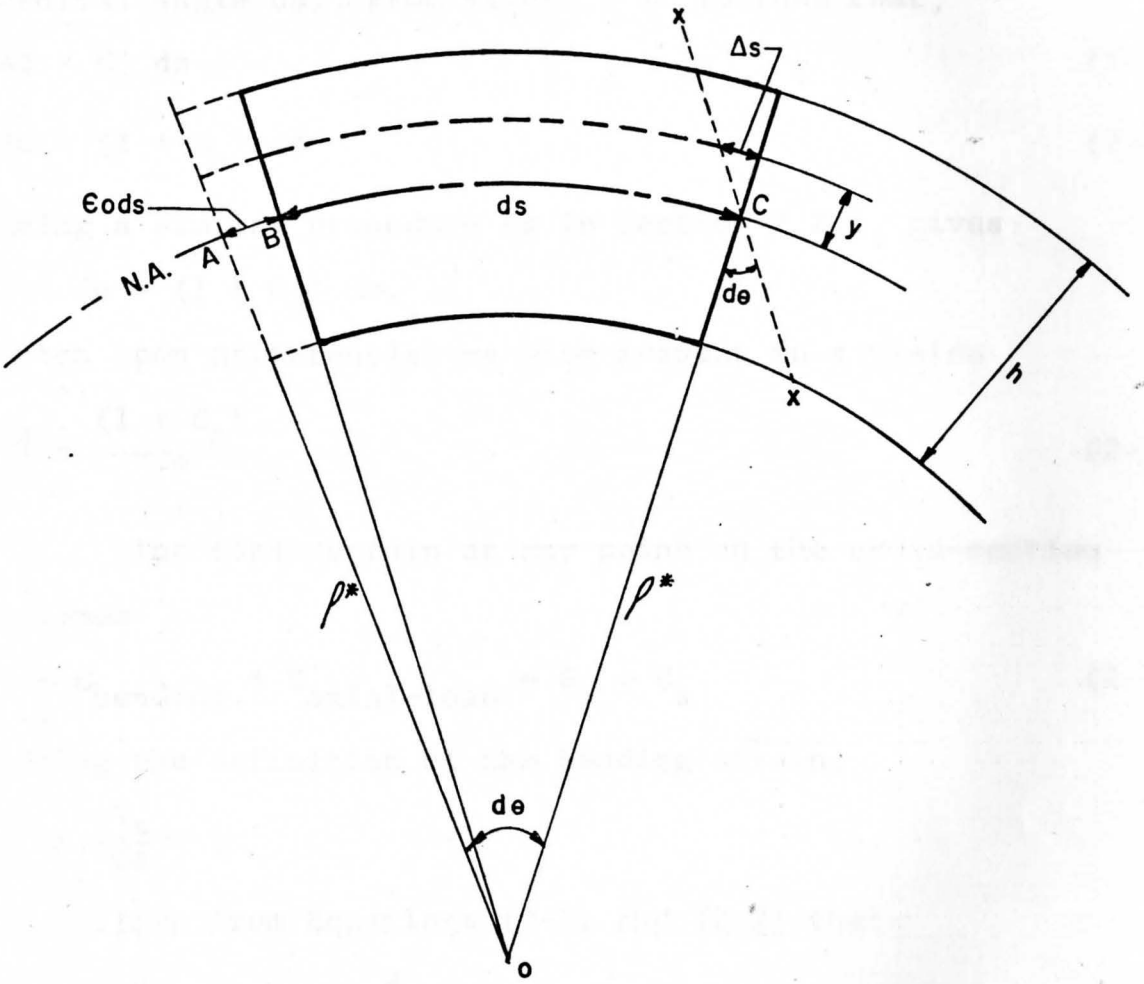

Figure 5. Deformed Element Geometry-Compressible Column

(undeformed shape shown in Figure 3b), these cross-sections are parallel to each other. After the column has deflected, it has the appearance shown in Figure 5, along with a subtended central angle $d\theta$. From Figure 5 it follows that,

$$\widehat{AB} = \epsilon_o \, ds \tag{2-4a}$$

$$\widehat{AC} = (1 + \epsilon_o) \, ds \tag{2-4b}$$

Using a similar procedure as in Section 2.2.1, gives:

$\rho^* \, d\theta = (1 + \epsilon_o) \, ds$,

which upon differentiating with respect to s yields

$$\frac{d\theta}{ds} = \frac{(1 + \epsilon_o)}{\rho^*} \tag{2-5}$$

The total strain at any point on the cross-section becomes

$$\epsilon = \epsilon_{bending} + \epsilon_{axial\text{-}load} \equiv \epsilon_b + \epsilon_a \tag{2-6}$$

Noting the definition of the bending strain,

$$\epsilon_b = \frac{\Delta s}{ds} \quad ;$$

it follows from Equations (2-1) and (2-2) that

$$\epsilon_b = \frac{\Delta s}{ds} = \frac{y}{\rho} = y \frac{d\theta}{ds}$$

Applying the results of Equation (2-5) to the latter equation gives

$$\epsilon_b = y \frac{(1 + \epsilon_o)}{\rho^*} \tag{2-7}$$

Noting the classical definition of strain, the axial strain is defined as

$$\epsilon_a = \frac{(1 + \epsilon_o) \, ds - ds}{ds} = \epsilon_o \tag{2-8}$$

2.2.3 Strain of a Compressible Column

Using the results obtained in Section 2.2.2, the general strain function is developed below.

Defining the strains due to tension as negative and strains due to compression as positive, it follows that, strains due to axial compressive load are positive (+) strains due to bending (see Figure 6) for positive "y" are negative (-), or tension and for negative "y" are positive (+), or compression.

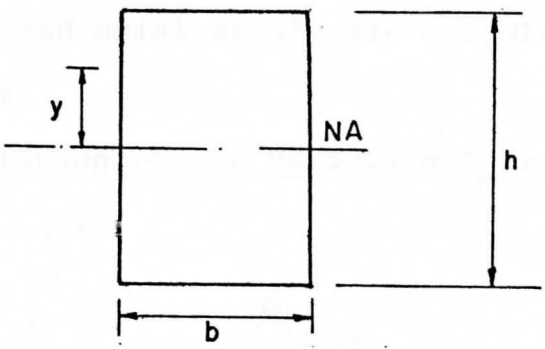

Figure 6. Column Cross-Section

The final expression of ϵ at any point on the section becomes

$$\epsilon = -y\frac{(1 + \epsilon_o)}{\rho^*} + \epsilon_o \qquad (2\text{-}9a)$$

Defining k as the curvature of the member with

$$k = \frac{1}{\rho^*} \qquad (2\text{-}9b)$$

the "True" strain function definition becomes

$$\epsilon = \epsilon_o - (1 + \epsilon_o)\, ky \qquad (2\text{-}10)$$

CHAPTER III

EXACT COMPRESSIBLE COLUMN THEORY

The nonlinear differential equations of equilibrium are formulated utilizing the minimum potential energy theorem of Variational Calculus. The potential energy of the compressive force P and the internal strain energy of combined bending and axial strain are computed as initial steps in the process.

3.1 Formulation of the Variational Problem

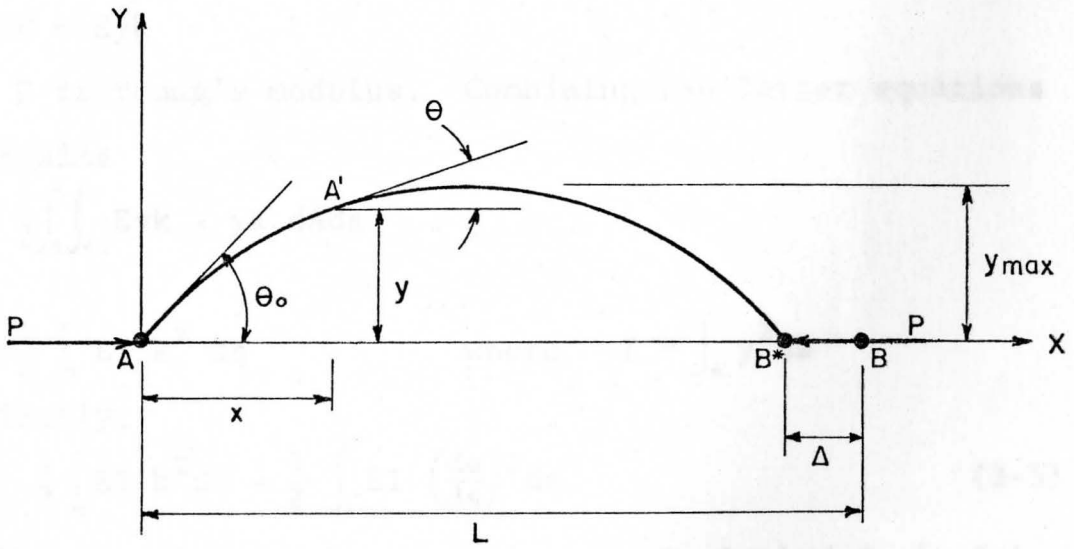

Figure 7. Column Center Line Geometry

The axial shortening of the column Δ (see Figure 7) becomes,

$$\Delta = L - \int_o^L \cos \theta \, ds \qquad (3\text{-}1)$$

From Equation (2-5) ds is replaced by $(1 + \epsilon_o)$ ds

Then, one obtains

$$\Delta = L - \int_o^L (1 + \epsilon_o) \cos \theta \, ds$$

or

$$\Delta = - \left\{ \int_o^L \left[(1 + \epsilon_o) \cos \theta - 1 \right] ds \right\} \qquad (3\text{-}2)$$

The potential energy of force P defined as V becomes

$$-P\Delta = -P \left[- \left\{ \int_o^L \left[(1 + \epsilon_o) \cos \theta - 1 \right] ds \right\} \right]$$

$$-P\Delta = P \left\{ \int_o^L \left[(1 + \epsilon_o) \cos \theta - 1 \right] ds \right\} \equiv -V \qquad (3\text{-}3)$$

The internal strain energy defined as U is given as

$$U = \frac{1}{2} \int_v \sigma \epsilon \, dv \qquad (3\text{-}4)$$

For bending strain only, noting Equation (2-1),

$$\epsilon_b = \frac{y}{\rho} = yk$$

Assuming Hooke's Law in the usual form

$$\sigma = E\epsilon = Eyk$$

where E is Young's modulus. Combining the latter equations one obtains

$$U_b = \frac{1}{2} \int_S \int_A Eyk \cdot yk \, dA ds$$

or

$$U_b = \frac{1}{2} \int_s EI \, k^2 \, ds \qquad \text{where} \quad I = \int_A y^2 da$$

and finally,

$$U_b = \frac{1}{2} \int_s EI \, k^2 ds = \frac{1}{2} \int_s EI \left(\frac{d\theta}{ds} \right)^2 ds \qquad (3\text{-}5)$$

For the general case when axial strain is included, it follows from Equation (2-10) that

$$\epsilon = \epsilon_o - (1 + \epsilon_o) \, ky$$

hence,

$$\sigma = E \left[\epsilon_o - (1 + \epsilon_o) \, ky \right]$$

The general strain energy becomes

$$U = \frac{1}{2}\int_V E\left[\epsilon_o - (1 + \epsilon_o)ky\right]^2 dv$$

or

$$U = \frac{1}{2}\int_s\int_A \left[\epsilon_o^2 - 2\epsilon_o(1 + \epsilon_o)ky + (1 + \epsilon_o)^2k^2y^2\right] dAds.$$

Integrating over the area of the cross-section (see Figure 6) gives

$$U = \frac{1}{2}\int_s E\left\{b\left[\epsilon_o y\right]_{-h/2}^{h/2} - 2\left[b\epsilon_o(1 + \epsilon_o)ky^2\right]_{-h/2}^{h/2}\right.$$

$$\left. + b\left[(1 + \epsilon_o)^2k^2\frac{y^3}{3}\right]\right\} ds$$

or

$$U = \frac{1}{2}\int_s E\left\{\epsilon_o^2 bh + (1 + \epsilon_o)^2k^2\frac{bh^3}{12}\right\} ds.$$

But $k = \frac{1}{\rho^*}$ and $\rho^* d\theta = (1 + \epsilon_o)ds$

$$\rho^*\frac{d\theta}{ds} = (1 + \epsilon_o) \qquad \frac{1}{\rho^*} = \frac{1}{(1 + \epsilon_o)} \times \frac{d\theta}{ds}$$

Noting Equations (2-5) and (2-9b), one obtains

$$k = \frac{1}{(1 + \epsilon_o)} \cdot \frac{d\theta}{ds} \tag{3-6}$$

Substituting k into the Strain Energy Expression gives

$$U = \frac{1}{2}\int_o^L E\left\{A\epsilon_o + I(1 + \epsilon_o)^2\frac{1}{(1 + \epsilon_o)^2}\left(\frac{d\theta}{ds}\right)^2\right\} ds \tag{3-7}$$

The total energy (Π) becomes

$$\Pi = U - V$$

or

$$\Pi = \frac{1}{2}\int_o^L E\left\{A\epsilon_o^2 + I\theta_s^2\right\} ds + P\int_o^L\left\{(1 + \epsilon_o)\cos\theta - 1\right\} ds \tag{3-8}$$

A constraint condition is added to the energy function to insure boundary condition compatability. The center line curve of the column must satisfy the simply-supported boundary conditions

$$y_{(o)} = 0$$

$$y_{(L)} = 0$$

This geometry imposes the integral constraint of the form

$$\int_o^L dy = 0$$

Noting,

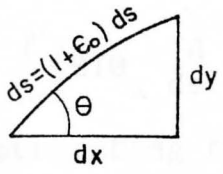

$$\sin \theta = \frac{dy}{(1 + \epsilon_o)\, ds} \quad \text{or}$$

$$dy = (1 + \epsilon_o) \sin \theta \, ds$$

Figure 8. Infinitesimal arc length of the Deformed Compressible Column.

Therefore,

$$\int_o^L dy = \int_o^L (1 + \epsilon_o) \sin \theta \, ds = 0$$

Introducing the integral constraint into Equation (3-8) yields

$$\Pi = \frac{1}{2}\int_o^L E \left\{ A\epsilon_o^{\,2} + I\theta_s^2 \right\} ds + p\int_o^L \left[(1 + \epsilon_o)\cos \theta - 1 \right] ds$$
$$- \hat{\lambda} \int_o^L (1 + \epsilon_o) \sin \theta \, ds \qquad (3\text{-}9).$$

Where " $\hat{\lambda}$ " the Lagrange Multiplier is an arbitrary constant to be determined.

3.2 Solution of the Variational Problem

The first variation of Π is computed as a necessary condition for equilibrium, as

$$\delta^{(1)}\Pi = 0$$

Performing the individual operations on ϵ and θ gives

$$\delta^{(1)}\Pi = \frac{1}{2}\int_o^L E\left\{A(2\epsilon_o\,\delta\epsilon_o) + 2I\frac{d}{ds}\,\frac{d(\delta\theta)}{ds}\right\}ds$$

$$- P\int_o^L\left[(1+\epsilon_o)\sin\theta\,\delta\theta - \cos\theta\,\delta\epsilon_o\right]ds$$

$$-\hat{\lambda}\int_o^L\left[(1+\epsilon_o)\cos\theta\,\delta\theta + \sin\theta\,\delta\epsilon_o\right]ds$$

or,

$$\delta^{(1)}\Pi = \int_o^L\left\{EA\epsilon_o + P\cos\theta - \hat{\lambda}\sin\theta\right\}\delta\epsilon_o\,ds$$

$$+\int_o^L\left\{EI\theta_s\,\frac{d}{ds}(\delta\theta) - P(1+\epsilon_o)\sin\theta\,\delta\theta - \hat{\lambda}(1+\epsilon_o)\cos\theta\,\delta\theta\right\}ds.$$

Integrating the first term in the second integral by parts gives

$$\delta^{(1)}\Pi = \int_o^L\left\{EA\epsilon_o + P\cos\theta - \hat{\lambda}\sin\theta\right\}\delta\epsilon_o ds + \left[EI\theta_s\,\delta\theta\right]_o^L$$

$$-\int_o^L\left\{EI\theta_{ss} + P(1+\epsilon_o)\sin\theta + \hat{\lambda}(1+\epsilon_o)\cos\theta\right\}\delta\theta ds \qquad (3\text{-}10)$$

where the subscript s implies the operator $\frac{d}{ds}$.

Taking E,A,I, as constants setting the coefficients of $\delta\epsilon_o$ and $\delta\theta$ equal to zero in Equation (3-10), one obtains

$$EA\epsilon_o + P\cos\theta - \hat{\lambda}\sin\theta = 0 \qquad (3\text{-}11)$$

$$EI\theta_{ss} + P(1+\epsilon_o)\sin\theta + \hat{\lambda}(1+\epsilon_o)\cos\theta = 0 \qquad (3\text{-}12)$$

with the boundary conditions at $s = 0$ and $s = L$

Either $EI\theta_s = 0$ or θ is specified for pinned-pinned conditions $EI\theta_s = M = 0$

The Lagrange multiplier $\hat{\lambda}$ is evaluated as follows: multipliying Equation (3-12) by ds, and integrating from "o" to "L" gives

$$EI\theta_{ss} \cdot ds + P(1 + \epsilon_o)\sin\theta \cdot ds + \hat{\lambda}(1 + \epsilon_o)\cos\theta \cdot ds = 0$$

and

$$\int_o^L EI\theta_{ss} ds + P\int_o^L (1 + \epsilon_o)\sin\theta\, ds + \hat{\lambda}\int_o^L (1 + C_o)\cos\, ds = 0$$

Noting the second integral is zero, since $\int_o^L dy = 0$, it follows that

$$EI\int_o^L \frac{d}{ds}(\theta_s)ds + \hat{\lambda}\int_o^L (1 + \epsilon_o)\cos\theta\, ds = 0$$

Integrating the first integral of the last equation gives

$$EI\left[\theta_s\right]_o^L + \hat{\lambda}\int_o^L (1 + \epsilon_o)\cos\theta\, ds = 0$$

Since $EI\theta_s = M = 0$ at $s = 0$ and $s = L$, one obtains

$$\hat{\lambda}\int_o^L (1 + \epsilon_o)\cos\theta\, ds = 0$$

The integral in the latter equation is nonzero by Equation (3-2) therefore, $\hat{\lambda} \equiv 0$ (3-13)

Thus, the simply-supported boundary conditions are uniquely satisfied by the optimization of Equation (3-8). It should be noted that for a cantilever beam $\hat{\lambda}$ is not necessarily equal to zero.

Introducing Equation (3-13) in Equations (3-11) and (3-12) gives

$$EA\epsilon_o + P\cos\theta = 0 \qquad (3\text{-}14)$$

$$EI\theta_{ss} + P(1 + \epsilon_o)\sin\theta = 0 \qquad (3\text{-}15)$$

From Equation (3-14), it follows that

$$\epsilon_o = -\frac{P}{EA} \cos \theta \qquad (3\text{-}15a)$$

which is the center line strain along the length of the column. For $\theta = 0$ or $\cos \theta = 1$ at $L/2$, then

$$\epsilon_o = -\frac{P}{EA}$$

Equation (3-15) is the basic non-linear differential equation of equilibrium of the column and is rewritten as

$$\theta_{ss} + \frac{P}{EI} (1 + \epsilon_o) \sin \theta = 0 \qquad (3\text{-}16)$$

3.3 Solution of the Non-Linear Equilibrium Equation

The solution of the nonlinear differential equation is formulated by carrying out quadrature process. Multiplying Equation (3-16) by θ_s, noting Equation (3-14)

$$\theta_{ss} \cdot \theta_s + \frac{P}{EI} \sin \theta \cdot \theta_s - \frac{P}{EI} \cdot \frac{P}{AE} \cos \theta \cdot \sin \theta \cdot \theta_s = 0$$

since $\epsilon_o = -\frac{P}{AE} \cos \theta$, one obtains

$$\frac{d}{ds} \left[\frac{1}{2} (\theta_s)^2 - \frac{P}{EI} \left[1 + \frac{\epsilon_o}{2} \right] \cos \theta \right] = 0$$

Integrating on the variable s gives

$$(\theta_s)^2 = 2 \frac{P}{EI} \left[1 + \frac{\epsilon_o}{2} \right] \cos \theta + C \qquad (3\text{-}17)$$

where C is a constant of integration to be determined by the boundary conditions

$x = 0 \quad \theta = \alpha' \;, \quad EI\theta_s = M = 0$

$x = L \quad 0 = -\alpha' \;, \quad EI\theta_s = M = 0$

Then at $x = 0, L$, Equation (3-17)

$$(0)^2 = 2 \frac{P}{EI} \left[1 + \frac{\hat{\epsilon}_o}{2} \right] \cos \alpha' + C$$

where $\hat{\epsilon}_o = -\frac{P}{AE}\cos\alpha'$

then,

$$C = -\frac{2P}{EI}\left[1 + \frac{\hat{\epsilon}_o}{2}\right]\cos\alpha' \qquad (3\text{-}18)$$

Substituting Equation (3-18) into Equation (3-17) yields

$$\theta_s = \left[\frac{2P}{EI}\left[\cos\theta - \cos\alpha' - \frac{P}{2AE}(\cos^2\theta - \cos^2\alpha')\right]\right]^{\frac{1}{2}} \qquad (3\text{-}19a)$$

which upon trigonometric substitution becomes

$$\theta_s = \left[\frac{2P}{EI}\left[1 - 2\sin^2\frac{\theta}{2} - 1 + 2\sin^2\frac{\alpha'}{2} - \frac{P}{2AE}\left(1 - \sin^2\theta - 1 + \sin^2\alpha'\right)\right]\right]^{\frac{1}{2}}$$

or

$$\theta_s = \left[\frac{2P}{EI}(2)\left(\sin^2\frac{\alpha'}{2} - \sin^2\frac{\theta}{2}\right)\left[1 - \frac{P}{2EA}(\cos\theta + \cos\alpha')\right]\right]^{\frac{1}{2}} \qquad (3\text{-}19b)$$

Separating variables in Equation (3-19b) gives

$$ds = \frac{d\theta}{\left[\frac{4P}{EI}\left[1 - \frac{P}{2EA}(\cos\theta + \cos\alpha')\right]\left[\sin^2\frac{\alpha'}{2} - \sin^2\frac{\theta}{2}\right]\right]^{\frac{1}{2}}} \qquad (3\text{-}19c)$$

Integrating the latter Equation yields

$$\int_o^L ds = \int_{-\alpha'}^{\alpha'} \frac{d\theta}{\left[\frac{4P}{EI}\right]^{\frac{1}{2}}\left[\left[1 - \frac{P}{2AE}(\cos\theta + \cos\alpha')\right](\sin^2\frac{\alpha'}{2} - \sin^2\frac{\theta}{2})\right]^{\frac{1}{2}}}$$

Using the symmetry of the deflected curve about x = L/2 gives

$$\int_o^L ds = \sqrt{\frac{EI}{4P}}\int_0^{\alpha'} \frac{2\,d\theta}{\left[\left[1 - \frac{P}{2EA}(\cos\theta + \cos\alpha')\right](\sin^2\frac{\alpha'}{2} - \sin^2\frac{\theta}{2})\right]^{\frac{1}{2}}}$$

Noting $ds = (1 + \epsilon_o)\,ds$ from Equation (2-5)

The last equation becomes

$$\int_o^L \left[1 - \frac{P}{EA} \cos \theta \right] ds =$$

$$\sqrt{\frac{EI}{4P}} \int_o^{\alpha'} \frac{2 d\theta}{\left[\left[1 - \frac{P}{2EA} (\cos \theta + \cos \alpha') \right] \left[\sin^2 \frac{\alpha'}{2} - \sin \frac{\theta}{2} \right] \right]^{\frac{1}{2}}}$$

$$L - \frac{P}{EA} \int_o^L \cos\theta ds =$$

$$\sqrt{\frac{EI}{4P}} \int_o^{\alpha'} \frac{2 d\theta}{\left[\left[1 - \frac{P}{2EA} (\cos \theta + \cos \alpha') \right] \left[\sin^2 \frac{\alpha'}{2} - \sin \frac{\theta}{2} \right] \right]^{\frac{1}{2}}}$$

Substituting "ds" previously computed in Equation (3-19c) gives

$$L = \frac{P}{EA} \int_o^{\alpha'} \frac{2 \cos \theta \, d\theta}{\left[\left[1 - \frac{P}{2EA} (\cos \theta + \cos \alpha') \right] \left[\sin^2 \frac{\alpha'}{2} - \sin \frac{\theta}{2} \right] \right]^{\frac{1}{2}}} -$$

$$+ \sqrt{\frac{EI}{4P}} \int_o^{\alpha'} \frac{2 \, d\theta}{\left[\left[1 - \frac{P}{2EA} (\cos \theta + \cos \alpha') \right] \left[\sin^2 \frac{\alpha'}{2} - \sin \frac{\theta}{2} \right] \right]^{\frac{1}{2}}}$$

or

$$L = \sqrt{\frac{EI}{P}} \int_o^{\alpha'} \frac{\left[1 + \frac{P}{EA} \right] \cos \theta \, d\theta}{\left[\left[1 - \frac{P}{2EA} (\cos \theta + \cos \alpha') \right] \left[\sin^2 \frac{\alpha'}{2} - \sin^2 \frac{\theta}{2} \right] \right]^{\frac{1}{2}}} \qquad (3\text{-}19d)$$

The Euler Buckling load (p. 467, (17)) "P_E" for a pinned-pinned column is given as

$$P_E = \frac{\pi^2 EI}{L^2}$$

which is used as a nondimensionalizing reference point.

Equation (3-19d) becomes

$$\sqrt{\frac{P}{P_E}} = \frac{1}{\pi}\int_0^{\alpha'} \frac{\left[1 + \frac{P}{EA}\cos\theta\right] d\theta}{\left[\left[1 - \frac{P}{2EA}(\cos\theta + \cos\alpha')\right]\left[\sin^2\frac{\alpha'}{2} - \sin^2\frac{\theta}{2}\right]\right]^{\frac{1}{2}}} \quad (3\text{-}19e)$$

For purposes of comparison with classical solution (axial strain neglected),

let $\sin\frac{\theta}{2} = \varphi \sin\phi$ where $\varphi = \sin\frac{\alpha'}{2}$

$$\cos\alpha' = 1 - 2\sin^2\frac{\alpha'}{2}$$

$$\cos\alpha' = 1 - 2\varphi^2.$$

Equation (3-19e) simplifies to the form

$$\sqrt{\frac{P}{P_E}} = \frac{1}{\pi}\int_0^{\alpha'} \frac{\left[1 + \frac{P}{EA}\cos\theta\right] d\theta}{\left[\left[1 - \frac{P}{2EA}(\cos\theta + 1 - 2\varphi^2)\right](\varphi^2 - \varphi^2\sin\phi)\right]^{\frac{1}{2}}}$$

Consider $\theta = 2 \arcsin(\varphi\sin\phi)$,

then; $d\theta = 2\,\frac{\varphi\cos\phi\, d\phi}{\sqrt{1 - \varphi^2\sin^2\phi}}$

which upon substitution gives

$$\sqrt{\frac{P}{P_E}} = \frac{1}{\pi}\int_0^{\alpha'} \frac{\left[1 + \frac{P}{AE}\cos\theta\right] 2\, d\phi}{\left[\left[1 - \frac{P}{2EA}(\cos\theta + 1 - \varphi^2)\right](1 - \varphi^2\sin^2\phi)\right]^{\frac{1}{2}}}$$

Finally noting

$$\cos \theta = 1 - 2 \sin^2 \frac{\theta}{2}$$

$$\cos \theta = 1 - 2 \gamma^2 \sin^2 \phi$$

it follows that

$$\sqrt{\frac{P}{P_E}} =$$

$$\frac{2}{\pi} \int_0^{\pi/2} \frac{\left[1 + \frac{P}{EA} \cos \theta (1 - 2 \gamma^2 \sin^2 \phi)\right] d\phi}{\left[\left[1 - \frac{P}{2EA} (1 - 2 \gamma^2 \sin^2 \phi + 1 - 2 \gamma^2)\right] (1 - \gamma^2 \sin^2 \phi)\right]^{\frac{1}{2}}}$$

or

$$\sqrt{\frac{P}{P_E}} = \frac{2}{\pi} \int_0^{\pi/2} \frac{\left[1 + \frac{P}{EA} \cos \theta (1 - 2 \gamma^2 \sin^2 \phi)\right] d\phi}{\left[\left[1 - \frac{P}{2EA} (1 - \gamma^2 (1 + \sin^2 \phi)\right]\left[1 - \gamma^2 \sin^2 \phi\right]\right]^{\frac{1}{2}}} \quad (3\text{-}20)$$

To compute the maximum deflection: (Ymax)

A expression of sin θ was found as (Constraint of π)

$$\sin \theta = \frac{dy}{(1 + \epsilon_o)\, ds}$$

Substituting this expression in "the basic non-linear differential equation"

$$\theta_{ss} + \frac{P}{EI} \cdot \frac{dy}{ds} = 0$$

$$\frac{d}{ds} (\theta_s) + \frac{P}{EI} \frac{d}{ds} (y) = 0$$

$$\frac{d}{ds}\left[\theta_s + \frac{P}{EI} y\right] = 0$$

Integrating

$$y = - \frac{EI}{P} \theta_s + C_1$$

For pinned-pinned conditions $EI\theta_s = 0$ at $x = 0;\ x = L$

$$0 = - \frac{EI}{P} \theta_s + C_1$$

Then

$$C_1 \equiv 0$$

$$y = - \frac{EI}{P} \theta_s \qquad (3\text{-}21)$$

Substituting Equation (3-19) in Equation (3-22)

$$Y = - \frac{EI}{P} \left[\frac{2P}{EI} \left[\cos \theta - \cos\alpha' - \frac{P}{2AE}(\cos^2\theta - \cos^2\alpha') \right] \right]^{\frac{1}{2}}$$

Ymax at $\theta = 0$; then $\hat{\epsilon}_o = - \frac{P}{EA} \cos(o) = - \frac{P}{EA}$

$$Ymax = - \frac{EI}{P} \left[\frac{2P}{EI} \left[1 - \cos\alpha' - \frac{P}{2AE}(1 - \cos^2\alpha') \right] \right]^{\frac{1}{2}}$$

$$Ymax = - \sqrt{\frac{2EI}{P}} \left[(1 - \cos\alpha') \left[1 - \frac{P}{2AE} (1 + \cos\alpha') \right] \right]^{\frac{1}{2}}$$

$$Ymax = - \sqrt{\frac{2EI}{P}} \left[2 \sin^2 \frac{\alpha'}{2} \left[1 - \frac{P}{2AE} \cos^2 \frac{\alpha'}{2} \right] \right]^{\frac{1}{2}}$$

$$Ymax = - 2 \sqrt{\frac{EI}{P}} \sin \frac{\alpha'}{2} \left[1 - \frac{P}{2AE} \cos^2 \frac{\alpha'}{2} \right]^{\frac{1}{2}} =$$

$$- 2\rho \sqrt{\frac{\pi^2 EI}{L^2 P}} \cdot \frac{L}{\pi} \left[1 - \frac{P}{2AE} \cos^2 \frac{\alpha'}{2} \right]^{\frac{1}{2}}$$

$$\frac{Ymax}{L} = -\frac{2\varphi}{\pi} \cdot \left[1 - \frac{P}{2AE}\cos^2\frac{\alpha'}{2}\right]^{\frac{1}{2}} \cdot \sqrt{\frac{P_E}{P}} \qquad (3\text{-}22)$$

Expression that in conjunction with Equation (3-20) relates $\frac{P}{P_E}$ versus $\frac{Ymax}{L}$ and their solution will give the non-linear load-deflection relation. Therefore a description of the postbuckling behavior is perform.

CHAPTER IV

INTERMEDIATE THEORY

4.1 Numerical Solution

The solution of the problem formulated in Chapter III is most conveniently performed and easily carried out. By a numerical technique, as presented by Dym and Shames[17]. The numerical technique utilized to solve the Basic Non-linear Differential Equations (3-14) and (3-15) is an amplified form of that employed by these authors

The process consists of using a power series expansion of the trigonometric functions present in the potential energy function. The functions are expanded in terms of the powers of the derivative term (dy/ds). Next the classical Rayleigh-Ritz process is applied to the expanded potential function. The resulting function is integrated and evaluated. Lastly, the latter function is extremized to obtain a final function that relates P/Pe versus Ymax/L.

Express cos θ as follows, noting $\frac{dy}{ds} = \sin \theta$

$$\cos \theta = (1-\sin^2\theta)^{\frac{1}{2}} = \left[1 - \left[\frac{dy}{ds}\right]^2\right]^{\frac{1}{2}}$$

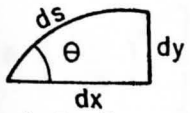

Fig. 9. A Deformed Curved Segment ds

Using the binomial expansion

$$\text{Cos } \theta = 1 - \frac{1}{2}\left(\frac{dy}{ds}\right)^2 - \frac{1}{8}\left(\frac{dy}{ds}\right)^4 - \frac{1}{16}\left(\frac{dy}{ds}\right)^6 - \frac{5}{128}\left(\frac{dy}{ds}\right)^8 - \ldots .$$

From which one uses the following terms:

$$\text{Cos } \theta \cong 1 - \frac{1}{2}\left(\frac{dy}{ds}\right)^2 - \frac{1}{8}\left(\frac{dy}{ds}\right)^4 \qquad (4\text{-}1)$$

Similar procedure is used to obtain the curvature expression noting that $\theta = \text{arc sin}\left(\frac{dy}{ds}\right)$

$$\frac{d\theta}{ds} = \frac{d}{ds}\left[\text{arc sin } \frac{dy}{ds}\right] = \left[1-\left(\frac{dy}{ds}\right)^2\right]^{-\frac{1}{2}} \left(\frac{d^2y}{ds^2}\right)$$

expanding

$$\frac{d\theta}{ds} = \left[1 + \frac{1}{2}\left(\frac{dy}{ds}\right)^2 + \frac{3}{8}\left(\frac{dy}{ds}\right)^4 + \frac{5}{16}\left(\frac{dy}{ds}\right)^6 + \ldots . \right]^{-\frac{1}{2}} \left(\frac{d^2y}{ds^2}\right)$$

To finally use:

$$\frac{d\theta}{ds} \cong \left[1 + \frac{1}{2}\left(\frac{dy}{ds}\right)^2 \right]^{-\frac{1}{2}} \left(\frac{d^2y}{ds^2}\right) \qquad (4\text{-}2)$$

Substituting Equations (4-1) and (4-2) into Equation (3-8) of Chapter III, the total potential energy Π is approximated by the expansion

$$\Pi \cong \frac{P^2}{2EA}\int_o^L \left[1 - \frac{1}{2}\left(\frac{dy}{ds}\right)^2 - \frac{1}{8}\left(\frac{dy}{ds}\right)^4\right]^2 ds +$$

$$\frac{EI}{2}\int_o^L \left[1 + \frac{1}{2}\left(\frac{dy}{ds}\right)^2\right]^2 \left(\frac{d^2y}{ds^2}\right)^2 ds + P\int_o^L \left\{1 - \frac{1}{2}\left(\frac{dy}{ds}\right)^2 - \frac{1}{8}\left(\frac{dy}{ds}\right)^4 - \frac{P}{EA}\left[\right.\right.$$

$$\left.\left. 1 - \frac{1}{2}\left(\frac{dy}{ds}\right)^2 - \frac{1}{8}\left(\frac{dy}{ds}\right)^4\right]^2 - 1 \right\} ds$$

After simplfication one obtains

$$\Pi = -\frac{P^2}{2EA}\int_o^L \left[1 - \frac{1}{2}\left(\frac{dy}{ds}\right)^2 - \frac{1}{8}\left(\frac{dy}{ds}\right)^4\right]^2 ds +$$

$$P\int_o^L \left[\left[1 - \frac{1}{2}\left(\frac{dy}{ds}\right)^2 - \frac{1}{8}\left(\frac{dy}{ds}\right)^4\right] - 1\right] ds$$

$$+ \frac{EI}{2}\int_o^L \left[1 - \frac{1}{2}\left(\frac{dy}{ds}\right)^2\right]^2 \cdot \left(\frac{d^2y}{ds^2}\right)^2 ds \qquad (4\text{-}3)$$

Continuing with this numerical technique the Rayleigh-Ritz method is employed (see p. 407 of (17)) using the eigenfunction with "s" as the variable, that is $y = B \sin \frac{\pi s}{L}$, as the single coordinate function. This function satisfies the geometric and natural boundary conditions of the pinned-pinned column thus

at: $s = 0$; $s = L$ $\qquad y = B \sin o \equiv 0$

$s = \frac{L}{2}$ $\qquad y = B \sin \frac{\pi}{2} \equiv B$

The derivatives of "Y", that is, $y = B \sin \frac{\pi s}{L}$ $\qquad (4\text{-}4a)$

$$\frac{dy}{ds} = B\left(\frac{\pi}{L}\right) \cos \frac{\pi s}{L}$$

Taking $a = \frac{B\pi}{L}$ $\qquad (4\text{-}4b)$

then

$$\frac{dy}{ds} = a \cos \frac{\pi s}{L}$$

$$\frac{d^2y}{ds^2} = -a \frac{\pi}{L} \sin \frac{\pi s}{L} \qquad (4\text{-}4c)$$

Substituting this latter values into "Π", Equation (4-3) yields

$$\pi = -\frac{P^2}{2EA}\int_0^L \left[1 - \frac{a^2}{2}\cos^2\frac{\pi s}{L} - \frac{a^4}{8}\cos^4\frac{\pi s}{L}\right]^2 ds +$$

$$P\int_0^L \left[-\frac{a^2}{2}\cos^2\frac{\pi s}{L} - \frac{a^4}{8}\cos^4\frac{\pi s}{L}\right] ds +$$

$$\frac{EI}{2}\int_0^L \left[1 + \frac{a^2}{2}\cos^2\frac{\pi s}{L}\right]^2 \left[-\frac{a}{L}\sin\frac{\pi s}{L}\right]^2 ds \qquad (4\text{-}5)$$

Upon integration and algebraic manipulation, Equation (4-5) becomes

$$\pi = -\frac{P^2 L}{2EA}\left[1 - \frac{a^2}{2} + \frac{5a^6}{128} + \frac{35a^8}{8192}\right] - \frac{PL}{4}\left[a^2 + \frac{3a^4}{16}\right] +$$

$$\frac{EI\pi^2 L}{4L^2}\left[a^2 + \frac{a^4}{4} + \frac{a^6}{32}\right] \qquad (4\text{-}6a)$$

Using P_E (Euler Buckling Load) which is defined in Chapter III, to nondimensionalize the above π expression yields

$$\pi = \frac{P_E L}{4}\left[a^2 + \frac{a^4}{4} + \frac{a^6}{32} - \left[a^2 + \frac{3a^4}{16}\right]\left(\frac{P}{P_E}\right) - \right.$$

$$\left. \frac{2P}{EA} \times \frac{P}{P_E}\left[1 - \frac{a^2}{2} + \frac{5a^6}{128} + \frac{35a^8}{8192}\right]\right] \qquad (4\text{-}6b)$$

Extremizing π of Equation (4-6b) with respect to "a", that is $\frac{\partial \pi}{\partial a} = 0$, which is a necessary condition for equilbrium:

$$\frac{P}{EA} \times \frac{P}{P_E}\left[2 - \frac{15a^4}{32} - \frac{35a^6}{512}\right] - \left[2 + \frac{3a^2}{4}\right]\left(\frac{P}{P_E}\right) + 2 + a^2 + \frac{3a^4}{16} = 0$$

(4-7)

From the expression $\frac{P}{EA}$ the following expressions are obtained:

$$\frac{P}{EA} = \frac{P}{EA} \times \frac{IL^2}{IL^2} \frac{\pi^2}{\pi^2} = \frac{P}{\pi^2 EI/L^2} \times \frac{I}{A} \times L^2 \times \pi^2 = \frac{P}{P_E} \times \left(\frac{r}{L}\right)^2 \times \pi^2$$

where $r = \sqrt{\frac{I}{A}}$ is the classical radius of gyration.

Defining $R \equiv \left(\frac{r}{L}\right)^2$ which is the reciprocal of the square of the slenderness ratio that defines the buckling loads or critical stress in a simple prismatic column.

Thus,

$$\frac{P}{AE} = \frac{P}{P_E} R \pi^2 \tag{4-8}$$

substituting Equation (4-8) into Equation (4-7) one obtains,

$$\left[2 - \frac{15a^4}{32} - \frac{35a^6}{512}\right] R \pi^2 \left(\frac{P}{P_E}\right)^2 - \left[2 + \frac{3a^2}{4}\right]\left(\frac{P}{P_E}\right) +$$

$$\left[2 + a^2 + \frac{3a^4}{16}\right] = 0 \tag{4-9}$$

Equation (4-9) is solved for the value of $\frac{P}{P_E}$ given a particular value of a, where a is defined from Equation (4-4a) as follows

$$Y\Big|_{S=L/2} \equiv Ymax = B$$

Noting Equation (4-4b), one obtains

$$a = Ymax \frac{\pi}{L}$$

and hence,

$$\frac{Ymax}{L} = \frac{a}{\pi} \tag{4-10}$$

The latter equation relates the paramenter a of Equation (4-9) to the maximum deflection of the column.

Equation (4-9) is recast in the following algebraic form

$$A\left(R\pi^2\right)\left(\frac{P}{P_E}\right)^2 - B\left(\frac{P}{P_E}\right) + C = 0 \qquad (4\text{-}11a)$$

where

$$A = \left[2 - \frac{15a^4}{32} - \frac{35a^6}{512}\right] \qquad (4\text{-}11b)$$

$$B = \left[2 + \frac{3a^2}{4}\right] \qquad (4\text{-}11c)$$

$$C = \left[2 + a^2 + \frac{3a^4}{16}\right] \qquad (4\text{-}11d)$$

Then, using the quadratic formula, one obtains

$$\frac{P}{P_E} = \frac{B \pm \sqrt{B^2 - 4AR\pi^2C}}{2AR\pi^2} \qquad (4\text{-}12)$$

which is the function that relates $\frac{P}{P_E}$ and $\frac{Ymax}{L}$. Four special cases of parameters are defined:

I) $B^2 \quad 4AR\pi^2C$ $\frac{P}{P_E}$ has real values

II) $B^2 = 4AR\pi^2C$ $\frac{P}{P_E}$ repeated value

III) $B^2 \quad 4AR\pi^2C$ $\frac{P}{P_E}$ has complex values which have no physical meaning

IV) $R=0$ Classical Elastica Condition.

4.2 Solution of Buckling Loads

To obtain the buckling loads, Equation (4-11a) is used with $\frac{Ymax}{L} = \frac{a}{\pi} = 0$ and for different values of R. Since Equation (4-9a) is a quadratic equation, one obtains a set of bifurcation points. (see Table 1; Figures10 and 11).

A bifurcation for the case R = 0, as given by Equation (4-11a) becomes

$$-2\left(\frac{P}{P_E}\right) + 2 = 0$$

$$\frac{P}{P_E} = 1 \qquad (4\text{-}13)$$

It should be noted that the latter bifurcation point defines the special case of the Euler buckling load for the bending mode of stability.

A trifurcation point exists for the special case of repeated roots (see Figure 10)

For $B^2 = 4AR\pi^2C$

From Equation (4-12)

$$2^2 - 4 \times 2R\pi^2 \times 2 = 0$$

$$R = \frac{1}{4\pi^2} = 0.02533029 \qquad (4\text{-}14a)$$

and substituting (4-14a) into (4-12) gives $\frac{P}{P_E} = 2$ (4-14b)

The trifurcation point the defines the limit between the higher and lower modes of postbuckling behavior, and also the limit of pure axial compression mode behavior. (see Figure 10)

The case of $R > 0.02533029$, defines the pure axial compression mode with no bending. The column theoretically shrinks to a zero length condition, (see Figure 10)

With $\frac{Ymax}{L} = 0$ Equation (4-9a) becomes

$$2\pi^2 R\left(\frac{P}{P_E}\right)^2 - 2\left(\frac{P}{P_E}\right) + 2 = 0 \qquad (4\text{-}15)$$

Solution of Equation (4-12). yields

$$\frac{P}{P_E} = \frac{2 \pm \sqrt{4 - 16\pi^2 R}}{4\pi^2 R} \qquad (4\text{-}16)$$

or

$$\frac{P}{P_E} = \frac{1}{2\pi^2 R} \pm \sqrt{\frac{1}{4\pi^4 R^2} - \frac{1}{\pi^2 R}} \qquad (4\text{-}16a)$$

Table 1 gives some dimensionless buckling loads for several values of R, as obtained by solving Equation (4-16a)

TABLE 1

R	P/P_E	P/P_E
0.0	--	1.00000000
0.01	1.12488712	9.00723125
0.02	3.69500193	1.37105725
0.025	2.25782280	1.79502455
0.02533029	2.00000000	2.00000000
0.03	Complex	Complex
0.05	Complex	Complex

DIMENSIONLESS BUCKLING LOADS

4.3 Solution of Postbuckling State

The postbuckling state is obtained by finding the postbuckling loads, as determined by Equation (4-9a), for several values of Ymax/L and different values of R. As in the case buckling loads, the quadratic equation (4-9a) gives two sets of solutions. The numerical results are tabulated in Tables 2a to 2g.

In the Tables 2a to 2g, the column entries Ymax/L, P/P_E, P/P_E, are self explanatory, column entry Δ/L and the

two values of ϵ_o are developed below.

From Figure 10, Δ is defined as the displacement along the X axis or the underformed column axis. The numerical value of Δ is computed from Equation (3-2), that is,

$$\Delta = -\left[\int_o^L \left[(1 + \epsilon_o)\cos\theta - 1\right] ds\right]$$

which is as a function of the expanded forms of cos θ and $\frac{d\theta}{ds}$ using Equations (4-1) and (4-2) respectively, first substituting Equation (3-15a) into the latter equation, one obtains

$$\Delta = -\left[\int_o^L \left[\cos\theta - \frac{P}{EA}\cos\theta - 1\right] ds\right]$$

then, upon substitution of Equation (4-1), it follows that,

$$\Delta = -\left[\int_o^L \left[1 - \frac{1}{2}\left(\frac{dy}{ds}\right)^2 - \frac{1}{8}\left(\frac{dy}{ds}\right)^4 - \frac{P}{EA}\left(1 - \frac{1}{2}\left(\frac{dy}{ds}\right)^2 - \frac{1}{8}\left(\frac{dy}{ds}\right)^4\right)^2 - 1\right] ds\right]$$

Substituting the derivatives of "y" as obtained in Equation (4-4c) gives

$$\Delta = -\left[\int_o^L \left[-\frac{P}{EA}\left[1 - \frac{a^2}{2}\cos^2\frac{\pi s}{L} - \frac{a^4}{8}\cos^4\frac{\pi s}{L}\right]^2 + \left[1 - \frac{a^2}{2}\cos^2\frac{\pi s}{L} - \frac{a^4}{8}\cos^4\frac{\pi s}{L}\right] - 1\right] ds\right]$$

After integration and some algebraic simplifications one

obtains

$$\frac{\Delta}{L} = \frac{1}{4}\left[4\frac{P}{EA}\left[1 - \frac{a^2}{2} + \frac{5a^6}{128} + \frac{35a^8}{8192}\right] + \left[a^2 + \frac{3a^4}{16}\right]\right] \qquad (4\text{-}17)$$

or by substituting Equation (4-7), yields

$$\frac{\Delta}{L} = \frac{1}{4}\left[4\frac{P}{P_E}\,\pi^2 R\left[1 - \frac{a^2}{2} + \frac{5a^6}{128} + \frac{35a^8}{8192}\right] + \left[a^2 + \frac{3a^4}{16}\right] \qquad (4\text{-}17a)$$

This equation is solved simultaneously with Equation (4-9a) and the results are presented in Tables 2a to 2g. Figure 11 shows a plot of P/P_E versus Δ/L for various values of R equal or less than 0.25533. This plot shows clearly the bifurcation points and the postbuckling path that the system must follow in a minimum energy state for a given displacement. In Figure 10 are plotted the values tabulated in Table 1 for the Buckling Loads which are the intersection of the curves with the vertical axis, and in Tables 2a to 2g for the Post-buckling Loads which are the curves themselves.

To evaluate ϵ_o, the center line axial strain as defined in Chapter II, Equation (4-9a) is used as follows:

$$AR\pi^2\left(\frac{P}{P_E}\right)^2 - B\left(\frac{P}{P_E}\right) + C = 0$$

where Equation (4-7) is substituted to give

$$A\frac{P}{EA}\left(\frac{P}{P_E}\right)^2 - B\left(\frac{P}{P_E}\right) + C = 0$$

solving for $\frac{P}{EA}$

$$\frac{P}{EA} = \frac{B}{A} - \frac{C}{A\left(\frac{P}{P_E}\right)} \qquad (4\text{-}18)$$

For the case $S = \frac{L}{2}$, $\theta = \frac{\pi}{2}$, $\cos\theta = 1$, and $\epsilon = \epsilon_{o_{max}} = \frac{P}{EA}$

Thus,

$$\epsilon_{o_{max}} = \frac{B}{A} - \frac{C}{A\left(\frac{P}{P_E}\right)} \qquad (4\text{-}18a)$$

These values are tabulated in Tables 2a to 2g. It should be noted that the value ϵ_o is bigger than 1 for values of $\frac{Ymax}{L} \geqslant 0.25$ for the case of the higher mode of postbuckling. This is inconsistent with the definition of strain given in Chapter II. Therefore, the higher values of $\frac{P}{P_E}$ for $\epsilon_o > 1$ shown in the tables are beyond the limitations of the theory and should be interpreted as such. A close agreement for values of $\frac{P}{P_E}$ and $\epsilon_o < 1$ as given by the exact[12] theory and the intermediate theory is observed for $\frac{Ymax}{L} \leqslant 0.25$ (see Appendix A).

TABLE 2a

R = 0.0

Ymax/L	$P/P_{E(higher)}$	$P/P_{E(lower)}$	Δ/L	$\epsilon_{o(higher)}$	$\epsilon_{o(lower)}$
0.05000000	----	1.00311253	0.00619704	----	----
0.10000000	----	1.01277732	0.02513062	----	----
0.15000000	----	1.02989213	0.05782809	----	----
0.20000000	----	1.05571161	0.10600173	----	----
0.25000000	----	1.09159168	0.1720487	----	----
0.30000000	----	1.13877668	0.25905111	----	----
0.35000000	----	1.19827795	0.37077594	----	----
0.40000000	----	1.27080790	0.51167509	----	----
0.45000000	----	1.35684895	0.68688536	----	----
0.50000000	----	1.45665234	0.90222847	----	----
0.55000000	----	1.57031912	1.16421105	----	----

DIMENSIONLESS POSTBUCKLING LOADS

TABLE 2b

R = 0.01

Ymax/L	$P/P_{E(higher)}$	$P/P_{E(lower)}$	Δ/L	$\epsilon_{o(higher)}$	$\epsilon_{o(lower)}$
0.05000000	9.09994531	1.12738763	0.11609308	0.89812860	0.11126870
0.10000000	9.39638275	1.13512538	0.13163868	0.92738581	0.11203239
0.15000000	9.95974422	1.14867101	0.15865931	0.98298735	0.11336928
0.20000000	10.93096899	1.16857217	0.19885844	1.07884340	0.11533345
0.25000000	12.62421783	1.19491354	0.25476259	1.24596036	0.11793324
0.30000000	15.84646370	1.22694910	0.33000125	1.56398328	0.12109502
0.35000000	23.40358897	1.26293576	0.42981493	2.30984165	0.12464676
0.40000000	56.11944205	1.30024170	0.56182913	5.53876692	0.12832967
0.45000000	-86.13041145	1.33580545	0.73707792	-8.50073088	0.13183882
0.50000000	-22.11163341	1.36662305	0.97121189	-2.18233074	0.13488029

DIMENSIONLESS POSTBUCKLING LOADS

TABLE 2c

R = 0.02

Ymax/L	$P/P_{E(higher)}$	$P/P_{E(lower)}$	Δ/L	$\epsilon_{o(higher)}$	$\epsilon_{o(lower)}$
0.05000000	3.74334632	1.37032015	0.27335051	0.73890695	0.27049036
0.10000000	3.89739481	1.36835926	0.28191510	0.76931490	0.27010329
0.15000000	4.18851120	1.36569641	0.29759184	0.82677897	0.26957767
0.20000000	4.68714819	1.36262239	0.32255426	0.92520597	0.26897088
0.25000000	5.55881049	1.35881049	0.36016692	1.09567516	0.26821844
0.30000000	7.18338954	1.35331686	0.41556619	1.41794426	0.26713404
0.35000000	10.98832439	1.34493797	0.49652070	2.16900830	0.26548011
0.40000000	27.37717849	1.33266838	0.61448396	5.40403843	0.26305819
0.45000000	-43.71330365	1.31600065	0.78578216	-8.62866028	0.25976810
0.50000000	-11.66748317	1.29497800	1.03296241	-2.30306887	0.25561841

DIMENSIONLESS POSTBUCKLING LOADS

TABLE 2d

R = 0.025

Ymax/L	$P/P_{E(higher)}$	$P/P_{E(lower)}$	Δ/L	$\epsilon_{o(higher)}$	$\epsilon_{o(lower)}$
0.05000000	2.32878133	1.77215184	0.43562679	0.57460376	0.43479354
0.10000000	2.51870620	1.69389706	0.42247371	0.62146584	0.41795235
0.15000000	2.82142281	1.62194328	0.41376664	0.69615818	0.40019846
0.20000000	3.28391368	1.55590279	0.41508836	0.81027322	0.38390362
0.25000000	4.03063177	1.49702078	0.43111433	0.99451853	0.36937507
0.30000000	5.38519905	1.44416607	0.46782868	1.32874461	0.35633370
0.35000000	8.47090383	1.39570606	0.53389009	2.09081174	0.34437667
0.40000000	21.61769862	1.35017888	0.64187475	5.33395334	0.33314328
0.45000000	-35.22436391	1.30652150	0.80961591	-8.69126343	0.32237127
0.50000000	- 9.56209041	1.26408627	1.06174757	-2.35935124	0.31190078

DIMENSIONLESS POSTBUCKLING LOADS

TABLE 2e

R = 0.02533029

Ymax/L	$P/P_{E(higher)}$	$P/P_{E(lower)}$	Δ/L	$\epsilon_{o(higher)}$	$\epsilon_{o(lower)}$
0.02500000	2.08345773	1.92583081	0.48151668	0.52087443	0.48145770
0.05000000	2.17809099	1.85949822	0.46533621	0.54452275	0.46487456
0.07500000	2.28638468	1.79986587	0.45150281	0.57159614	0.44996647
0.10000000	2.41164870	1.74602406	0.44011249	0.60291218	0.43650601
0.15000000	2.73259773	1.65282882	0.42533669	0.68314943	0.41320721
0.20000000	3.20162358	1.57508381	0.42303269	0.80040590	0.39377095
0.25000000	3.94662410	1.50895030	0.43662879	0.98665602	0.37723757
0.30000000	5.28907401	1.45123920	0.47162306	1.32226850	0.36280980
0.35000000	8.33858902	1.39936462	0.53647835	2.08464725	0.34984116
0.40000000	21.31701710	1.35136940	0.64371124	5.32925427	0.33784234
0.45000000	-34.78147338	1.30590472	0.81117871	-8.69536834	0.32647617
0.50000000	- 9.45194371	1.26214188	1.06360650	-2.36298593	0.31553574

DIMENSIONLESS POSTBUCKLING LOADS

TABLE 2f

R = 0.03

Ymax/L	$P/P_{E(higher)}$	$P/P_{E(lower)}$	Δ/L	$\epsilon_{o(higher)}$	$\epsilon_{o(lower)}$
0.22623463	2.14639939	2.14639939	0.61663179	0.63552339	0.63552339
0.23000000	2.35753595	1.97925358	0.5797607	0.69803842	0.58603349
0.24000000	2.61158682	1.85190354	0.55391901	0.77325986	0.54832666
0.25000000	2.82892103	1.77745610	0.54116405	0.83760994	0.52628366
0.30000000	4.11691730	1.57422031	0.53214593	1.21897035	0.46619775
0.33000000	5.40109645	1.49833429	0.55212311	1.59920056	0.44563700
0.37000000	9.01285739	1.41861300	0.60608530	2.66860011	0.42003448
0.40000000	17.77121652	1.36868139	0.67005575	5.26184630	0.40525031
0.45000000	-29.56217373	1.29730506	0.83312311	-8.75300880	0.38411661
0.50000000	- 8.15080272	1.23579926	1.08936783	-2.41335595	0.36590550

DIMENSIONLESS POSTBUCKLING LOADS

TABLE 2g

R = 0.05

Ymax/L	$P/P_{E(higher)}$	$P/P_{E(lower)}$	Δ/L	$\epsilon_{o(higher)}$	$\epsilon_{o(lower)}$
0.34669980	2.38790114	2.38790114	0.92876349	1.17838199	1.17838199
0.35000000	2.88249923	2.05080571	0.85012534	1.42245636	1.01203205
0.36000000	3.69973981	1.80185058	0.79982824	1.82574842	0.88917762
0.37000000	4.58613179	1.67275044	0.78245711	2.26316533	0.82546926
0.38000000	5.73346566	1.58250168	0.77802003	2.82935189	0.78093320
0.40000000	10.02873183	1.45520693	0.79233041	4.94898079	0.71811583
0.42000000	29.30181957	1.36427944	0.82972419	14.45986837	0.67324490
0.44000000	-38.24187225	1.29327795	0.88756835	-18.87160753	0.63820697
0.46000000	-12.06848997	1.23493195	0.96596439	- 5.95556109	0.60941449
0.48000000	- 7.30182299	1.18535261	1.06624467	- 3.60330521	0.58434806
0.50000000	- 5.29120869	1.14220662	1.19050590	- 2.61110683	0.56365637

DIMENSIONLESS POSTBUCKLING LOADS

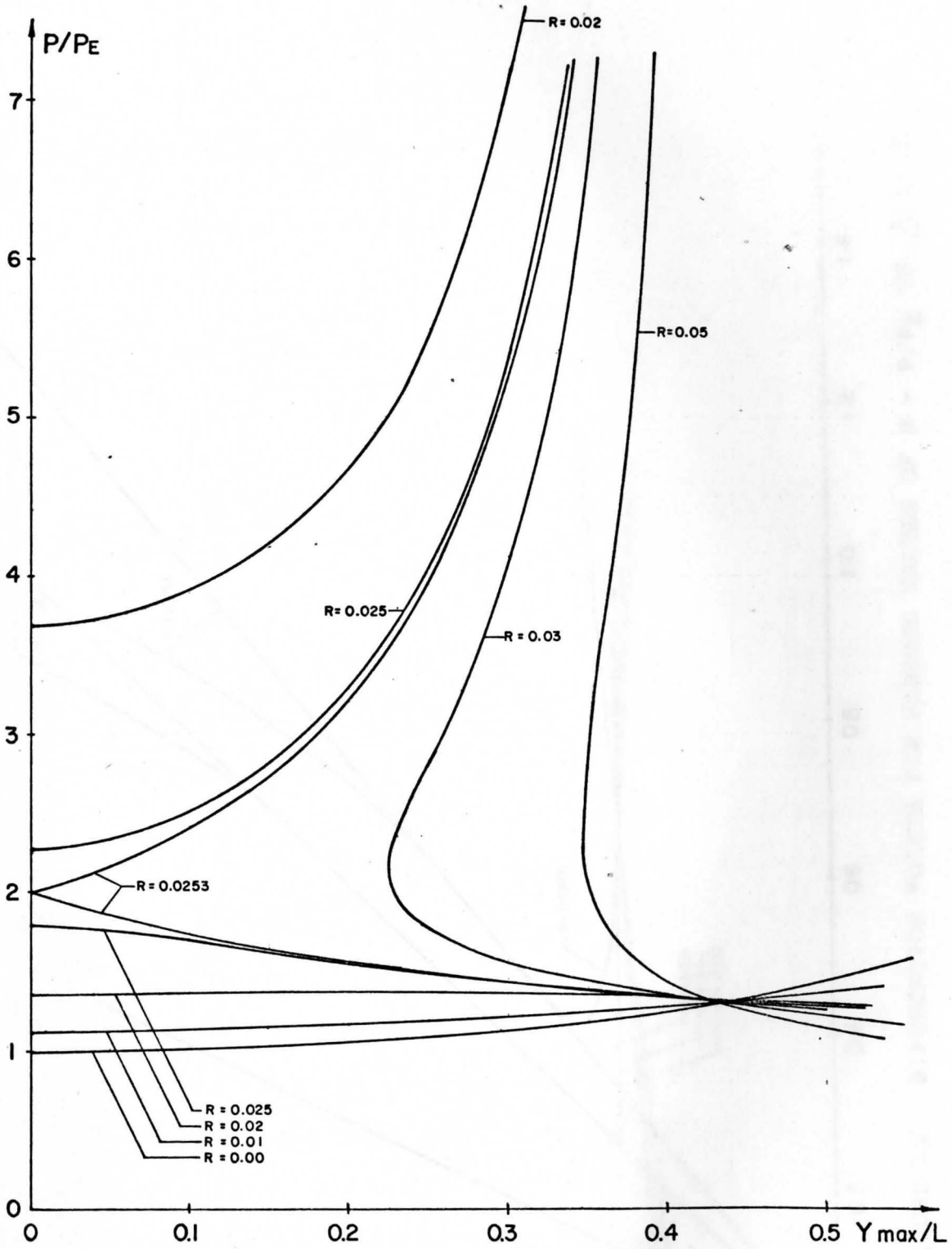

FIGURE 10 DIMENSIONLESS BUCKLING AND POSTBUCKLING LOADS VERSUS YMAX/L, FOR VARIOUS VALUES OF R.

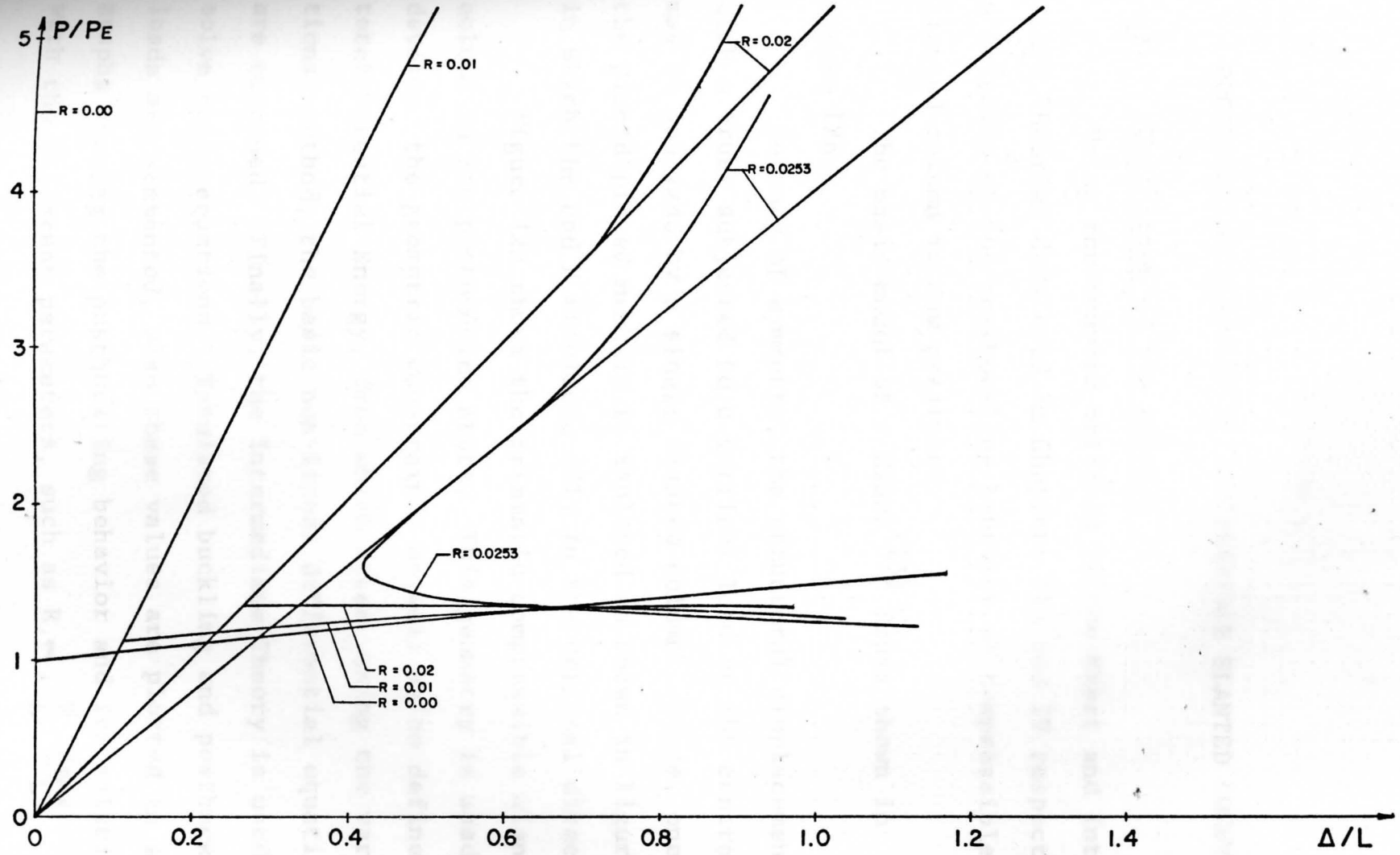

FIGURE 11 BIFURCATION POINTS FOR VARIOUS VALUES OF R - P/P_E VS. Δ/L CURVES

CHAPTER V

POSTBUCKLING BEHAVIOR OF COMPRESSIBLE SLANTED COLUMNS

5.1 Definition of the Problem

Using the results obtained in the Exact and Intermediate Theories developed in Chapters III and IV respectively a solution of the postbuckling behavior of compressible slanted column is now presented.

The basic model of a Mises[15] Truss shown in Figure 12a.

Because of symmetry, the structural displacements of such a truss subjected to a vertical load at the central joint may be analyzed by a single slanted column. Hence, one of the pinned-pinned members is isolated as shown in Figure 12b, in which the end B displaces only in the vertical direction.

Figure 12c shows the prismatic compressible slanted column in its postbuckled state. This geometry is used to develop the geometric constraints as well as to define the total Potential Energy, from which after using the variational method, the basic non-linear differential equations are obtained. Finally, the Intermediate Theory is used to solve these equations. Tabulated buckling and postbuckling loads are presented, also these values are plotted in several graphs showing the postbuckling behavior and its relations with the different parameters, such as R, α, $\frac{V}{L}$, $\frac{Ymax}{L}$

(explained later).

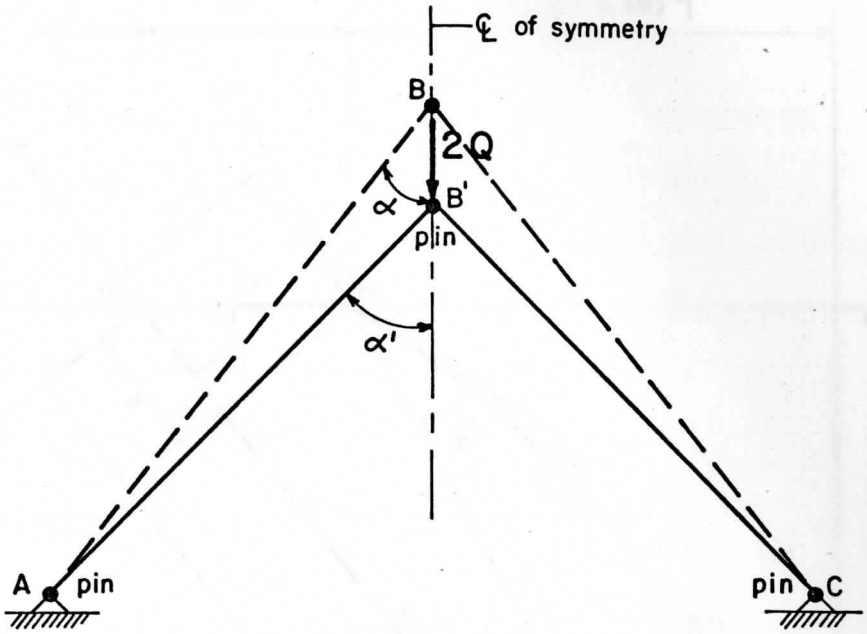

Figure 12a. Basic Truss Model

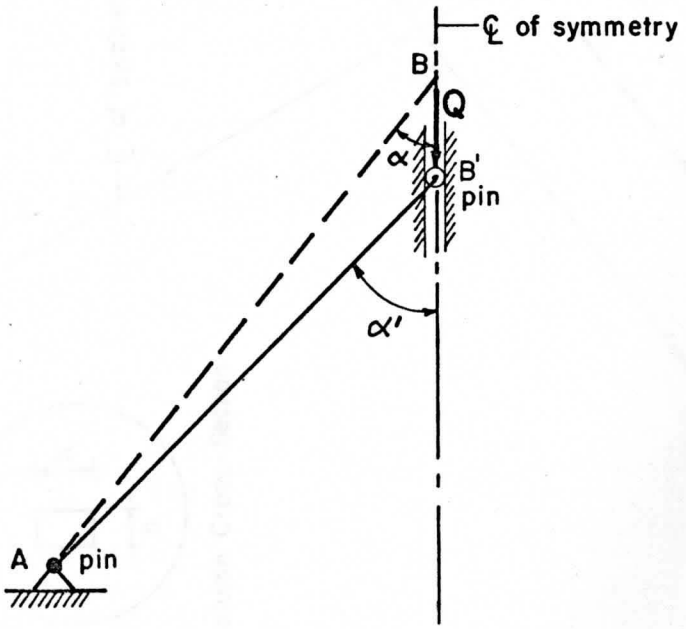

Figure 12b. Slanted Column

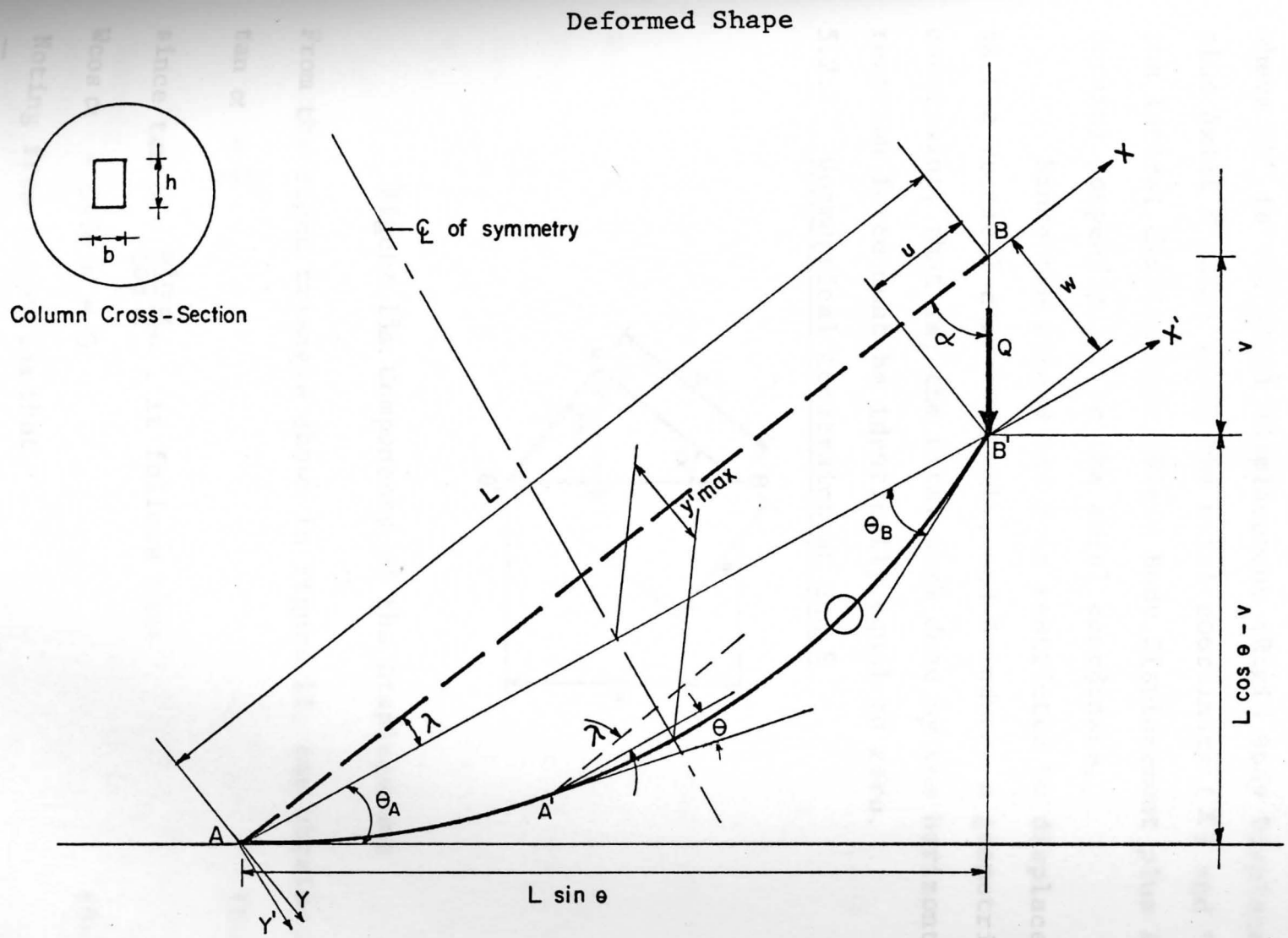

Figure 12c Slanted Compressible Column in Postbuckling State

5.2 Total Potential Energy

Consider the compressible slanted elastic column AB, of length L (see Figure 12c) subjected a compressive force Q, where "U" is the axial displacement (Rigid Body Displacement plus Axial Strain) along the axial coordinate (X) and "W" the lateral displacement (Rigid Body Displacement plus Axial Strain) perpendicular to the axial coordinate.

Since the pinned end B is restricted to displacemnt in the vertical direction only, end B induces a geometrical constraint, that is, the total work done by the horizontal reaction force must be identically equal to zero.

5.2.1 Geometrical Constraint at End B

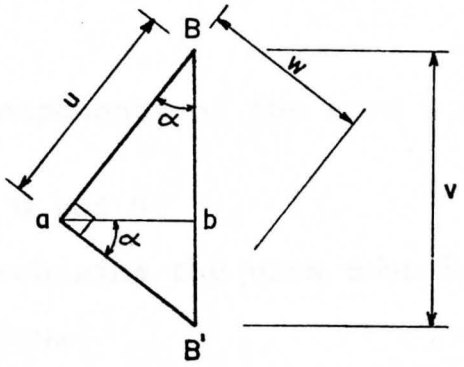

Figure 13a. Components of the Displacement

From the right triangle shown in Figure 11, one obtains,

$$\tan \alpha = \frac{W}{L} \qquad (5\text{-}1a)$$

since $\tan \alpha = \frac{\sin \alpha}{\cos \alpha}$, it follows that

$$W\cos \alpha - U\sin \alpha = 0 \qquad (5\text{-}1b)$$

Noting from Figure 13a that,

$$\overline{ab} = U\sin \alpha = W\cos \alpha \ ,$$

Equation (5-2a) defines zero horizontal displacement. Then defining "H" as the horizontal reaction at end B, it follows that

$$H[\ W\cos\alpha \ - U\sin\alpha\ ] = 0 \qquad (5\text{-}2)$$

5.2.2 Evaluation of the External Work Done

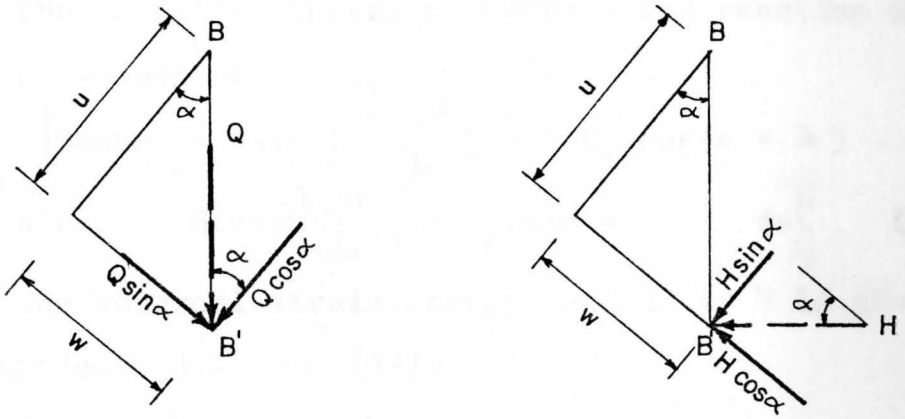

Figure 13b. Components of the Load Q and Reaction H

Work done by Load Q and H:

From Figure 13b one obtains the work done by the Load Q and Reaction H as follows:

$$W_{(x)} = (U)Q\cos\alpha + (U)H\sin\alpha \quad \text{(Work along X)} \qquad (5\text{-}3a)$$

$$W_{(y)} = (W)Q\sin\alpha - (W)H\cos\alpha \quad \text{(Work along Y)} \qquad (5\text{-}3b)$$

Noting total work as $W_T = W_{(x)} + W_{(y)}$, that is,

$$W_T = [Q\cos\alpha + H\sin\alpha\ ]U + [Q\sin\alpha - H\cos\alpha\ ]W \qquad (5\text{-}3c)$$

Evaluation of U and W, using the same procedure employed in Chapter III to evaluate $\triangle$ (see Equations (3-1) and (3-2), Noting from Figure 12c that the tangent at any point A' along the deformed shape of the column makes an angle with the coordinate axis X equal to $(\theta + \lambda)$, it follows,

$$U = L - \int_o^L (1 + \epsilon_o)\cos(\theta + \lambda)\, ds \qquad (5\text{-}4a)$$

or

$$U = -\left[\int_o^L \left[(1 + \epsilon_o)\cos(\theta + \lambda) - 1\right] ds\right] \qquad (5\text{-}4b)$$

and

$$W = \int_o^L (1 + \epsilon_o)\sin(\theta + \lambda)\, ds \qquad (5\text{-}4c)$$

The Potential Energy of force Q and reaction H defined as V becomes

$$-V = -\left[\left[Q\cos\alpha + H\sin\alpha\right]\left[-\int_o^L \left[(1 + \epsilon_o)\cos(\theta + \lambda) - 1\right] ds\right]\right.$$
$$\left.+\left[Q\sin\alpha - H\cos\alpha\right]\left[\int_o^L (1 + \epsilon_o)\sin(\theta + \lambda)\, ds\right]\right] \qquad (5\text{-}5)$$

The internal strain energy defined as U is given as, see Equations (3-4) to (3-7)

$$U = \frac{1}{2}\int_o^L E\left[A\epsilon_o^2 + I\theta_s^2\right] ds \qquad (5\text{-}6)$$

Therefore, combining Equations (5-5) and (5-6), one obtains the expression for the Total Potential Energy as

$$\Pi = U - V$$

$$\Pi = \frac{1}{2}\int_o^L E\left[A\epsilon_o^2 + I\theta_s^2\right] ds + Q\cos\alpha \int_o^L \left[(1 + \epsilon_o)\cos(\theta + \lambda) - 1\right] ds$$
$$- Q\sin\alpha \int_o^L (1 + \epsilon_o)\sin(\theta + \lambda)\, ds$$
$$+ H\sin\alpha \int_o^L \left[(1 + \epsilon_o)\cos(\theta + \lambda) - 1\right] ds$$
$$+ H\cos\alpha \int_o^L (1 + \epsilon_o)\sin(\theta + \lambda)\, ds \qquad (5\text{-}7a)$$

Equation (5-7a) is simplified by algebraic minipulation to,

$$\Pi = \frac{1}{2}\int_o^L E\left[A\epsilon_o^2 + I\theta_s^2\right] ds + Q\int_o^L (1 + \epsilon_o)\cos(\theta + \lambda + \alpha)\, ds$$
$$+ H\int_o^L (1 + \epsilon_o)\sin(\theta + \lambda + \alpha)\, ds - \left[Q\cos\alpha + H\sin\alpha\right]\int_o^L ds \qquad (5\text{-}7b)$$

Note, that α and λ remain constant for a given Q.

5.3 Solution of the Variational Problem

The first variation of the functional Π is computed to satisfy the necessary conditions of equilibrium, that is,

$$\delta^{(1)}\Pi = 0$$

or

$$\delta^{(1)}\Pi = \frac{1}{2}\int_o^L \left[2EA\epsilon_o\,\delta\epsilon_o + 2EI\frac{d}{ds}\frac{d(\delta\theta)}{ds}\right] ds$$

$$+ Q\int_o^L \left[\cos(\theta+\lambda+\alpha)\,\delta\epsilon_o - (1+\epsilon_o)\sin(\theta+\lambda+\alpha)\,\delta\theta\right] ds$$

$$+ H\int_o^L \left[\sin(\theta+\lambda+\alpha)\,\delta\epsilon_o + (1+\epsilon_o)\cos(\theta+\lambda+\alpha)\,\delta\theta\right] ds$$

Integrating by parts the term with second derivative and rearranging terms with common variable one obtains,

$$\delta^{(1)}\Pi = \left[EI\theta_s\,\delta s_s\right]_o^L - \int_o^L \left[EI\theta_{ss} - (1+\epsilon_o)\left(Q\sin(\theta+\lambda+\alpha) - H\cos(\theta+\lambda+\alpha)\right)\right]\delta\theta ds$$

$$+ \int_o^L \left[EA\epsilon_o + Q\cos(\theta+\lambda+\alpha) + H\sin(\theta+\lambda+\alpha)\right]\delta\epsilon_o ds$$

Setting the coefficients of $\delta\epsilon_o$, $\delta\theta$, equal to zero and taking E,A,I as constants on the above $\delta^{(1)}\Pi$ expression it follows that,

$$EA\epsilon_o + Q\cos(\theta+\lambda+\alpha) + H\sin(\theta+\lambda+\alpha) = 0 \qquad (5\text{-}8a)$$

$$EI\theta_{ss} + (1+\epsilon_o)\left[Q\sin(\theta+\lambda+\alpha) - H\cos(\theta+\lambda+\alpha)\right] = 0 \qquad (5\text{-}8b)$$

The boundary conditions at S = 0, L are either $EI\theta_s = M = 0$ or θ is specified. For pinned-pinned conditions $EI\theta_s = M = 0$.

To evaluate the expression for ϵ_o and H Equation (5-8b) is integrated from 0 to L. A quadrature is carried out first, noting

$$\frac{d}{ds}\left[\frac{EI}{2}(\theta_s)^2 + (1+\epsilon_o)\left[-Q\cos(\theta+\lambda+\alpha) - H\sin(\theta+\lambda+\alpha)\right]\right] = 0$$

integration yields

$$\frac{1}{2}\left[EI(\theta_s)\cdot\theta_s\right]_o^L - Q\left[(1+\epsilon_o)\left[\cos(\theta_A+\lambda+\alpha) - \cos(\theta_B+\lambda+\alpha)\right]\right]$$
$$- H\left[(1+\epsilon_o)\left[\sin(\theta_A+\lambda+\alpha) - \sin(\theta_B+\lambda+\alpha)\right]\right] = 0$$

where θ_A and θ_B are the end angles at A and B (see Figure 10), respectively. Because of symmetry $\theta_B = -\theta_A$. Noting that $EI\theta_s \equiv o$ at S = 0,L from boundary conditions, it follows,

$$Q(1+\epsilon_o)\left[-2\sin(\lambda+\alpha)\sin\theta_A\right] + H(1+\epsilon_o)\left[2\sin\theta_A\cos(\lambda+\alpha)\right] = 0$$

or

$$-Q\sin(\lambda+\alpha) + H\cos(\lambda+\alpha) = 0$$

and finally,

$$H = Q\tan(\lambda+\alpha) \qquad (5\text{-}9)$$

Substituting Equation (5-9) into Equation (5-8a) it follows that

$$\epsilon_o = -\frac{Q}{EA}\left[\cos(\theta+\lambda+\alpha) + \frac{\sin(\lambda+\alpha)}{\cos(\lambda+\alpha)}\sin(\theta+\lambda+\alpha)\right]$$

or

$$\epsilon_o = -\frac{Q}{EA}\left[\frac{\cos\theta}{\cos(\lambda+\alpha)}\right] \qquad (5\text{-}10)$$

Substituting Equation (5-9) into Equation (5-8b) one obtains the basic nonlinear differential equation as,

$$EI\theta_{ss} + Q(1 + \epsilon_o)\left[\sin(\theta + \lambda + \alpha) - \frac{\sin(\lambda+\alpha)}{\cos(\lambda+\alpha)}\cos(\theta + \lambda + \alpha)\right] = 0$$

or upon simplification

$$EI\theta_{ss} + Q(1 + \epsilon_o)\left[\frac{\sin\theta}{\cos(\lambda+\alpha)}\right] = 0 \qquad (5\text{-}11)$$

It should be noted that the latter equation simplifies to the results of the vertical column for the condition $\alpha = \lambda = 0$ (see Equation (3-15) Chapter III). If in addition Q is substituted by P and $\epsilon_o = 0$, Equation (5-11) becomes the differential equation for the Classical Elastica Problem.

5.4 Numerical Solution

The numerical technique presented in Chapter IV is utilized to obtain a solution to basic Nonlinear Differential Equation (5-11), that is, the potential energy function is expressed using the power series expansion of the trigonometric functions from which upon applying the Rayleigh-Ritz process, a function that relates $\frac{P}{P_E}$ versus $\frac{Ymax}{L}$ is obtained. Lastly, a geometric constraint function is formulated and the displacement U is evaluated. These three functions are solved simultaneously to find the buckling and postbuckling behavior of the compressible slanted column. The numerical resluts obtained are tabulated in Tables 3a.1 to 3a.31; 4a.1 to 4a.30; and 5. These values are plotted in Figures 18a to 18f; 19a to 19f; 20a to 20e; 21 and 22.

Upon substitution of Equation (5-10) into Equation (5-7b) it follows,

$$\Pi = \frac{1}{2}\int_o^L \left[EA\left[-\frac{Q}{EA}\cdot\frac{\cos\theta}{\cos(\lambda+\alpha)}\right]^2 + EI\theta_s^{\,2}\right] ds$$

$$+ Q\int_o^L\left[1 - \frac{Q}{EA} \times \frac{\cos\theta}{\cos(\lambda+\alpha)}\right]\cos(\theta+\lambda+\alpha)\,ds$$

$$+ H\int_o^L\left[1 - \frac{Q}{EA} \times \frac{\cos\theta}{\cos(\lambda+\alpha)}\right]\sin(\theta+\lambda+\alpha)\,ds$$

$$- \left[Q\cos\alpha + H\sin\alpha\right]\int_o^L ds$$

Substituting Equation (5-9) into the latter expression one obtains,

$$\Pi = \frac{1}{2}\int_o^L\left[\frac{Q^2}{EA} \times \frac{\cos^2\theta}{\cos^2(\lambda+\alpha)} + EI\theta_s{}^2\right]ds$$

$$+ Q\int_o^L\left[1 - \frac{Q}{EA} \times \frac{\cos\theta}{\cos(\lambda+\alpha)}\right]\cos(\theta+\lambda+\alpha)ds - Q\cos\alpha\int_o^L ds$$

$$+ Q\int_o^L\left[1 - \frac{Q}{EA} \times \frac{\cos\theta}{\cos(\lambda+\alpha)}\right]\frac{\sin(\lambda+\alpha)}{\cos(\lambda+\alpha)}\sin(\theta+\lambda+\alpha)ds$$

$$- Q\,\frac{\sin\alpha\sin(\lambda+\alpha)}{\cos(\lambda+\alpha)}\int_o^L ds$$

simplifying

$$\Pi = \frac{Q^2}{2EA}\int_o^L\frac{\cos^2\theta}{\cos^2(\lambda+\alpha)}\,ds + \frac{EI}{2}\int_o^L\theta_s{}^2 ds$$

$$+ Q\int_o^L\left[1 - \frac{Q}{EA} \times \frac{\cos\theta}{\cos(\lambda+\alpha)}\right]\left[\frac{\cos\theta}{\cos(\lambda+\alpha)}\right]ds -$$

$$- Q\int_o^L\frac{\cos\lambda}{\cos(\lambda+\alpha)}\,ds$$

and grouping common terms one obtains

$$\Pi = -\frac{Q^2}{2EA}\int_o^L\frac{\cos^2\theta}{\cos(\lambda+\alpha)}\,ds + \frac{Q}{\cos(\lambda+\alpha)}\int_o^L\left[\cos\theta - \cos\lambda\right]ds$$

$$+\frac{EI}{2}\int_o^L\theta_s{}^2 ds \qquad (5\text{-}12)$$

Substituting Equations (4-1) and (4-2) of Chapter IV into Equation (5-12), the total potential energy is approximated by the expansion

$$\Pi \cong -\frac{Q^2}{2EA\cos(\lambda+\alpha)}\int_o^L\left[1-\frac{a^2}{2}\cos^2\frac{\pi s}{L}-\frac{a^4}{8}\cos^4\frac{\pi s}{L}\right]^2 ds$$

$$+\frac{Q}{\cos(\lambda+\alpha)}\int_o^L\left[\left[1-\frac{a^2}{2}\cos^2\frac{\pi s}{L}-\frac{a^2}{8}\cos^4\frac{\pi s}{L}\right]-\cos\lambda\right]ds$$

$$+\frac{EI\,\pi^2(L)}{4L^2}\left[a^2+\frac{a^4}{4}+\frac{a^6}{32}\right] \qquad (5\text{-}13)$$

The Rayleigh-Ritz method is employed using a similar single coordinate function, to that used on Chapter IV (see Equations (4-4a) to (4-4c)), that is

$$\frac{Y'max}{L} = B\sin\frac{\pi s}{L} \qquad (5\text{-}14a)$$

where Y'max is defined in Figure 12c as the maximum deflection of the column with respect to the auxiliary coordinate axis X'. The next expressions follows with

$$a = \frac{B\pi}{L} \qquad (5\text{-}14b)$$

then

$$\frac{dy'}{ds} = a\cos\frac{\pi s}{L}$$

$$\frac{d^2y'}{ds^2} = -a\frac{\pi}{L}\sin\frac{\pi s}{L} \qquad (5\text{-}14c)$$

This auxiliary coordinate system is used only to carry out the variational process which is independant of the angles λ and α which are constant parameters throughout this process for a given Q. Substituting Equations (5-14b) and (5-14c) into Equation (5-13) and extremizing Π with respect to "a", that is, $\frac{\partial\Pi}{\partial a} = 0$, which is a necessary condition of equilibrium yields

$$\frac{\partial \Pi}{\partial a} = \frac{L}{4}\left[\frac{EI\,\pi^2(L)}{4L^2}\left[2a + a^3\,\frac{3a^5}{16}\right] - \frac{Q}{4\cos(\alpha+\lambda)}\left[2a - \frac{3a^3}{4}\right]\right.$$

$$\left. - \frac{2Q^2}{EA\cos(\alpha+\lambda)}\left[-a + \frac{15a^5}{64} + \frac{35a^7}{1024}\right]\right] = 0$$

Upon simplification and substitution of P_E (Euler Buckling Load for a simple column), the latter expression becomes

$$\frac{Q}{EA} \times \frac{Q}{P_E}\left[2 - \frac{15a^4}{32} - \frac{35a^6}{512}\right] - \left[2 + \frac{3a^2}{4}\right]\frac{Q}{P_E} + \left[2 + a^2 + \frac{3a^4}{16}\right]$$

$$\times \cos(\lambda+\alpha) = 0 \qquad (5\text{-}14)$$

substituting Equation (4-8) into Equation (5-14) gives

$$\left[2 - \frac{15a^4}{32} - \frac{35a^6}{512}\right]R\,\pi^2\left(\frac{Q}{P_E}\right)^2 - \left[2 + \frac{3a^2}{4}\right]\left(\frac{Q}{P_E}\right)$$

$$+ \left[2 + a^2\,\frac{3a^4}{16}\right]\cos(\lambda+\alpha) = 0 \qquad (5\text{-}15a)$$

Equation (5-15a) is compacted in the following algebraic form

$$A(R\,\pi^2)\left(\frac{Q}{P_E}\right)^2 - B\left(\frac{Q}{P_E}\right) + C(\cos(\lambda+\alpha)) = 0 \qquad 5\text{-}15b)$$

where

$$A = \left[2 - \frac{15a^4}{32} - \frac{35a^6}{512}\right] \qquad (5\text{-}16a)$$

$$B = \left[2 + \frac{3a^2}{4}\right] \qquad (5\text{-}16b)$$

$$C = \left[2 + a^2 + \frac{3a^4}{16}\right] \qquad (5\text{-}16c)$$

Using the quadratic formula on Equation (5-15b), one obtains

$$\frac{Q}{P_E} = \frac{B \pm \sqrt{B^2 - 4A\pi^2 R\cos(\lambda+\alpha)C}}{2AR\pi^2} \qquad (5\text{-}17)$$

using Equation (4-10) or Chapter IV, that is,

$$\frac{Ymax}{L} = \frac{a}{\pi}$$

then by analogy, one obtains

$$\frac{Y'max}{L} = \frac{a}{\pi} \qquad (5\text{-}18)$$

with Equation(5-18) substituted into Equation (5-17) the function that relates $\frac{Q}{P_E}$ and $\frac{Y'max}{L}$ is obtained.

In general, as in the case of vertical column presented in Chapter IV, there are four special cases of parameters defined as,

I) $B^2 > 4AR\pi^2\cos(\alpha+\lambda)C$ — $\frac{Q}{P_E}$ has real values

II) $B^2 = 4AR\pi^2\cos(\alpha+\lambda)C$ — $\frac{Q}{P_E}$ repeated value

III) $B^2 < 4AR\pi^2\cos(\alpha+\lambda)C$ — $\frac{Q}{P_E}$ has complex values which have no physical meaning

IV) $R = 0$ — Elastica condition for slanted column.

5.4 Solution of Buckling and Postbuckling Loads

To obtain the buckling and postbuckling loads it is required to find a function that geometrically relates the angles α and λ. This function is derived from the geometric configuration of the slanted column in its postbuckling state shown in Figure 12c.

5.4.1 Evaluation of Geometric Constraints Relating α and λ

From Figure 14 consider triangle AB'C, then

$$\tan(\alpha+\lambda) = \frac{AC}{CB'} = \frac{L\sin\alpha}{L\cos\alpha - V} \qquad (5\text{-}18a)$$

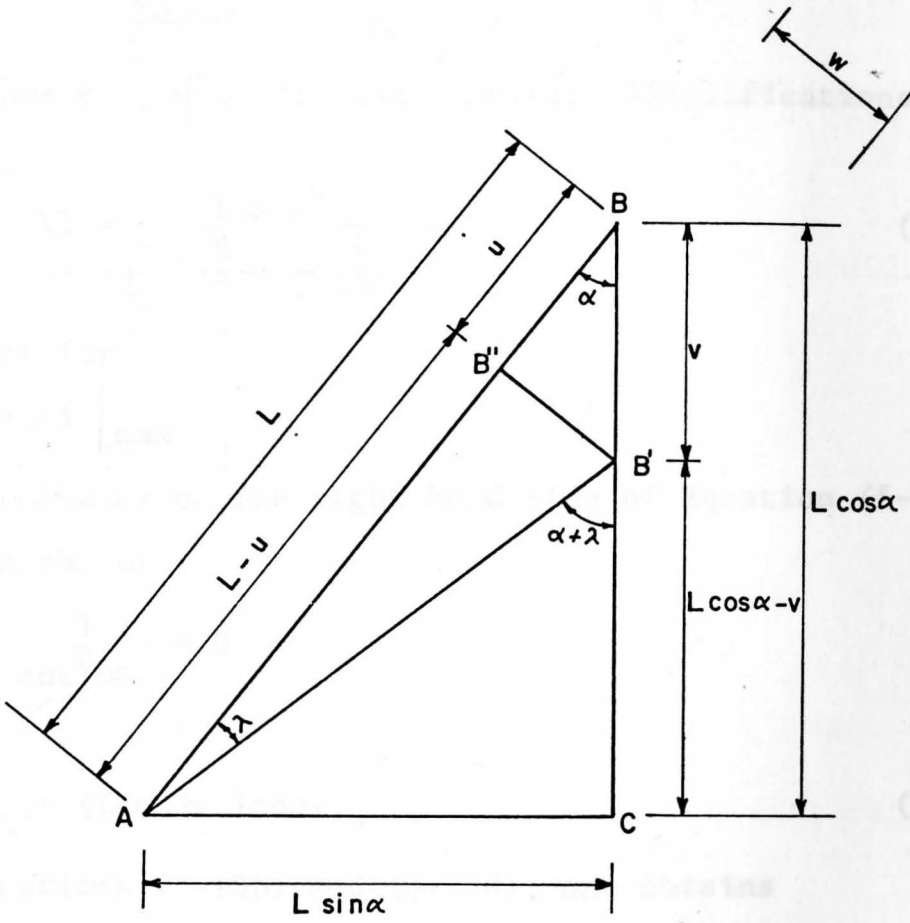

Figure 14. Geometric Parameters of a Slanted Column in Postbuckling State

From triangle BB'B"

$$V = \frac{U}{\cos\alpha} \qquad (5\text{-}18b)$$

substituting Equation (5-18b) into Equation (5-18a), yields

$$\tan(\alpha+\lambda) = \frac{L\sin\alpha}{\left[L\cos\alpha - \frac{U}{\cos\alpha}\right]}$$

which upon trigonometric and algebraic simplifications becomes,

$$\tan(\alpha+\lambda) = \frac{\tan\lambda}{\left[1 - \frac{U}{L} \times \frac{1}{\cos^2\alpha}\right]}. \qquad (5\text{-}18c)$$

note that for

$$\tan(\alpha+\lambda)\Big|_{max}$$

the denominator on the right hand side of Equation (5-18c) must vanish or

$$1 - \frac{U}{L} \times \frac{1}{\cos^2\alpha} = 0$$

hence

$$U_{max} = (L\cos\alpha)\cos\alpha \qquad (5\text{-}18d)$$

From Equations (5-18b) and (5-18d), one obtains

$$V_{max} = L\cos\alpha \qquad (5\text{-}18e)$$

which is an obvious geometric constraint observed in Figure 14. It is required now to evaluate a function that defines $\frac{U}{L}$, to be used in Equation (5-18c) in order to obtain a value of the $\tan(\alpha+\lambda)$. The derivation of the value of $\frac{U}{L}$ is presented in the next section.

5.4.2 Evaluation of Parameter U/L

From Equation (5-4b), that is,

$$U = -\int_o^L \left[(1 + \epsilon_o)\cos(\theta + \lambda) - 1\right] ds$$

substituting Equation (5-10) into the latter equation, one obtains

$$U = -\int_o^L \left[\left[1 - \frac{Q}{EA} \times \frac{\cos\theta}{\cos(\alpha + \lambda)}\right]\cos(\theta + \lambda) - 1\right] ds$$

then, upon trigonometric and algebraic operations it becomes.

$$U = \int_o^L \left[1 - \left[\cos\theta\cos\lambda - \sin\theta\sin\lambda - \frac{Q}{EA} \times \frac{1}{\cos(\alpha + \lambda)}\left[\cos^2\theta\cos\lambda - \cos\theta\sin\theta\sin\lambda\right]\right]\right] ds$$

then, upon substitution of Equations (4-1)and (5-14c) it follows that,

$$U = \int_o^L \left[1 - \left[\left[1 - \frac{a^2}{2}\cos^2\frac{\pi s}{L} - \frac{a^4}{8}\cos^4\frac{\pi s}{L}\right]\cos\lambda - a\cos\frac{\pi s}{L}\sin\lambda - \frac{Q}{EA} \times \frac{1}{\cos(\alpha+\lambda)}\left[\left[1 - \frac{a^2}{2}\cos^2\frac{\pi s}{L} - \frac{a^4}{8}\cos^4\frac{\pi s}{L}\right]^2\cos\lambda + \left[a\cos\frac{\pi s}{L} - \frac{a^3}{2}\cos^3\frac{\pi s}{L} - \frac{a^5}{8}\cos^5\frac{\pi s}{L}\right]\sin\lambda\right]\right]\right] ds$$

after integration and some algebraic simplifications, one obtains

$$U = \frac{L}{4}\left[4 - \left[4 - a^2 - \frac{3a^4}{16}\right]\cos\lambda + \frac{4Q\cos\lambda}{EA\cos(\alpha+\lambda)}\left[1 - \frac{a^2}{2} + \frac{5a^6}{128} + \frac{35a^8}{8192}\right]\right] \qquad (5\text{-}19)$$

For the axial compression mode only a = 0, that is $\frac{Y'max}{L} = 0$, and Equation (5-19) becomes

$$U = L\left[1 - \cos\lambda + \frac{Q\cos\lambda}{EA\cos(\alpha+\lambda)}\right] \qquad (5\text{-}20)$$

5.4.3 Solution of the Three Simultaneous Nonlinear Equations

Equations (5-17), (5-18c), and (5-19) are solved simultaneously to obtain a transient solution utilizing an iterative process illustrated by the flow diagram shown on Figure 15. The summary of equations used in flow diagram is:

Equation (5-17) $$\frac{Q}{P_E} = \frac{B \pm \sqrt{B^2 - 4A\pi^2 R \cos(\alpha + \lambda) C}}{2AR\pi^2}$$

Equation (5-18b) $$V = \frac{U}{\cos \alpha}$$

Equation (5-18c) $$\tan(\alpha + \lambda) = \frac{\tan \alpha}{\left(1 - \frac{U}{L} \times \frac{1}{\cos^2 \alpha}\right)}$$

Equation (5-19) $$U = \frac{L}{4}\left[4 - \left[4 - a^2 - \frac{3a^4}{16}\right]\cos\lambda + \frac{4Q\cos\lambda}{EA\cos(\alpha+\lambda)}\left[1 - \frac{a^2}{2} + \frac{5a^6}{128} + \frac{35a^8}{8192}\right]\right]$$

The numerical results obtained upon the solution of these equations are tabulated in Tables 3a.1 to 3a.31 for various values of angles α and the parameters $\frac{Y'max}{L}$ and $\frac{Q}{P_E}$ * represents the higher mode of postbuckling and $\frac{Q}{P_E}$ ** represents the lower mode of postbuckling. λ is the angle defined in Figure 12c, $\frac{U}{L}$ and $\frac{V}{L}$ are dimensionless expressions of U and V defined in Figure 12c and by Equations (5-4b) and (5-4c). These results are also plotted in Figures 18a to 18f and Figures 20a to 20e.

5.4.4 Q/P_E versus V/L

The bifurcation points are clearly defined by the graphs that relate $\frac{Q}{P_E}$ and $\frac{V}{L}$. Several graphs are presented

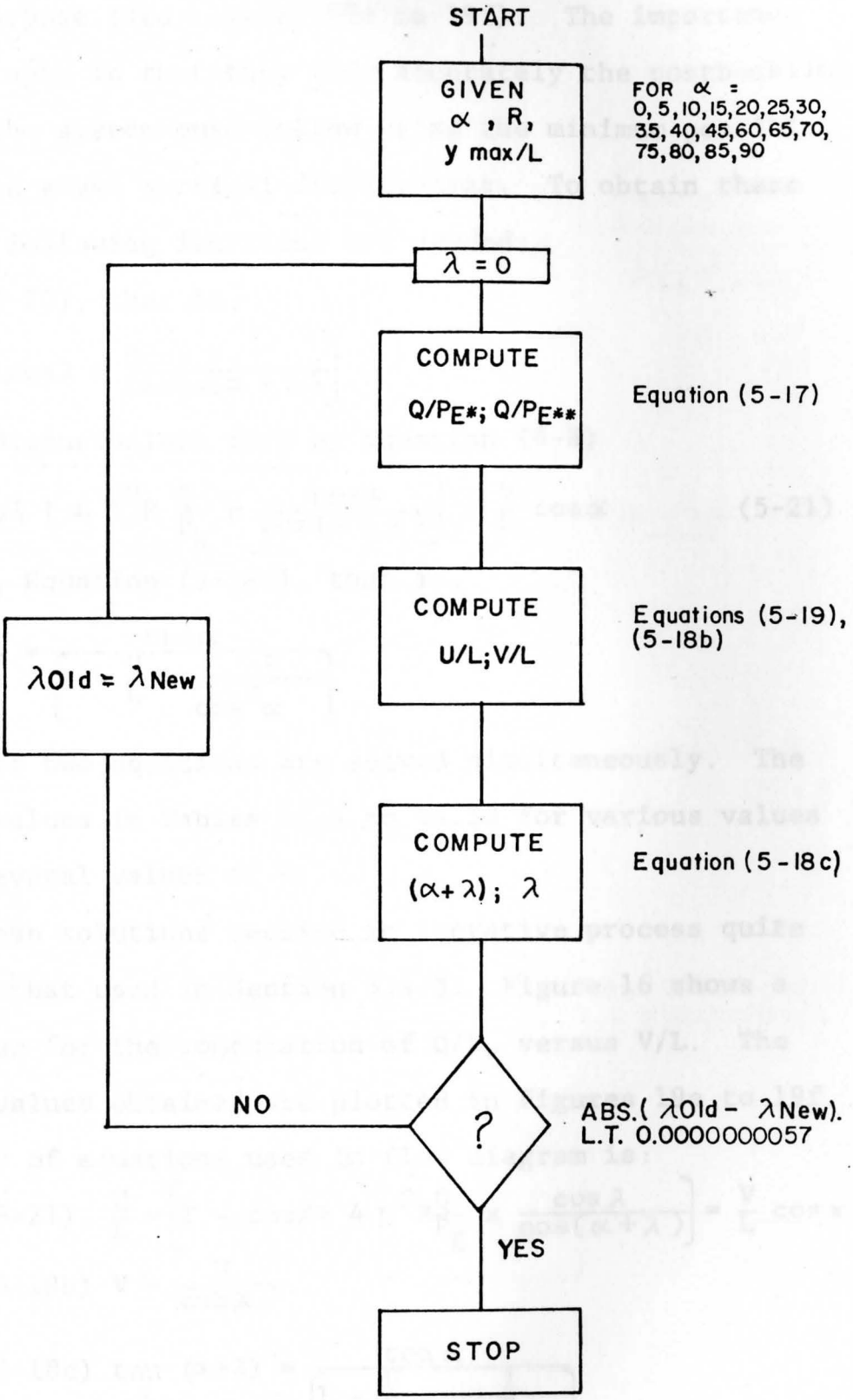

Figure 15 Flow Diagram for Q/P_E vs. Y'max/L

for this purpose (see Figures 19a to 19f). The importance of these graphs is that they show accurately the postbuckling path that the system must follow using the minimum possible energy for a given vertical displacement. To obtain these values the following functions are needed:

Equation (5-20), that is,

$$U = L\left[1 - \cos\lambda + \frac{Q\cos\lambda}{EA\cos(\alpha+\lambda)}\right]$$

or in its dimensionless form by Equation (4-8)

$$\frac{U}{L} = \left[1 - \cos\lambda + 4\pi^2 R\,\frac{Q}{P_E} \times \frac{\cos\lambda}{\cos(\alpha+\lambda)}\right] = \frac{V}{L}\cos\alpha \qquad (5\text{-}21)$$

and lastly, Equation (5-18c), that is,

$$\tan(\alpha+\lambda) = \frac{\tan\alpha}{\left[1 - \frac{U}{L} \times \frac{1}{\cos^2\alpha}\right]}$$

these latter two equations are solved simultaneously. The tabulated values in Tables 41.a to 4a.30 for various values of α and several values of R.

These solutions require in iterative process quite similar to that used in Section 5.4.3. Figure 16 shows a flow diagram for the computation of Q/P_E versus V/L. The numerical values obtained are plotted in Figures 19a to 19f. The summary of equations used in flow diagram is:

Equation (5-21) $\frac{U}{L} = \left[1 - \cos\lambda + 4\pi^2 R\frac{Q}{P_E} \times \frac{\cos\lambda}{\cos(\alpha+\lambda)}\right] = \frac{V}{L}\cos\alpha$

Equation (5-18b) $V = \frac{U}{\cos\alpha}$

Equation (5-18c) $\tan(\alpha+\lambda) = \frac{\tan\alpha}{\left[1 - \frac{U}{L} \times \frac{1}{\cos^2\alpha}\right]}$

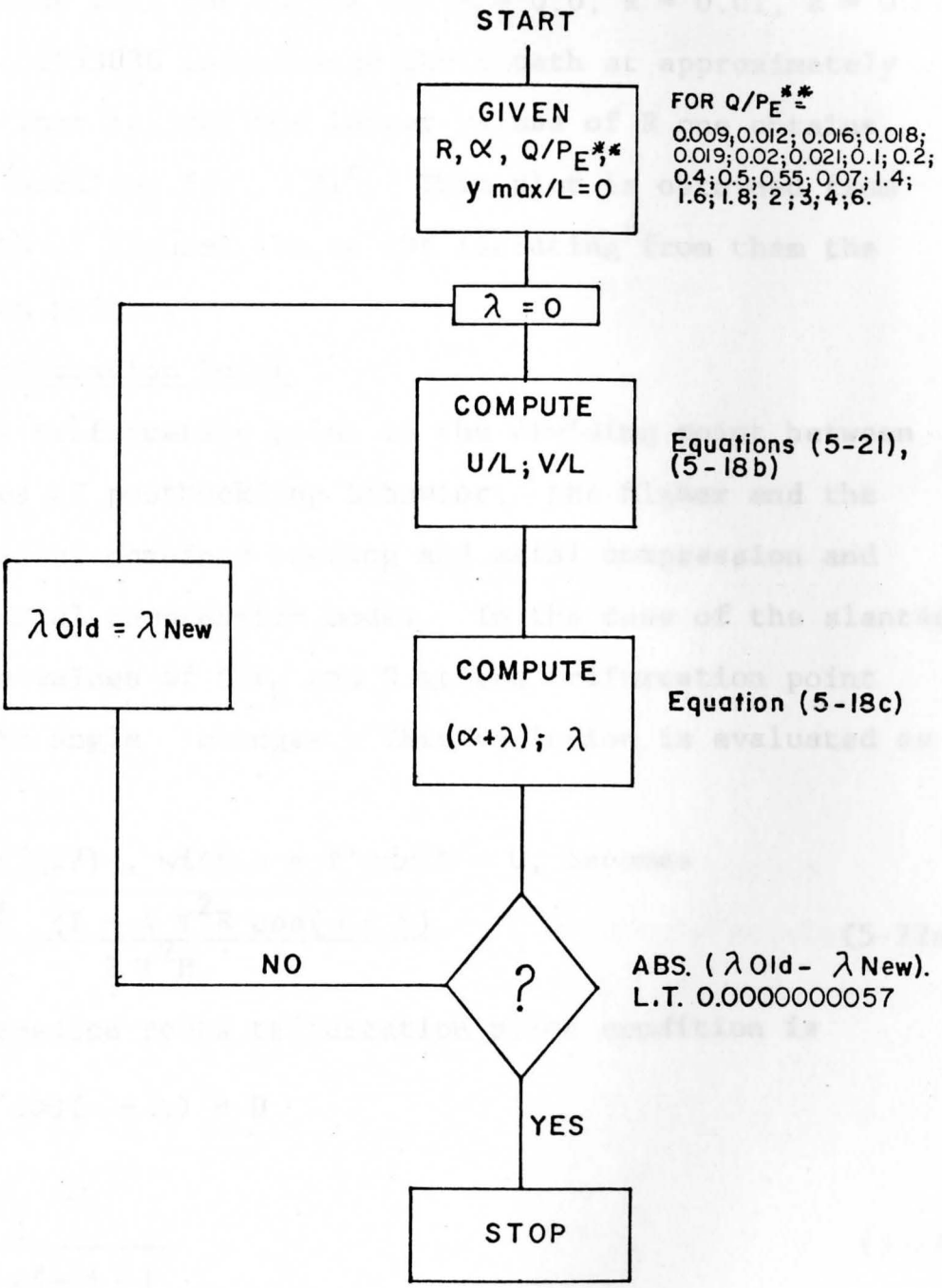

Figure 16 Flow Diagram for Q/P_E vs. V/L

Figure 21 illustrates the path that the bifurcation point follows for a range of the parameter . The graph clearly shows that the curves for R = 0.0, R = 0.01, R = 0.02, and R = 0.02533030 interchange their path at approximately = 31°. That is, for the larger values of R one obtains a smaller buckling for 31°. This plot is obtained from the results of Figures 19a to 19f isolating from them the bifurcation points.

5.5 Trifurcation Point

The trifurcation point is the dividing point between three modes of postbuckling behavior, the higher and the lower modes of combined bending and axial compression and the pure axial compression modes. In the case of the slanted column the values of Q/P_E and R at the trifurcation point vary as the angle changes. This variation is evaluated as follows:

Equation (5-17) , with a = Y'max/L = 0, becomes

$$\frac{Q}{P_E} = \frac{1 \pm \sqrt{1 = 4\pi^2 R \cos(\alpha+\lambda)}}{2\pi^2 R} \qquad (5\text{-}22a)$$

and for repeated roots trifurcation point condition is

$$1 - 4\pi R^2 \cos(\alpha+\lambda) = 0$$

or

$$R = \frac{1}{4\pi^2 \cos(\alpha+\lambda)} \qquad (5\text{-}22b)$$

Equation (5-22a) reduces to

$$\frac{Q}{P_E} = \frac{1}{2\pi^2 R} \qquad (5\text{-}22c)$$

Equation (5-21) reduces to

$$\frac{U}{L} = \left[1 - \cos\lambda + \frac{1}{2} \times \frac{\cos\lambda}{\cos(\alpha + \lambda)}\right] = \frac{V}{L}\cos\alpha \qquad (5\text{-}23)$$

Solving simultaneously the four Equations (5-22b), (5-22c), (5-23), and (5-18c) using an iterative process as done previously one obtains, the values of Q/P_E and R as α varies. The corresponding flow diagram is presented in Figure 17. The summary of equations used in flow diagram is:

Equation (5-22b) $$R = \frac{1}{4\pi^2\cos(\alpha + \lambda)}$$

Equation (5-22c) $$\frac{Q}{P_E} = \frac{1}{2\pi^2 R}$$

Equation (5-23) $$\frac{U}{L} = 1 - \cos + \frac{1}{2}\frac{\cos\lambda}{\cos(\alpha + \lambda)} = \frac{V}{L}\cos$$

Equation (5-18b) $$V = \frac{U}{\cos\alpha}$$

Equation (5-18c) $$\tan(\alpha + \lambda) = \frac{\tan\alpha}{1 - \frac{U}{L} \times \frac{1}{\cos^2\alpha}}$$

Finally, the numerical results are tabulated in Table 5. The limit of the angle α is determined as approximately $\alpha_{limit} = 13.01$. For values of $\alpha > \alpha$ limit the trifurcation point no longer exists.

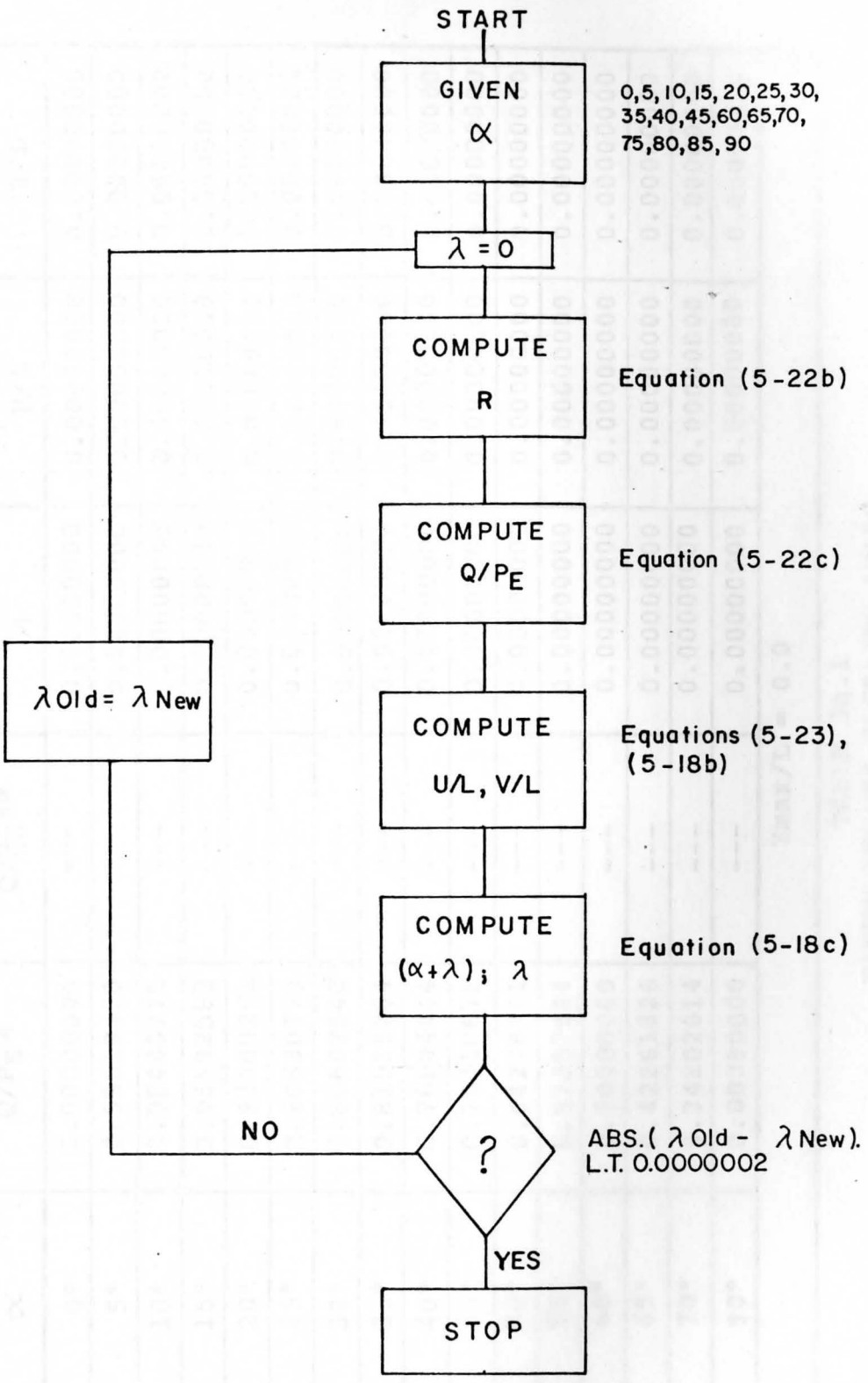

Figure 17 Flow Diagram for "R" Trifurcation

R = 0.00					
α	Q/P_E*	Q/P_E**	λ	U/L	V/L
0°	1.00000000	---	0.00000000	0.00000000	0.00000000
5°	0.99619470	---	0.00000000	0.00000000	0.00000000
10°	0.98480775	---	0.00000000	0.00000000	0.00000000
15°	0.96592583	---	0.00000000	0.00000000	0.00000000
20°	0.93969262	---	0.00000000	0.00000000	0.00000000
25°	0.90630779	---	0.00000000	0.00000000	0.00000000
30°	0.86602540	---	0.00000000	0.00000000	0.00000000
35°	0.81915204	---	0.00000000	0.00000000	0.00000000
40°	0.76604444	---	0.00000000	0.00000000	0.00000000
45°	0.70710678	---	0.00000000	0.00000000	0.00000000
50°	0.64278761	---	0.00000000	0.00000000	0.00000000
55°	0.57357644	---	0.00000000	0.00000000	0.00000000
60°	0.50000000	---	0.00000000	0.00000000	0.00000000
65°	0.42261826	---	0.00000000	0.00000000	0.00000000
70°	0.34202014	---	0.00000000	0.00000000	0.00000000
90°	0.00000000	---	0.00000000	0.00000000	0.00000000
Ymax/L = 0.0					

TABLE 3a.1
DIMENSIONLESS BUCKLING LOADS

R = 0.000					
α	Q/P_E^*	Q/P_E **	λ	U/L	V/L
0°	1.00311253	---	0.00000000	0.00619704	0.00619704
5°	0.99924754	---	0.03125855	0.00619719	0.00622086
10°	0.98768085	---	0.06300393	0.00619764	0.00629325
15°	0.96849705	---	0.09575393	0.00619843	0.00641709
20°	0.94183602	---	0.13009255	0.00619960	0.00659748
25°	0.90789132	---	0.16671496	0.00620125	0.00684232
30°	0.86690772	---	0.20649002	0.00620349	0.00716318
35°	0.81917778	---	0.25055338	0.00620654	0.00757679
40°	0.76503701	---	0.30045452	0.00621070	0.00810750
45°	0.70485690	---	0.35840162	0.00621648	0.00879144
50°	0.63903433	---	0.42769410	0.00622473	0.00968396
55°	0.56797381	---	0.51353996	0.00623696	0.01087381
60°	0.49205437	---	0.62473586	0.00625612	0.01251223
65°	0.41155783	---	0.77752317	0.00628855	0.01487997
70°	0.32648339	---	1.00592651	0.00635020	0.01856675
83.61000000	0.00562058	---	6.06896221	0.01176695	0.10572707
Ymax/L = 0.5					

TABLE 3a.2
DIMENSIONLESS POSTBUCKLING LOADS

R = 0.000					
α	Q/P_E^*	Q/P_E^{**}	λ	U/L	V/L
0°	1.01277731	---	0.00000000	0.02513062	0.02513062
5°	1.00872173	---	0.12923327	0.02513310	0.02522910
10°	0.99658093	---	0.26053960	0.02514070	0.02552853
15°	0.97643212	---	0.39612998	0.02515392	0.02604125
20°	0.94840173	---	0.53851162	0.02517367	0.02678926
25°	0.91266170	---	0.69069256	0.02520145	0.02780672
30°	0.86942355	---	0.85647174	0.02523953	0.02914410
35°	0.81892910	---	1.04088112	0.02529148	0.03087520
40°	0.76143577	---	1.25090376	0.02536294	0.03310897
45°	0.69719203	---	1.49671419	0.02546322	0.03601043
50°	0.62639366	---	1.79397664	0.02560844	0.03983966
55°	0.54909796	---	2.16848444	0.02582874	0.04503103
60°	0.46503348	---	2.66665925	0.02618629	0.05237257
65°	0.37309794	---	3.38358659	0.02683003	0.06348526
70°	0.26960639	---	4.56143305	0.02821838	0.08250503
77.12000000	0.00798763	---	12.42811188	0.04797492	0.21522119
Ymax/L = 0.10					

TABLE 3a.3
DIMENSIONLESS POSTBUCKLING LOADS

R = 0.000					
α	Q/P_E^*	Q/P_E^{**}	λ	U/L	V/L
0°	1.02989213	---	0.00000000	0.05782809	0.05782809
5°	1.02547616	---	0.30774233	0.05784168	0.05806262
10°	1.01224891	---	0.62068831	0.05788337	0.05877632
15°	0.99027078	---	0.94441653	0.05795608	0.06000055
20°	0.95963730	---	1.28531716	0.05806515	0.06179164
25°	0.92047019	---	1.65117119	0.05821930	0.06423789
30°	0.87290238	---	2.05200025	0.05843226	0.06747177
35°	0.81705283	---	2.50141937	0.05872585	0.07169102
40°	0.75298303	---	3.01895383	0.05913567	0.07719613
45°	0.68061688	---	3.63433018	0.05972286	0.08446089
50°	0.59957922	---	4.39621268	0.06060013	0.09427706
55°	0.50882546	---	5.39241003	0.06199774	0.10808977
60°	0.40561078	---	6.80646952	0.06446839	0.12893678
65°	0.28144857	---	9.14048067	0.06979196	0.16514184
70°	0.07466542	---	15.84250634	0.09361580	0.27371429
70.41500000	0.00774954	---	19.15386722	0.10998592	0.32811545
Ymax/L = 0.15					

TABLE 3a.4
DIMENSIONLESS POSTBUCKLING LOADS

R = 0.000					
α	Q/P_E^*	Q/P_E^{**}	λ	U/L	V/L
0°	1.05571161	---	0.00000000	0.10600173	0.10600173
5°	1.05068275	---	0.59464214	0.10604987	0.10645497
10°	1.03560505	---	1.20019619	0.10619786	0.10783613
15°	1.01050161	---	1.82846234	0.10645692	0.11021231
20°	0.97539837	---	2.49318911	0.10684798	0.11370525
25°	0.93030178	---	3.21154099	0.10740575	0.11850913
30°	0.87515886	---	4.00637869	0.10818641	0.12492290
35°	0.80978510	---	4.91015700	0.10928258	0.13340939
40°	0.73372672	---	5.97224304	0.11085398	0.14470959
45°	0.64597141	---	7.27425844	0.11319713	0.16008492
50°	0.54424556	---	8.96745735	0.11692904	0.18190929
55°	0.42285485	---	11.38805188	0.12360243	0.21549426
60°	0.26202118	---	15.62933820	0.13905754	0.27811509
63.37555000	0.00936675	---	26.11600893	0.19727537	0.44020865
Ymax/L = 0.20					

TABLE 3a.5
DIMENSIONLESS POSTBUCKLING LOADS

R = 0.000					
α	Q/P_E^*	Q/P_E^{**}	λ	U/L	V/L
0°	1.09159168	---	0.00000000	0.17204871	0.17204871
5°	1.08552682	---	1.04253544	0.17218576	0.17284348
10°	1.06731341	---	2.10666824	0.17260830	0.17527106
15°	1.03688577	---	3.21609576	0.17335269	0.17946791
20°	0.99410081	---	4.39922462	0.17448802	0.18568628
25°	0.93867522	---	5.69304605	0.17613248	0.19434069
30°	0.87006395	---	7.14974673	0.17848665	0.20609863
35°	0.78721501	---	8.84945584	0.18190467	0.22206460
40°	0.68802010	---	10.92842596	0.18706379	0.24419443
45°	0.56784695	---	13.65427281	0.19544841	0.27640579
50°	0.41416020	---	17.70289250	0.21125540	0.32865506
55°	0.15872256	---	26.63928462	0.25993820	0.45318842
55.88750000	0.00618641	---	33.78778434	0.31188715	0.55612737
Ymax/L = 0.25					

TABLE 3a.6
DIMENSIONLESS POSTBUCKLING LOADS

R = 0.01					
α	Q/P_E*	Q/P_E**	λ	U/L	V/L
0°	9.00723125	1.12488711	0.00000000	0.11102191	0.11102191
5°	9.01342203	1.11870039	0.62585338	0.11099869	0.11142269
10°	9.03190258	1.10021984	1.26037888	0.11093380	0.11264513
15°	9.06244670	1.06967572	1.91309364	0.11084136	0.11475142
20°	9.10469722	1.02742519	2.59534899	0.11074651	0.11785397
25°	9.15821078	0.97391163	3.32166279	0.11068821	0.12213092
30°	9.22251771	0.90960470	4.11173783	0.11072506	0.12785428
35°	9.29720989	0.83491253	4.99384129	0.11094680	0.13544102
40°	9.38207960	0.75004281	6.01103171	0.11149839	0.14555079
45°	9.47737255	0.65474987	7.23393141	0.11263431	0.15928894
50°	9.58434430	0.54777811	8.79088187	0.11485843	0.17868795
55°	9.70683452	0.42528789	10.95609526	0.11936934	0.20811404
60°	9.85805491	0.27406751	14.53474879	0.13019774	0.26039540
64.32000000	10.12605705	0.00606131	25.33291801	0.18542165	0.42788506
Ymax/L = 0.00					

TABLE 3a.7
DIMENSIONLESS BUCKLING LOADS

R = 0.01					
α	Q/P_E*	Q/P_E**	λ	U/L	V/L
0°	9.09994531	1.12738763	0.00000000	0.11609308	0.11609308
5°	9.10621422	1.12112277	0.65823626	0.11607576	0.11651915
10°	9.12493024	1.10240675	1.32584263	0.11602890	0.11781883
15°	9.15587068	1.07146631	2.01310067	0.11596776	0.12005866
20°	9.19868525	1.02865175	2.73227447	0.11591962	0.12335908
25°	9.25294270	0.97439429	3.49906299	0.11592712	0.12791142
30°	9.31819426	0.90914274	4.33481775	0.11605500	0.13400876
35°	9.39406812	0.83326887	5.27029050	0.11640359	0.14210254
40°	9.48042228	0.74691472	6.35261648	0.11713711	0.15291162
45°	9.57762972	0.64970728	7.65985647	0.11854817	0.16765240
50°	9.68722488	0.54011211	9.33611165	0.12122750	0.18859647
55°	9.81381087	0.41352612	11.69819744	0.12662464	0.22076326
60°	9.97405936	0.25327763	15.74495762	0.13998825	0.27997640
63.63000000	10.22111887	0.00621408	26.01527780	0.19481979	0.43861920
Ymax/L = 0.05					

TABLE 3a.8
DIMENSIONLESS POSTBUCKLING LOADS

R = 0.01					
α	Q/P_E*	Q/P_E**	λ	U/L	V/L
0°	9.39638275	1.13512538	0.00000000	0.13163868	0.13163868
5°	9.40290016	1.12861201	0.75987408	0.13164122	0.13214406
10°	9.42236546	1.10914671	1.53138306	0.13165522	0.13368621
15°	9.45456827	1.07694390	2.32729844	0.13169999	0.13634586
20°	9.49918245	1.03232972	3.16288001	0.13181055	0.14026986
25°	9.55581928	0.97569286	4.05774517	0.13204283	0.14569314
30°	9.62410351	0.90740867	5.03879383	0.13248408	0.15297943
35°	9.70379245	0.82771972	6.14529457	0.13327388	0.16269735
40°	9.79498126	0.73653091	7.43870750	0.13464908	0.17577187
45°	9.89851595	0.63299622	9.02417192	0.13705094	0.19381926
50°	10.01702016	0.51449201	11.10645531	0.14142676	0.22002094
55°	10.15839549	0.37311668	14.18467769	0.15036829	0.26215904
60°	10.36019927	0.17131290	20.42143947	0.17692808	0.35385602
61.61500000	10.52561373	0.00589440	28.05172118	0.22356652	0.47027637
Ymax/L = 0.10					

TABLE 3a.9
DIMENSIONLESS POSTBUCKLING LOADS

R = 0.01					
α	Q/P_E*	Q/P_E**	λ	U/L	V/L
0°	9.95974422	1.14867100	0.00000000	0.15865931	0.15865931
5°	9.96672716	1.14169205	0.94552161	0.15870321	0.15930943
10°	9.98759784	1.12082138	1.90711156	0.15884426	0.16129469
15°	10.02217386	1.08624536	2.90245709	0.15911128	0.16472412
20°	10.07018393	1.03823529	3.95282885	0.15955753	0.16979757
25°	10.13133639	0.97708283	5.08589229	0.16027067	0.17683911
30°	10.20542542	0.90299380	6.34029925	0.16139280	0.18636034
35°	10.29251242	0.81590679	7.77410182	0.16316195	0.19918395
40°	10.39327356	0.71514566	9.48215008	0.16600608	0.21670553
45°	10.50979552	0.59862370	11.63808139	0.17078736	0.24152977
50°	10.64794440	0.46047482	14.62280094	0.17960547	0.27941645
55°	10.82884700	0.27957222	19.65529423	0.20006043	0.34879462
58.39500000	11.10074866	0.00766656	31.17877795	0.27131881	0.51772447
Ymax/L = 0.15					

TABLE 3a.10
DIMENSIONLESS POSTBUCKLING LOADS

R = 0.01					
α	Q/P_E*	Q/P_E**	λ	U/L	V/L
0°	10.93096899	1.16857216	0.00000000	0.19885844	0.19885844
5°	10.93873133	1.16081364	1.24502079	0.19898165	0.19974172
10°	10.96195979	1.13758518	2.51410284	0.19936726	0.20244282
15°	11.00053397	1.09901101	3.83392614	0.20006541	0.20712295
20°	11.05430462	1.04524035	5.23706832	0.20117101	0.21408171
25°	11.12319846	0.97634651	6.76695260	0.20284587	0.22381565
30°	11.20740044	0.89214453	8.48650210	0.20536512	0.23713520
35°	11.30770618	0.79183879	10.49545000	0.20922005	0.25541050
40°	11.42631199	0.67323298	12.97075608	0.21537698	0.28115464
45°	11.56906077	0.53048420	16.28463549	0.22608372	0.31973061
50°	11.75526726	0.34427772	21.52865458	0.24869369	0.38689861
54.10000000	12.09240311	0.00713805	35.51282793	0.34062281	0.58089848
Ymax/L = 0.20					

TABLE 3a.11
DIMENSIONLESS POSTBUCKLING LOADS

R = 0.01					
α	Q/P_E^*	Q/P_E^{**}	λ	U/L	V/L
0°	12.62421783	1.19491354	0.00000000	0.25476259	0.25476259
5°	12.63326959	1.18586503	1.71559130	0.25503733	0.25601153
10°	12.66041279	1.15872183	3.47002423	0.25589279	0.25984035
15°	12.70567334	1.11346127	5.30701381	0.25742906	0.26651017
20°	12.76919481	1.04993980	7.28155985	0.25984111	0.27651713
25°	12.85144374	0.96769087	9.47046700	0.26347716	0.29071487
30°	12.95362567	0.86550894	11.99291649	0.26897110	0.31058105
35°	13.07864704	0.74048757	15.05839434	0.27757753	0.33885957
40°	13.23390894	0.58522567	19.10839099	0.29222323	0.38147029
45°	13.44399773	0.37513688	25.46812928	0.32262767	0.45626435
48.79500000	13.81449806	0.00463331	40.96188647	0.43185532	0.65556275
Ymax/L = 0.25					

TABLE 3a.12
DIMENSIONLESS POSTBUCKLING LOADS

R = 0.02					
α	Q/P_E*	Q/P_E**	λ	U/L	V/L
0°	3.69500193	1.37105725	0.00000000	0.27063585	0.27063585
5°	3.69500428	1.37105692	1.85233573	0.26988915	0.27092009
10°	3.75536813	1.31069308	3.69008094	0.26780663	0.27193798
15°	3.82585189	1.24020932	5.51232030	0.26479539	0.27413637
20°	3.91724675	1.14881446	7.33942318	0.26138298	0.27815795
25°	4.02533991	1.04072130	9.21577513	0.25812738	0.28481204
30°	4.14712112	0.91894009	11.21415677	0.25562011	0.29516466
35°	4.28119966	0.78486155	13.45053183	0.25460145	0.31081095
40°	4.42845745	0.63760376	16.12684671	0.25627723	0.33454612
45°	4.59424866	0.47181254	19.66744537	0.26330344	0.37236723
50°	4.79975779	0.26630342	25.38607071	0.28478649	0.44304904
53.37000000	5.06349175	0.00256743	36.48297136	0.35475674	0.59458581
Ymax/L = 0.00					

TABLE 3a.13
DIMENSIONLESS BUCKLING LOADS

R = 0.02					
α	Q/P_E*	Q/P_E**	λ	U/L	V/L
0°	3.74334632	1.37032015	0.00000000	0.27335051	0.27335051
5°	3.75880564	1.35486285	1.87830032	0.27264277	0.27368422
10°	3.80370751	1.30996098	3.74404272	0.27067097	0.27484850
15°	3.87430981	1.23935869	5.59801554	0.26782853	0.27727649
20°	3.96603147	1.14763703	7.46207165	0.26463134	0.28161479
25°	4.07473448	1.03893402	9.38239738	0.26163513	0.28868242
30°	4.19747481	0.91619369	11.43476493	0.25944386	0.29957995
35°	4.33295969	0.78070881	13.74095506	0.25883469	0.31597879
40°	4.48229104	0.63137745	16.51585132	0.26110619	0.34084989
45°	4.65147973	0.46218877	20.22158550	0.26919613	0.38070076
50°	4.86517043	0.24849807	26.36778961	0.29375784	0.45700598
52.95500000	5.11170481	0.00196166	36.93299683	0.36199649	0.60088181
Ymax/L = 0.05					

TABLE 3a.14
DIMENSIONLESS POSTBUCKLING LOADS

R = 0.02					
α	Q/P_E^*	Q/P_E^{**}	λ	U/L	V/L
0°	3.89739481	1.36835926	0.00000000	0.28191510	0.28191510
5°	3.91284833	1.35290776	1.96143877	0.28132226	0.28239687
10°	3.95784887	1.30790721	3.91649861	0.27967898	0.28399347
15°	4.02892491	1.23683117	5.87132380	0.27734293	0.28712653
20°	4.12178074	1.14397535	7.85268031	0.27480080	0.29243690
25°	4.23251310	1.03324298	9.91290310	0.27260775	0.30078936
30°	4.35840291	0.90735318	12.13805110	0.27141458	0.31340266
35°	4.49850765	0.76724843	14.67016332	0.27213061	0.33221010
40°	4.65473758	0.61101851	17.77104367	0.27639318	0.36080563
45°	4.83565824	0.43009785	22.04643242	0.28824065	0.40763378
50°	5.08274522	0.18301087	29.95500940	0.32595312	0.50709293
51.70000000	5.26475103	0.00100303	38.24326642	0.38364443	0.61900195
Ymax/L = 0.10					

TABLE 3a.15
DIMENSIONLESS POSTBUCKLING LOADS

R = 0.02					
α	Q/P_E^*	Q/P_E^{**}	λ	U/L	V/L
0°	4.18851121	1.36569641	0.00000000	0.29759184	0.29759184
5°	4.20404851	1.35016110	2.11867983	0.29718647	0.29832168
10°	4.24947633	1.30473328	4.24174062	0.29608546	0.30065306
15°	4.32174498	1.23246463	6.38522555	0.29460336	0.30499584
20°	4.41703309	1.13717651	8.58586026	0.29319800	0.31201478
25°	4.53187485	1.02233476	10.90917440	0.29244770	0.32268032
30°	4.66403685	0.89017276	13.46383021	0.29312255	0.33846874
35°	4.81340979	0.74079981	16.43801222	0.29644679	0.36189468
40°	4.98396817	0.57024144	20.20859352	0.30491981	0.39804450
45°	5.19191605	0.36229356	25.80210680	0.32590221	0.46089525
49.57500000	5.55103252	0.00317510	40.24846116	0.41896916	0.64610655
Ymax/L = 0.15					

TABLE 3a.16
DIMENSIONLESS POSTBUCKLING LOADS

R = 0.02					
α	Q/P_E^*	Q/P_E^{**}	λ	U/L	V/L
0°	4.68714819	1.36262238	0.00000000	0.32255426	0.32255426
5°	4.70300544	1.34676704	2.38378495	0.32241092	0.32364248
10°	4.74961587	1.30015662	4.78867404	0.32208072	0.32704934
15°	4.82448881	1.22528367	7.24736323	0.32185105	0.33320472
20°	4.92449954	1.12527294	9.81536845	0.32218588	0.34286305
25°	5.04694582	1.00282667	12.58523518	0.32376410	0.35723414
30°	5.19063003	0.85914246	15.71452913	0.32765493	0.37834330
35°	5.35749645	0.69227604	19.49974500	0.33586881	0.41002007
40°	5.55748078	0.49229171	24.63603305	0.35339293	0.46132165
45°	5.84186518	0.20790731	34.03743962	0.40314888	0.467013853
46.56500000	6.04744719	0.00232339	43.30895270	0.47160085	0.68593372
Ymax/L = 0.20					

TABLE 3a.17
DIMENSIONLESS POSTBUCKLING LOADS

R = 0.02					
α	Q/P_E*	Q/P_E**	λ	U/L	V/L
0°	5.55075519	1.35881049	0.00000000	0.36016692	0.36016692
5°	5.56743176	1.34213554	2.82202993	0.36037997	0.36175656
10°	5.61677442	1.29279289	5.69172265	0.36112104	0.36669191
15°	5.69702878	1.21253852	8.67070108	0.36270460	0.37549943
20°	5.80613657	1.10343073	11.85162210	0.36570837	0.38917871
25°	5.94286587	0.96670144	15.38675297	0.37113337	0.40950032
30°	6.10856566	0.80100165	19.55435963	0.38088214	0.43980479
35°	6.31151576	0.59805155	24.97019425	0.39941820	0.48759954
40°	6.58953009	0.32002821	33.76387047	0.44343078	0.57885770
42.59000000	6.90605790	0.00350778	47.22597564	0.54041260	0.73404161
Ymax/L = 0.25					

TABLE 3a.18
DIMENSIONLESS POSTBUCKLING LOADS

R = 0.02533030					
α	Q/P_E^*	Q/P_E^{**}	λ	U/L	V/L
0°	2.00000000	2.00000000	0.00000000	0.50000000	0.50000000
5°	2.22462002	1.77538172	4.10970769	0.45093046	0.45265294
10°	2.42291871	1.57708303	7.19860478	0.41735440	0.42379276
15°	2.60787735	1.39212439	9.82123135	0.39248925	0.40633476
20°	2.78548934	1.21451240	12.24735996	0.37359186	0.39756814
25°	2.95958548	1.04041626	14.66408625	0.35945246	0.39661190
30°	3.13354609	0.86645566	17.25245614	0.34976160	0.40386989
35°	3.31161951	0.68838223	20.25572934	0.34513569	0.42133284
40°	3.50146532	0.49853642	24.12548619	0.34799624	0.45427678
45°	3.72482646	0.27517529	30.15264906	0.36745216	0.51965575
48.58500000	3.99901270	0.00098745	41.35843736	0.43710338	0.66076788
Ymax/L = 0.00					

TABLE 3a.19
DIMENSIONLESS BUCKLING LOADS

R = 0.02533030					
α	Q/P_E*	Q/P_E**	λ	U/L	V/L
0°	2.17809153	1.85949783	0.00000000	0.46533660	0.46533660
5°	2.29292662	1.74466434	3.99155160	0.44369452	0.44538936
10°	2.47184247	1.56574848	7.13985133	0.41534200	0.42174931
15°	2.65086961	1.38672135	9.82106887	0.39248523	0.40633060
20°	2.82642616	1.21116479	12.30467029	0.37471923	0.39876787
25°	3.00015677	1.03743419	14.78242429	0.36138940	0.39874907
30°	3.17475994	0.86283101	17.44176341	0.35240654	0.40692399
35°	3.35434405	0.68324690	20.53758836	0.34854729	0.42549764
40°	3.54693325	0.49065770	24.55184723	0.35250622	0.46016413
45°	3.77669734	0.26089361	30.91989626	0.37459326	0.52975479
48.25000000	4.03659846	0.00099090	41.69341570	0.44290778	0.66514487
Ymax/L = 0.05					

TABLE 3a.20
DIMENSIONLESS POSTBUCKLING LOADS

R = 0.02533030					
α	Q/P_E^*	Q/P_E^{**}	λ	U/L	V/L
0°	2.41164902	1.74602389	0.00000000	0.44011244	0.44011244
5°	2.47893763	1.67873688	3.77742384	0.43008893	0.43173180
10°	2.62217646	1.53549804	7.02138501	0.41124335	0.41758743
15°	2.78654567	1.37112883	9.85687014	0.39337049	0.40724709
20°	2.95667390	1.20100061	12.50973487	0.37872411	0.40302977
25°	3.12964682	1.02802768	15.17528476	0.36775143	0.40576880
30°	3.30651568	0.85115883	18.05864870	0.36091546	0.41674925
35°	3.49115032	0.66652419	21.45364501	0.35947864	0.43884235
40°	3.69305800	0.46461651	25.95279317	0.36710547	0.47922210
45°	3.94699394	0.21068057	33.61029127	0.39927579	0.56466114
47.23000000	4.15639531	0.00127760	42.69774439	0.46048981	0.67813128
Ymax/L = 0.10					

TABLE 3a.21
DIMENSIONLESS POSTBUCKLING LOADS

R = 0.02533030					
α	Q/P_E^*	Q/P_E^{**}	λ	U/L	V/L
0°	2.73259798	1.65282873	0.00000000	0.42533665	0.42533665
5°	2.77806945	1.60735884	3.63230871	0.42048773	0.42209393
10°	2.89142905	1.49399923	6.97285846	0.40954842	0.41586636
15°	3.03870878	1.34671951	10.03201609	0.39766719	0.41169536
20°	3.20201601	1.18341228	12.96658294	0.38748667	0.41235469
25°	3.37492100	1.01050729	15.96668324	0.38025934	0.41956974
30°	3.55685485	0.82857343	19.26818872	0.37713185	0.43547432
35°	3.75199729	0.63343100	23.25035907	0.38026443	0.46421712
40°	3.97431252	0.41111577	28.79159572	0.39575013	0.51661504
45°	4.30785127	0.07757701	40.75665865	0.46290202	0.65464221
45.48500000	4.38340178	0.00202493	44.40239949	0.49055307	0.69969461
Ymax/L = 0.15					

TABLE 3a.22
DIMENSIONLESS POSTBUCKLING LOADS

R = 0.02533030					
α	Q/P_E*	Q/P_E**	λ	U/L	V/L
0°	3.20162381	1.57508375	0.00000000	0.42303267	0.42303267
5°	3.23605895	1.54065011	3.63737210	0.42082813	0.42243562
10°	3.32933668	1.44737238	7.14280231	0.41544339	0.42185227
15°	3.46225918	1.31444989	10.51624040	0.40925891	0.42369600
20°	3.62017857	1.15653049	13.87477006	0.40428254	0.43022848
25°	3.79586311	0.98084596	17.41257064	0.40211573	0.44368560
30°	3.98841959	0.78828947	21.43035609	0.40470596	0.46731417
35°	4.20464813	0.57206093	26.51183086	0.41602995	0.50787875
40°	4.47482777	0.30188130	34.46192888	0.44991600	0.58732356
42.95500000	4.77488377	0.00182379	46.94605664	0.53480043	0.73071237
Ymax/L = 0.20					

TABLE 3a.23
DIMENSIONLESS POSTBUCKLING LOADS

R = 0.02533030					
α	Q/P_E*	Q/P_E**	λ	U/L	V/L
0°	3.94662432	1.50895026	0.00000000	0.43662878	0.43662878
5°	3.97549487	1.48008100	3.86913029	0.43599570	0.43766113
10°	4.05746327	1.39811260	7.71762844	0.43456960	0.44127353
15°	4.18220991	1.27336596	11.58792919	0.43351143	0.44880405
20°	4.34004633	1.11552954	15.61285313	0.43431680	0.46219028
25°	4.52582389	0.92975198	20.04233208	0.43893715	0.48431354
30°	4.74165416	0.71392171	25.35895009	0.45082645	0.52056951
35°	5.00662850	0.44894737	32.82523952	0.47951075	0.58537448
39.53000000	5.45363917	0.00193542	50.36844915	0.59402037	0.77016333
Ymax/L = 0.25					

TABLE 3a.24
DIMENSIONLESS POSTBUCKLING LOADS

R = 0.03092258					
α	Q/P_E*	Q/P_E**	λ	U/L	V/L
0°	COMPLEX	COMPLEX			
5°	COMPLEX	COMPLEX			
10°	COMPLEX	COMPLEX			
15°	COMPLEX	COMPLEX			
20°	COMPLEX	COMPLEX			
25°	COMPLEX	COMPLEX			
30°	COMPLEX	COMPLEX			
35°	2.75829166	0.51831668	29.13031667	0.44317211	0.54101325
40°	2.99156607	0.28504228	34.91536616	0.45410499	0.59279196
45°	COMPLEX	COMPLEX			
50°	COMPLEX	COMPLEX			
55°	COMPLEX	COMPLEX			
60°	COMPLEX	COMPLEX			
65°	COMPLEX	COMPLEX			
70°	COMPLEX	COMPLEX			
75°	COMPLEX	COMPLEX			
Ymax/L = 0.00					

TABLE 3a.25
DIMENSIONLESS BUCKLING LOADS

R = 0.03092258					
α	Q/P_E^*	Q/P_E^{**}	λ	U/L	V/L
0°	COMPLEX	COMPLEX			
5°	COMPLEX	COMPLEX			
10°	COMPLEX	COMPLEX			
15°	COMPLEX	COMPLEX			
20°	COMPLEX	COMPLEX			
25°	COMPLEX	COMPLEX			
30°	COMPLEX	COMPLEX			
35°	2.79463506	0.51276457	29.41031094	0.44600139	0.54446717
40°	3.03276208	0.27463754	35.46028771	0.45911561	0.59933286
45°	COMPLEX	COMPLEX			
50°	COMPLEX	COMPLEX			
55°	COMPLEX	COMPLEX			
60°	COMPLEX	COMPLEX			
65°	COMPLEX	COMPLEX			
70°	COMPLEX	COMPLEX			
75°	COMPLEX	COMPLEX			
Ymax/L = 0.05					

TABLE 3a.26
DIMENSIONLESS POSTBUCKLING LOADS

R = 0.03092258					
α	Q/P_E*	Q/P_E**	λ	U/L	V/L
0°	COMPLEX	COMPLEX			
5°	COMPLEX	COMPLEX			
10°	COMPLEX	COMPLEX			
15°	COMPLEX	COMPLEX			
20°	COMPLEX	COMPLEX			
25°	COMPLEX	COMPLEX			
30°	COMPLEX	COMPLEX			
35°	2.91148526	0.49428105	30.34112675	0.45531338	0.55583501
40°	3.16678273	0.23898359	37.32558518	0.47608711	0.62148758
45°	COMPLEX	COMPLEX			
50°	COMPLEX	COMPLEX			
55°	COMPLEX	COMPLEX			
60°	COMPLEX	COMPLEX			
65°	COMPLEX	COMPLEX			
70°	COMPLEX	COMPLEX			
75°	COMPLEX	COMPLEX			
Ymax/L = 0.10					

TABLE 3a.27
DIMENSIONLESS POSTBUCKLING LOADS

R = 0.03092258					
α	Q/P_E*	Q/P_E**	λ	U/L	V/L
0°	COMPLEX	COMPLEX			
5°	COMPLEX	COMPLEX			
10°	COMPLEX	COMPLEX			
15°	COMPLEX	COMPLEX			
20°	COMPLEX	COMPLEX			
25°	COMPLEX	COMPLEX			
30°	2.89848168	0.69384963	27.07195100	0.46957073	0.54221337
35°	3.13616999	0.45616132	32.25202212	0.47400666	0.57865529
40°	3.43467413	0.15765718	41.58378712	0.51396983	0.67093996
45°	COMPLEX	COMPLEX			
50°	COMPLEX	COMPLEX			
55°	COMPLEX	COMPLEX			
60°	COMPLEX	COMPLEX			
65°	COMPLEX	COMPLEX			
70°	COMPLEX	COMPLEX			
75°	COMPLEX	COMPLEX			
Ymax/L = 0.15					

TABLE 3a.28
DIMENSIONLESS POSTBUCKLING LOADS

R = 0.03092258					
α	Q/P_E*	Q/P_E**	λ	U/L	V/L
0°	COMPLEX	COMPLEX			
5°	COMPLEX	COMPLEX			
10°	COMPLEX	COMPLEX			
15°	COMPLEX	COMPLEX			
20°	COMPLEX	COMPLEX			
25°	3.01990153	0.89294829	24.24690267	0.49132466	0.54211679
30°	3.26211377	0.65073605	29.07707942	0.49061192	0.56650985
35°	3.53208047	0.38076935	35.99944701	0.50922394	0.62164765
39.38000000	3.91087233	0.00197749	50.51273129	0.59654143	0.77176726
Ymax/L = 0.20					

TABLE 3a.29
DIMENSIONLESS POSTBUCKLING LOADS

R = 0.03092258					
α	Q/P_E^*	Q/P_E^{**}	λ	U/L	V/L
0°	2.57300521	1.89593993	0.00000000	0.57787693	0.57787693
5°	2.69394262	1.77500252	6.41579379	0.56241614	0.56456448
10°	2.91309429	1.55585085	11.70676865	0.54026470	0.54859916
15°	3.14619172	1.32275342	16.44977738	0.52424594	0.54273934
20°	3.38408063	1.08486451	21.18589502	0.51571463	0.54881204
25°	3.63174199	0.83720315	26.44421700	0.51611485	0.56946972
30°	3.90428485	0.56466030	33.13293393	0.53063299	0.61272220
35°	4.26361282	0.20533232	44.66163997	0.58529953	0.71451879
36.45500000	4.46698431	0.00196083	53.44212438	0.64607863	0.80325690
Ymax/L = 0.25					

TABLE 3a.30
DIMENSIONLESS POSTBUCKLING LOADS

R = 0.09786875					
α	Q/P_E*	Q/P_E**	λ	U/L	V/L
0°	COMPLEX	COMPLEX			
5°	COMPLEX	COMPLEX			
10°	COMPLEX	COMPLEX			
15°	COMPLEX	COMPLEX			
20°	COMPLEX	COMPLEX			
25°	COMPLEX	COMPLEX			
30°	COMPLEX	COMPLEX			
35°	COMPLEX	COMPLEX			
40°	COMPLEX	COMPLEX			
45°	COMPLEX	COMPLEX			
50°	COMPLEX	COMPLEX			
55°	COMPLEX	COMPLEX			
60°	COMPLEX	COMPLEX			
65°	COMPLEX	COMPLEX			
70°	COMPLEX	COMPLEX			
75°	COMPLEX	COMPLEX			
Ymax/L = 0.00, 0.05, 0.10, 0.15, 0.20, 0.25					

TABLE 3a.31
DIMENSIONLESS BUCKLING AND POSTBUCKLING LOADS

R = 0.00					
α	Q/P_E	Q/P_E**	λ	U/L	V/L
5°	---	0.99619470			
15°	---	0.96592583			
30°	---	0.86602540			
45°	---	0.70710678			
60°	---	0.50000000			
70°	---	0.34202014			
Ymax/L = 0.0					

TABLE 4a.1
DIMENSIONLESS POSTBUCKLING LOADS FOR Q/P_E - V/L CURVES

R = 0.01					
α	Q/P_E	Q/P_E**	λ	U/L	V/L
5°	---	6.00000000	7.82380803	0.61097991	0.61331375
	---	4.00000000	3.33834280	0.40002189	0.40154991
	---	2.00000000	1.24327844	0.19875846	0.19951768
	---	1.11870039	0.62585338	0.11099869	0.11142269
	---	0.70000000	0.37389154	0.06941204	0.06967718
	---	0.55000000	0.28908992	0.05452697	0.05473525
	---	0.50000000	0.26142065	0.04956671	0.04975605
	---	0.40000000	0.20695048	0.03964827	0.03979972
	---	0.20000000	0.10135725	0.01981924	0.01989495
Ymax/L = 0.0					

TABLE 4a.2
DIMENSIONLESS POSTBUCKLING LOADS FOR Q/P_E - V/L CURVES

R = 0.01					
α	Q/P_E	Q/P_E**	λ	U/L	V/L
15°	---	4.00000000	12.88738647	0.46059340	0.47684138
	---	3.00000000	7.37893468	0.32583371	0.33732780
	---	2.00000000	4.09638173	0.21090830	0.21834834
	---	1.60000000	3.08203569	0.16732386	0.17322640
	---	1.06967572	1.91309364	0.11084136	0.11475142
	---	0.70000000	1.19350516	0.07214283	0.07468775
	---	0.50000000	0.83170317	0.05139369	0.05320666
	---	0.40000000	0.65737900	0.04106293	0.04251147
	---	0.20000000	0.32101808	0.02048195	0.02120448
Ymax/L = 0.0					

TABLE 4a.3
DIMENSIONLESS POSTBUCKLING LOADS FOR Q/P_E - V/L CURVES

R = 0.01					
α	Q/P_E	Q/P_E**	λ	U/L	V/L
30°	---	2.00000000	13.33142388	0.29100271	0.33602098
	---	1.80000000	10.79042002	0.24818035	0.28657398
	---	1.60000000	8.83996968	0.21220950	0.24503842
	---	1.40000000	7.22783081	0.18010186	0.20796372
	---	0.90960470	4.11173783	0.11072506	0.12785428
	---	0.70000000	3.01754736	0.08366577	0.09660891
	---	0.50000000	2.06742522	0.05884601	0.06794952
	---	0.40000000	1.62166059	0.04674376	0.05397504
	---	0.20000000	0.78100448	0.02306659	0.02663500
Ymax/L = 0.0					

TABLE 4a.4
DIMENSIONLESS POSTBUCKLING LOADS FOR Q/P_E - V/L CURVES

R = 0.01					
α	Q/P_E	Q/P_E**	λ	U/L	V/L
45°	---	0.70000000	8.02135565	0.12351508	0.17467670
	---	0.65474987	7.23393141	0.11263431	0.15928894
	---	0.55000000	5.65255946	0.09006293	0.12736822
	---	0.50000000	4.98610186	0.08024346	0.11348139
	---	0.40000000	3.77858063	0.06195281	0.08761450
	---	0.20000000	1.72499179	0.02923544	0.04134515
	---	0.10000000	0.82923872	0.01426745	0.02017722
	---	0.02100000	0.16918576	0.00294416	0.00416368
	---	0.02000000	0.16107222	0.00280337	0.00396456
Ymax/L = 0.0					

TABLE 4a.5
DIMENSIONLESS POSTBUCKLING LOADS FOR Q/P_E - V/L CURVES

R = 0.01					
α	Q/P_E	Q/P_E**	λ	U/L	V/L
60°	---	0.27406751	14.53474879	0.13019774	0.26039540
	---	0.20000000	5.38172157	0.05158419	0.10316837
	---	0.10000000	2.22230237	0.02191366	0.04382732
	---	0.02100000	0.42112693	0.00422570	0.00845140
	---	0.02000000	0.40061363	0.00402068	0.00804137
	---	0.01900000	0.38014800	0.00381606	0.00763212
	---	0.01800000	0.35972975	0.00361183	0.00722366
	---	0.01600000	0.31903430	0.00320453	0.00640906
	---	0.01200000	0.23819998	0.00239453	0.00478905
Ymax/L = 0.0					

TABLE 4a.6
DIMENSIONLESS POSTBUCKLING LOADS FOR Q/P_E - V/L CURVES

R = 0.01					
α	Q/P_E	Q/P_E**	λ	U/L	V/L
70°	---	0.02100000	1.03624328	0.00654037	0.01912277
	---	0.02000000	0.98259844	0.00620382	0.01813876
	---	0.01900000	0.92944727	0.00587015	0.01716317
	---	0.01800000	0.87677799	0.00553929	0.01619581
	---	0.01600000	0.77284014	0.00488576	0.01428501
	---	0.01200000	0.57027590	0.00360971	0.01055408
	---	0.00900000	0.42270115	0.00267806	0.00783012
Ymax/L = 0.0					

TABLE 4a.7
DIMENSIONLESS POSTBUCKLING LOADS FOR Q/P_E - V/L CURVES

R = 0.02					
α	Q/P_E	Q/P_E**	λ	U/L	V/L
5°	---	3.00000000	7.82380803	0.61097991	0.61331375
	---	2.00000000	3.33834280	0.40002189	0.40154991
	---	1.80000000	2.81011543	0.35940373	0.36077659
	---	1.60000000	2.34693940	0.31901345	0.32023203
	---	1.37105692	1.85233573	0.26988915	0.27092009
	---	0.70000000	0.80902345	0.13897352	0.13950438
	---	0.50000000	0.55202540	0.09920304	0.09958198
	---	0.40000000	0.43197060	0.07933917	0.07964224
	---	0.20000000	0.20695048	0.03964827	0.03979972
Ymax/L = 0.0					

TABLE 4a.8
DIMENSIONLESS POSTBUCKLING LOADS FOR Q/P_E - V/L CURVES

R = 0.02					
α	Q/P_E	Q/P_E**	λ	U/L	V/L
15°	---	2.00000000	12.88738647	0.46059340	0.47684138
	---	1.80000000	10.22848150	0.40242044	0.41661630
	---	1.60000000	8.22532030	0.35043017	0.36279201
	---	1.40000000	6.61021575	0.30191356	0.31256391
	---	1.24020932	5.51232030	0.26479539	0.27413637
	---	0.70000000	2.62007574	0.14586989	0.15101563
	---	0.50000000	1.77203970	0.10351000	0.10716144
	---	0.40000000	1.38136309	0.08256434	0.08547690
	---	0.20000000	0.65737900	0.04106293	0.04251147
Ymax/L = 0.0					

TABLE 4a.9
DIMENSIONLESS POSTBUCKLING LOADS FOR Q/P_E - V/L CURVES

R = 0.02					
α	Q/P_E	Q/P_E**	λ	U/L	V/L
30°	---	0.91894009	11.21415677	0.25562011	0.29516466
	---	0.70000000	7.22783081	0.18010186	0.20796372
	---	0.55000000	5.21333545	0.13646858	0.15758034
	---	0.50000000	4.62047887	0.12279209	0.14178809
	---	0.40000000	3.52572919	0.09642704	0.11134435
	---	0.20000000	1.62166059	0.04674376	0.05397504
	---	0.10000000	0.78100448	0.02306659	0.02663500
	---	0.02000000	0.15183708	0.00456907	0.00527591
	---	0.01800000	0.13655893	0.00411121	0.00474722
Ymax/L = 0.0					

TABLE 4a.10
DIMENSIONLESS POSTBUCKLING LOADS FOR Q/P_E - V/L CURVES

R = 0.02					
α	Q/P_E	Q/P_E**	λ	U/L	V/L
45°	---	0.47181254	19.66744537	0.26330344	0.37236723
	---	0.40000000	10.12371907	0.15150280	0.21425732
	---	0.20000000	3.77858063	0.06195281	0.08761450
	---	0.10000000	1.72499179	0.02923544	0.04134515
	---	0.02000000	0.32445150	0.00563092	0.00796332
	---	0.01800000	0.29158737	0.00506343	0.00716078
	---	0.01600000	0.25881802	0.00449694	0.00635964
	---	0.01200000	0.19356106	0.00336692	0.00476154
	---	0.00900000	0.14486244	0.00252196	0.00356658
Ymax/L = 0.0					

TABLE 4a.11
DIMENSIONLESS POSTBUCKLING LOADS FOR Q/P_E - V/L CURVES

R = 0.02					
α	Q/P_E	Q/P_E**	λ	U/L	V/L
60°	---	0.10000000	5.38172157	0.05158419	0.10316837
	---	0.02100000	0.86341373	0.00862623	0.01725246
	---	0.02000000	0.82032961	0.00819897	0.01639794
	---	0.01900000	0.77743108	0.00777349	0.01554698
	---	0.01800000	0.73474541	0.00734977	0.01469954
	---	0.01600000	0.65000204	0.00650751	0.01301502
	---	0.01200000	0.48295566	0.00484313	0.00968625
	---	0.00900000	0.35972975	0.00361183	0.00722366
Ymax/L = 0.0					

TABLE 4a.12
DIMENSIONLESS POSTBUCKLING LOADS FOR Q/P_E - V/L CURVES

R = 0.02					
α	Q/P_E	Q/P_E**	λ	U/L	V/L
70°	---	0.02100000	2.30439405	0.01443509	0.04220538
	---	0.02000000	2.16944109	0.01360040	0.03976490
	---	0.01900000	2.03803507	0.01278643	0.03738501
	---	0.01800000	1.90993760	0.01199179	0.03506164
	---	0.01600000	1.66283761	0.01045563	0.03057022
	---	0.01200000	1.20026519	0.00756806	0.02212753
	---	0.00900000	0.87677799	0.00553929	0.01619581
Ymax/L = 0.0					

TABLE 4a.13
DIMENSIONLESS POSTBUCKLING LOADS FOR Q/P_E - V/L CURVES

R = 0.02533030					
α	Q/P_E	Q/P_E**	λ	U/L	V/L
5°	---	2.00000000	5.29213113	0.51426851	0.51623294
	---	1.80000000	4.28066082	0.46107630	0.46283753
	---	1.77538172	4.10970769	0.45093046	0.45265294
	---	1.60000000	3.46015115	0.40867347	0.41023453
	---	1.40000000	2.77847180	0.35679651	0.35815941
	---	0.70000000	1.08184442	0.17752675	0.17820487
	---	0.50000000	0.72714720	0.12668932	0.12717325
	---	0.40000000	0.56507420	0.10131057	0.10169756
	---	0.20000000	0.26726533	0.05061882	0.05081217
Ymax/L = 0.0					

TABLE 4a.14
DIMENSIONLESS POSTBUCKLING LOADS FOR Q/P_E - V/L CURVES

R = 0.02533030					
α	Q/P_E	Q/P_E**	λ	U/L	V/L
15°	---	1.80000000	21.28602483	0.59250490	0.61340621
	---	1.60000000	13.58970598	0.47428419	0.49101512
	---	1.40000000	10.08386727	0.39892843	0.41300110
	---	1.39212439	9.82123135	0.39248925	0.40633476
	---	0.70000000	3.54044737	0.18759066	0.19420814
	---	0.50000000	2.34805615	0.13271989	0.13740174
	---	0.40000000	1.81470179	0.10573999	0.10947009
	---	0.20000000	0.85044226	0.05249102	0.05434270
	---	0.10000000	0.41244089	0.02616258	0.02708550
Ymax/L = 0.0					

TABLE 4a.15
DIMENSIONLESS POSTBUCKLING LOADS FOR Q/P_E - V/L CURVES

R = 0.02533030					
α	Q/P_E	Q/P_E**	λ	U/L	V/L
30°	---	0.86645566	17.25245614	0.34976160	0.40386989
	---	0.70000000	10.65102262	0.24570497	0.28371566
	---	0.50000000	6.34997563	0.16160100	0.18660076
	---	0.40000000	4.74347676	0.12566301	0.14510314
	---	0.20000000	2.11578472	0.06014087	0.06944469
	---	0.10000000	1.00710559	0.02954824	0.03411937
	---	0.02000000	0.19419393	0.00583624	0.00673911
	---	0.01800000	0.17461991	0.00525106	0.00606340
	---	0.01600000	0.15508057	0.00466622	0.00538809
Ymax/L = 0.0					

TABLE 4a.16
DIMENSIONLESS POSTBUCKLING LOADS FOR Q/P_E - V/L CURVES

R = 0.02533030					
α	Q/P_E	Q/P_E**	λ	U/L	V/L
45°	---	0.27517529	30.15264906	0.36745216	0.51965575
	---	0.20000000	5.12353810	0.08228400	0.11636715
	---	0.10000000	2.25391613	0.03786813	0.05355362
	---	0.02000000	0.41582428	0.00720534	0.01018988
	---	0.01900000	0.39466794	0.00684124	0.00967497
	---	0.01800000	0.37355103	0.00647756	0.00916065
	---	0.01600000	0.33143481	0.00575142	0.00813374
	---	0.01200000	0.24766811	0.00430405	0.00608684
	---	0.00900000	0.18524538	0.00322273	0.00455763
Ymax/L = 0.0					

TABLE 4a.17
DIMENSIONLESS POSTBUCKLING LOADS FOR Q/P_E - V/L CURVES

R = 0.02533030					
α	Q/P_E	Q/P_E**	λ	U/L	V/L
60°	---	0.10000000	8.36559501	0.07825730	0.15651459
	---	0.02100000	3.17445959	0.01978692	0.05785309
	---	0.02000000	1.06154152	0.01058478	0.02116957
	---	0.01900000	1.00525375	0.01002904	0.02005808
	---	0.01800000	0.94933729	0.00947637	0.01895273
	---	0.01600000	0.83859368	0.00838001	0.01676002
	---	0.01200000	0.62130051	0.00622193	0.01244385
	---	0.00900000	0.46182857	0.00463223	0.00926447
Ymax/L = 0.0					

TABLE 4a.18
DIMENSIONLESS POSTBUCKLING LOADS FOR Q/P_E - V/L CURVES

R = 0.02533030					
α	Q/P_E	Q/P_E**	λ	U/L	V/L
70°	---	0.02100000	3.17445959	0.01978692	0.05785309
	---	0.02000000	2.96844765	0.01852427	0.05416133
	---	0.01900000	2.77154867	0.01731486	0.05062527
	---	0.01800000	2.58275172	0.01615280	0.04722763
	---	0.01600000	2.22624499	0.01395189	0.04079259
	---	0.01200000	1.58116427	0.00994693	0.02908287
	---	0.00900000	1.14381486	0.00721460	0.02109407
Ymax/L = 0.0					

TABLE 4a.19
DIMENSIONLESS POSTBUCKLING LOADS FOR Q/P_E - V/L CURVES

R = 0.03092258					
α	Q/P_E	Q/P_E**	λ	U/L	V/L
5°	---	2.00000000	8.54410369	0.63197797	0.63439202
	---	1.80000000	6.43738342	0.56324971	0.56540123
	---	1.60000000	4.95355954	0.49765537	0.49955633
	---	1.40000000	3.83277338	0.43366853	0.43532507
	---	0.70000000	1.37419791	0.21519023	0.21601222
	---	0.50000000	0.90903632	0.15351851	0.15410492
	---	0.40000000	0.70137644	0.12275008	0.12321897
	---	0.20000000	0.32745055	0.06131887	0.06156310
	---	0.10000000	0.15848275	0.03064718	0.03076425
Ymax/L = 0.0					

TABLE 4a.20
DIMENSIONLESS POSTBUCKLING LOADS FOR Q/P_E - V/L CURVES

R = 0.03092258					
α	Q/P_E	Q/P_E**	λ	U/L	V/L
15°	---	1.40000000	16.10672875	0.51869299	0.53699049
	---	0.70000000	4.55423679	0.22915265	0.23723628
	---	0.55000000	3.32551412	0.17821019	0.18449676
	---	0.50000000	2.95487897	0.16152508	0.16722307
	---	0.40000000	2.26280590	0.12851608	0.13304964
	---	0.20000000	1.04380074	0.06366789	0.06591385
	---	0.10000000	0.50273549	0.03170893	0.03282750
	---	0.02000000	0.09769890	0.00632354	0.00654661
	---	0.01800000	0.08786698	0.00569079	0.00589154
Ymax/L = 0.0					

TABLE 4a.21
DIMENSIONLESS POSTBUCKLING LOADS FOR Q/P_E - V/L CURVES

R = 0.03092258					
α	Q/P_E	Q/P_E**	λ	U/L	V/L
30°	---	0.70000000	16.44003135	0.33822409	0.39054753
	---	0.55000000	9.76959637	0.22972087	0.26525882
	---	0.50000000	8.37848736	0.20325235	0.23469560
	---	0.40000000	6.08376953	0.15583789	0.17994610
	---	0.20000000	2.62008319	0.07343950	0.08480063
	---	0.10000000	1.23212921	0.03591501	0.04147113
	---	0.02000000	0.23565103	0.00707338	0.00816763
	---	0.01800000	0.21185800	0.00636374	0.00734821
	---	0.01600000	0.18811619	0.00565461	0.00652939
Ymax/L = 0.0					

TABLE 4a.22
DIMENSIONLESS POSTBUCKLING LOADS FOR Q/P_E - V/L CURVES

R = 0.03092258					
α	Q/P_E	Q/P_E**	λ	U/L	V/L
45°	---	0.20000000	6.65266525	0.10445265	0.14771835
	---	0.10000000	2.79623975	0.04656789	0.06585694
	---	0.02100000	0.53151536	0.00919169	0.01299901
	---	0.02000000	0.50563246	0.00874798	0.01237151
	---	0.01900000	0.47980874	0.00830489	0.01174489
	---	0.01800000	0.45404390	0.00786242	0.01111914
	---	0.01600000	0.40268957	0.00697932	0.00987025
	---	0.01200000	0.30067380	0.00522040	0.00738276
	---	0.00900000	0.22475879	0.00390747	0.00552600
Ymax/L = 0.0					

TABLE 4a.23
DIMENSIONLESS POSTBUCKLING LOADS FOR Q/P_E - V/L CURVES

R = 0.03092258					
α	Q/P_E	Q/P_E**	λ	U/L	V/L
60°	---	0.02100000	1.37426919	0.01366148	0.02732297
	---	0.02000000	1.30355998	0.01296744	0.02593488
	---	0.01900000	1.23344738	0.01227832	0.02455665
	---	0.01800000	1.16391867	0.01159403	0.02318806
	---	0.01600000	1.02656413	0.01023952	0.02047903
	---	0.01200000	0.75834783	0.00758410	0.01516821
	---	0.00900000	0.56253660	0.00563672	0.01127344
Ymax/L = 0.0					

TABLE 4a.24
DIMENSIONLESS POSTBUCKLING LOADS FOR Q/P_E - V/L CURVES

R = 0.03092258					
α	Q/P_E	Q/P_E**	λ	U/L	V/L
70°	---	0.02100000	4.23827471	0.02626434	0.07679180
	---	0.02000000	3.91762805	0.02431933	0.07110498
	---	0.01900000	3.62213533	0.02252134	0.06584800
	---	0.01800000	3.34704878	0.02084261	0.06093973
	---	0.01600000	2.84524387	0.01776782	0.05194962
	---	0.01200000	1.98045011	0.01242935	0.03634098
	---	0.00900000	1.41688485	0.00892224	0.02608689
Ymax/L = 0.0					

TABLE 4a.25
DIMENSIONLESS POSTBUCKLING LOADS FOR Q/P_E - V/L CURVES

R = 0.09786875					
α	Q/P_E	Q/P_E**	λ	U/L	V/L
5°	---	0.70000000	12.40187265	0.71537960	0.71811224
	---	0.55000000	5.94850127	0.54357924	0.54565562
	---	0.50000000	4.84326496	0.49199917	0.49387853
	---	0.40000000	3.21959703	0.39134278	0.39283765
	---	0.20000000	1.21025953	0.19450528	0.19524826
	---	0.10000000	0.53897691	0.09708566	0.09745652
	---	0.02000000	0.09915383	0.01939674	0.01947084
	---	0.01800000	0.08906017	0.01745666	0.01752334
	---	0.01600000	0.07900677	0.01551667	0.01557594
Ymax/L = 0.0					

TABLE 4a.26
DIMENSIONLESS POSTBUCKLING LOADS FOR Q/P_E - V/L CURVES

R = 0.09786875					
α	Q/P_E	Q/P_E**	λ	U/L	V/L
15°	---	0.40000000	12.24125746	0.44742570	0.46300917
	---	0.20000000	3.98192611	0.20621528	0.21348977
	---	0.10000000	1.72941859	0.10127113	0.10484859
	---	0.02100000	0.33009745	0.02104907	0.02179160
	---	0.02000000	0.31402060	0.02004443	0.02075152
	---	0.01900000	0.29798040	0.01904004	0.01971170
	---	0.01800000	0.28197672	0.01803588	0.01867212
	---	0.01600000	0.25007834	0.01602826	0.01659368
	---	0.01200000	0.18671368	0.01201580	0.01243967
Ymax/L = 0.0					

TABLE 4a.27
DIMENSIONLESS POSTBUCKLING LOADS FOR Q/P_E - V/L CURVES

R = 0.09786875					
α	Q/P_E	Q/P_E**	λ	U/L	V/L
30°	---	0.20000000	12.71617986	0.28101443	0.32448751
	---	0.10000000	4.49832018	0.11992304	0.13847519
	---	0.02100000	0.80338281	0.02371193	0.02738018
	---	0.02000000	0.76376882	0.02256897	0.02606040
	---	0.01900000	0.72429679	0.02142746	0.02474230
	---	0.01800000	0.68496569	0.02028739	0.02342587
	---	0.01600000	0.60672223	0.01801153	0.02079792
	---	0.01200000	0.45188249	0.01347659	0.01556142
	---	0.00900000	0.33716367	0.01008973	0.01165062
Ymax/L = 0.0					

TABLE 4a.28
DIMENSIONLESS POSTBUCKLING LOADS FOR Q/P_E - V/L CURVES

R = 0.09786875					
α	Q/P_E	Q/P_E**	λ	U/L	V/L
45°	---	0.02100000	1.77667635	0.03008558	0.04254743
	---	0.02000000	1.68528050	0.02858126	0.04042000
	---	0.01900000	1.59464660	0.02708500	0.03830398
	---	0.01800000	1.50475971	0.02559665	0.03619913
	---	0.01600000	1.01285675	0.02063487	0.02693691
	---	0.01200000	0.98034761	0.01682407	0.02379283
	---	0.00900000	0.72715143	0.01253280	0.01772406
Ymax/L = 0.0					

TABLE 4a.29
DIMENSIONLESS POSTBUCKLING LOADS FOR Q/P_E - V/L CURVES

R = 0.09786875					
α	Q/P_E	Q/P_E**	λ	U/L	V/L
60°	---	0.02100000	5.61140634	0.05368066	0.10736132
	---	0.02000000	5.21055616	0.05001685	0.10003369
	---	0.01900000	4.83528117	0.04656527	0.09313055
	---	0.01800000	4.48163678	0.04329316	0.08658631
	---	0.01600000	3.82776132	0.03719188	0.07438376
	---	0.01200000	2.68091741	0.02632281	0.05264562
	---	0.00900000	1.92385525	0.01902438	0.03804877
Ymax/L = 0.0					

TABLE 4a.30
DIMENSIONLESS POSTBUCKLING LOADS FOR Q/P_E - V/L CURVES

α	α λ	Q/P_E	λ	U/L	V/L
0°	0°	2.00000000	0.00000000	0.50000000	0.02533029
2°	4.01231647	1.99509806	2.01231647	0.50153609	0.02539253
4°	8.10188392	1.98003805	4.10188392	0.50630867	0.02558567
6°	12.36522353	1.95360487	6.36522353	0.51488334	0.02593185
8°	16.95340778	1.91308439	8.95340778	0.52853169	0.02648111
10°	22.17553113	1.85206372	12.17553113	0.55028683	0.02735359
11°	25.26086006	1.80874855	14.26086006	0.56664715	0.02800864
12°	29.06673993	1.74810879	17.06673993	0.59089232	0.02898023
13°	36.73524572	1.60281572	23.73524572	0.65571423	0.03160725
13.00849500	37.36837791	1.58949943	24.35988291	0.66214654	0.03187204
13.00850000	37.36993910	1.58946636	24.36143910	0.66216262	0.03187270
13.00863500	37.43256439	1.58813857	24.42392939	0.66280860	0.03189935

TABLE 5 TRIFURCATION POINTS FOR VARIOUS VALUES OF

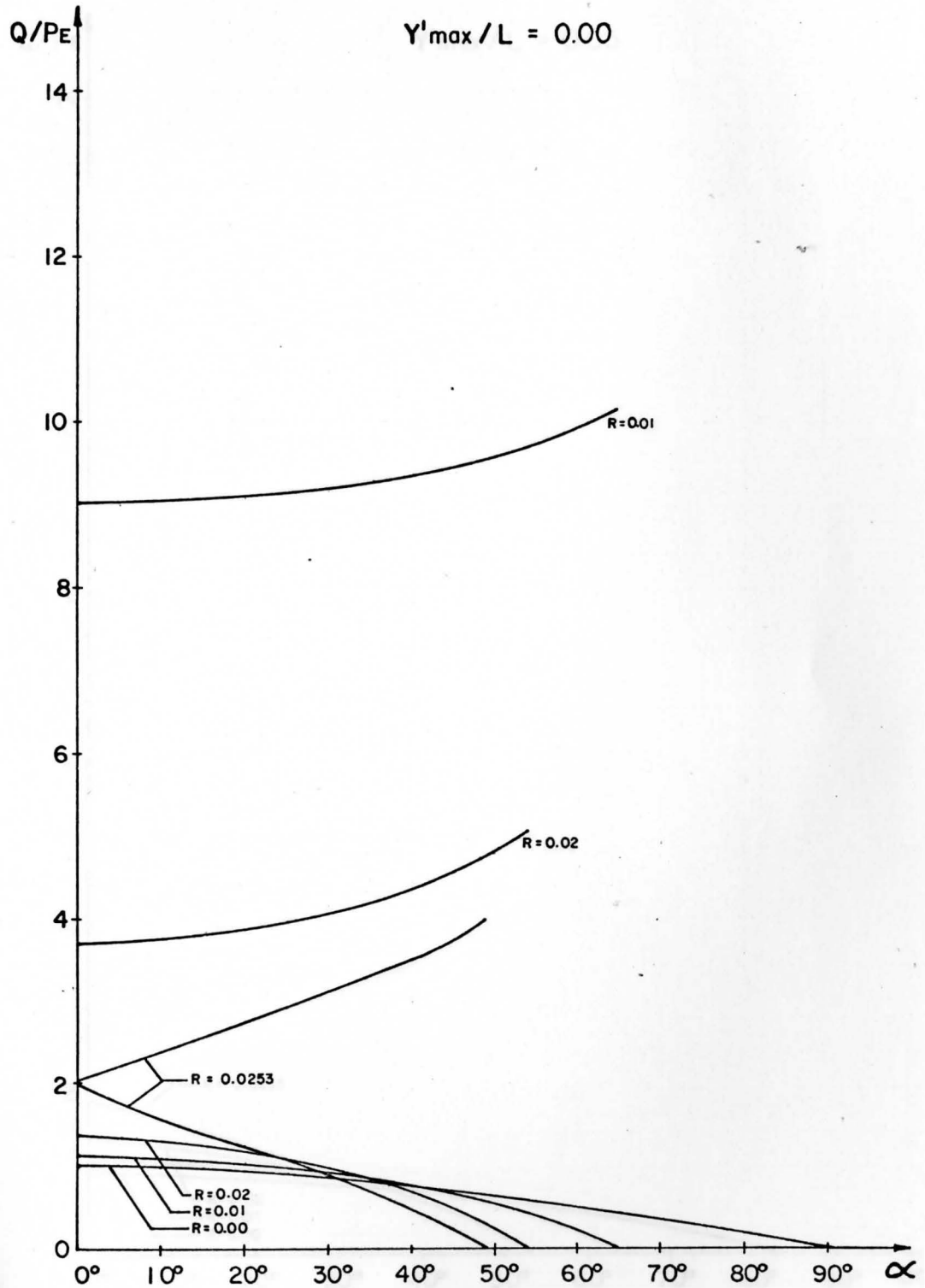

FIGURE 18a DIMENSIONLESS BUCKLING AND POSTBUCKLING LOADS VS. α, FOR VARIOUS VALUES OF R.

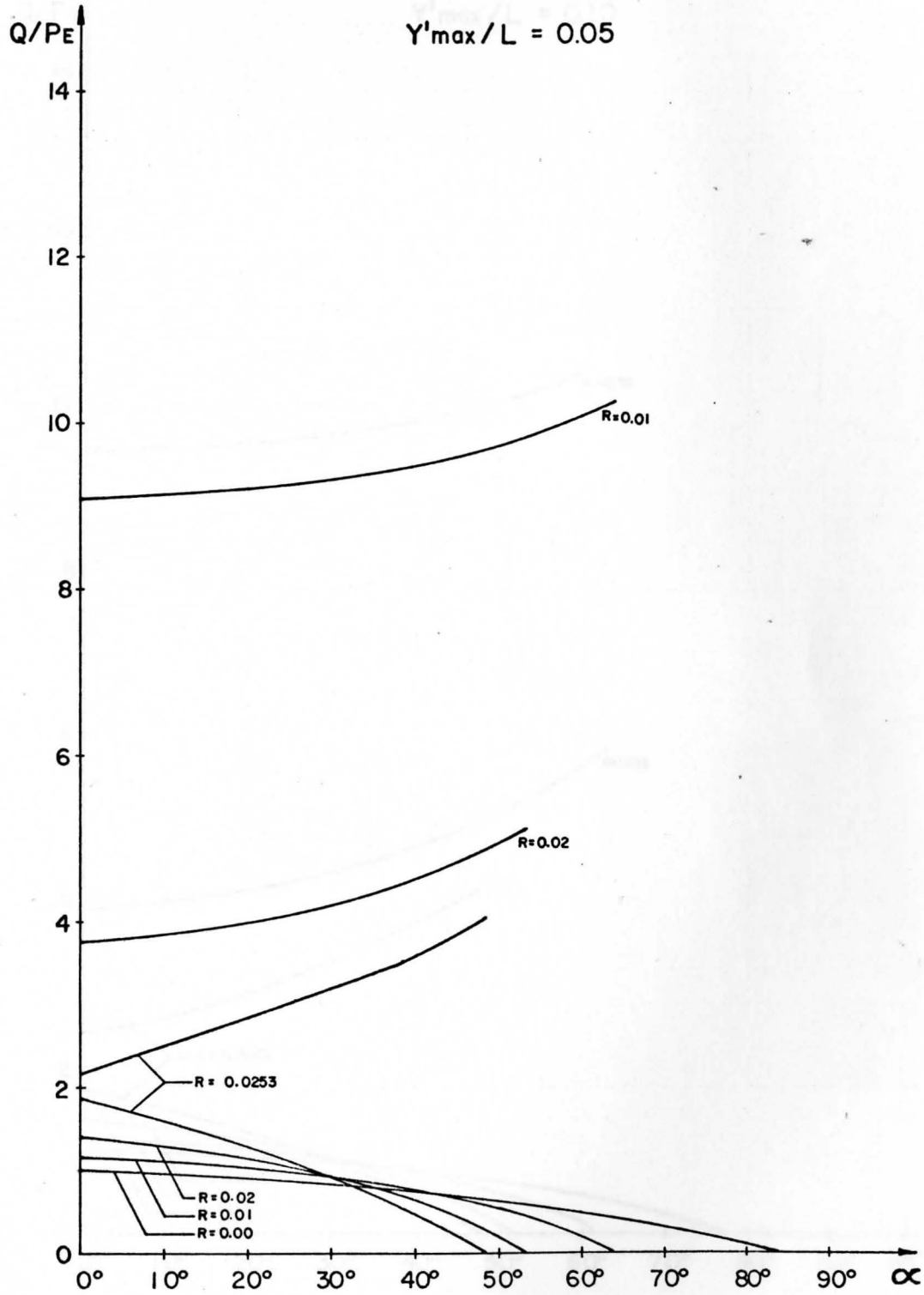

FIGURE 18b DIMENSIONLESS BUCKLING AND POSTBUCKLING LOADS VS. α , FOR VARIOUS VALUES OF R.

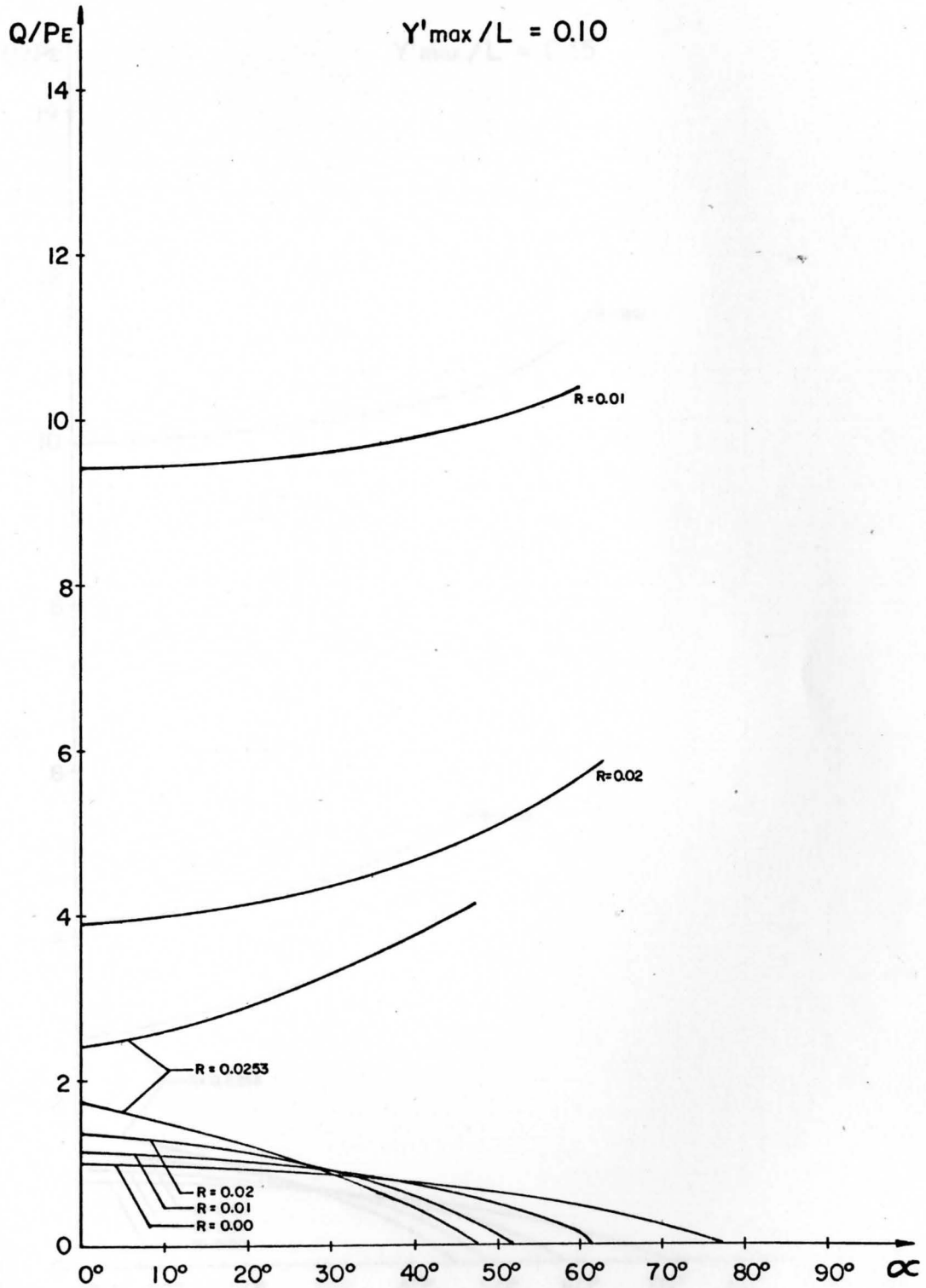

FIGURE 18c DIMENSIONLESS BUCKLING AND POSTBUCKLING LOADS VS. α, FOR VARIOUS VALUES OF R.

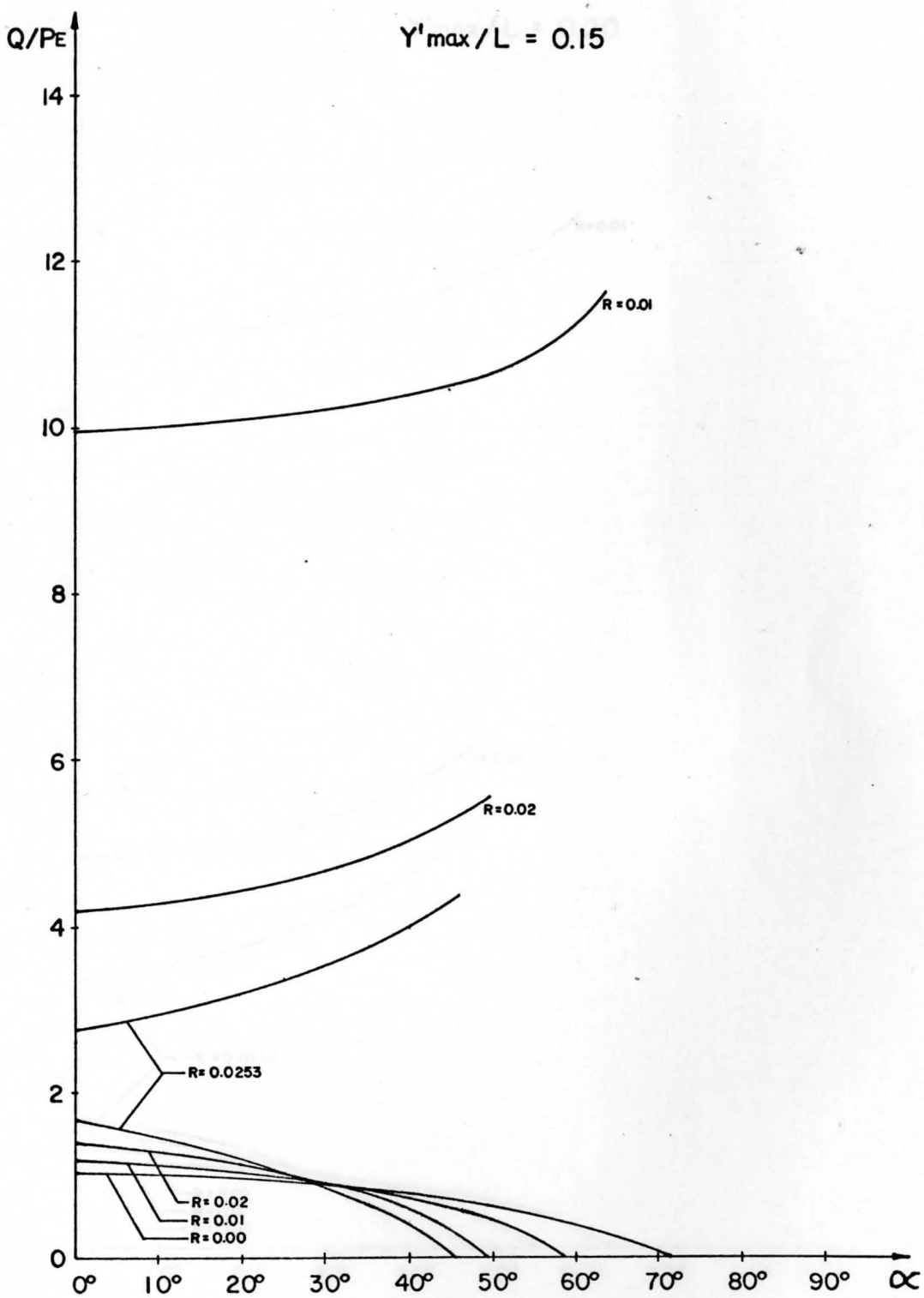

FIGURE 18d DIMENSIONLESS BUCKLING AND POSTBUCKLING LOADS VS. α, FOR VARIOUS VALUES OF R.

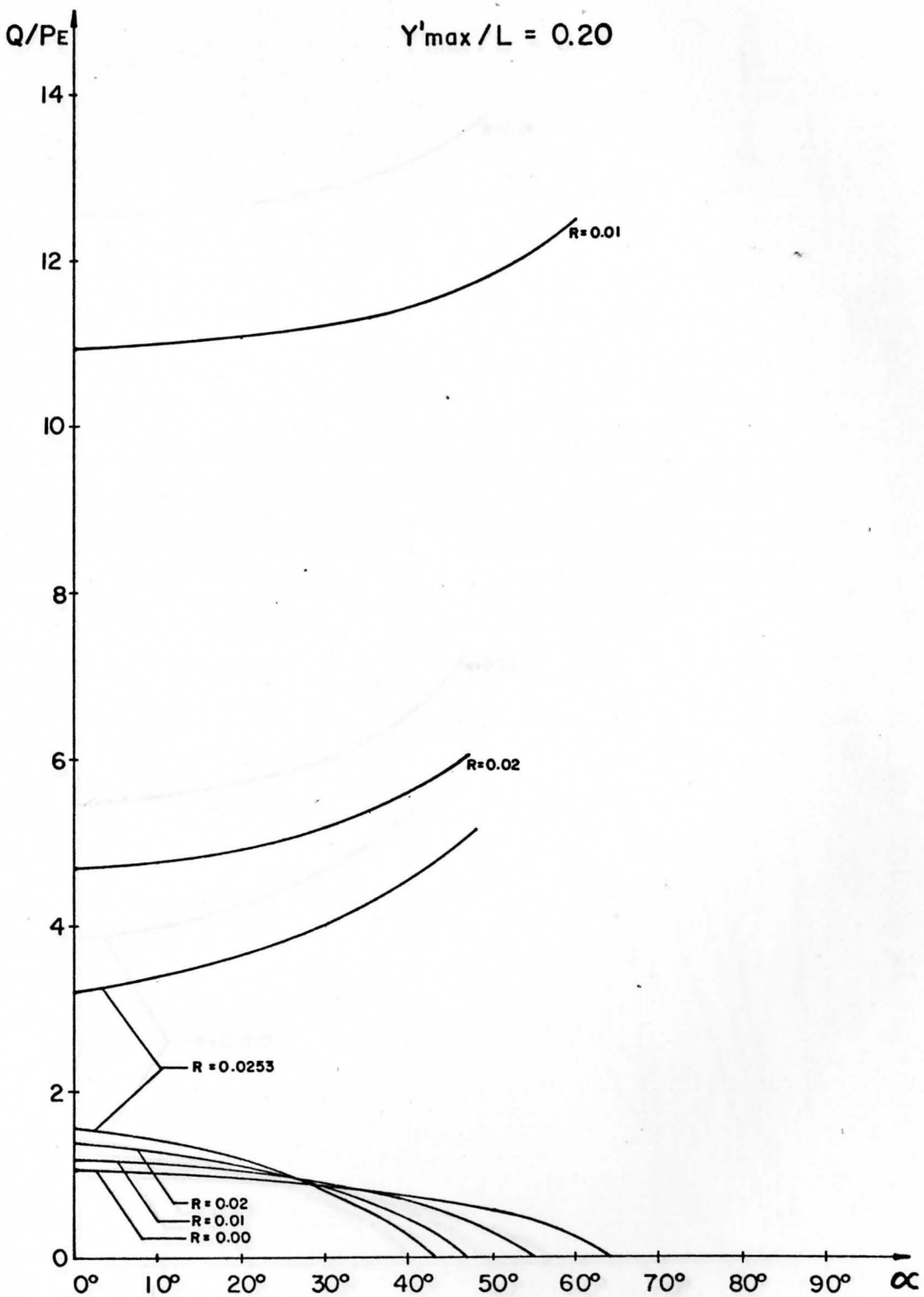

FIGURE 18e DIMENSIONLESS BUCKLING AND POSTBUCKLING LOADS VS. α, FOR VARIOUS VALUES OF R.

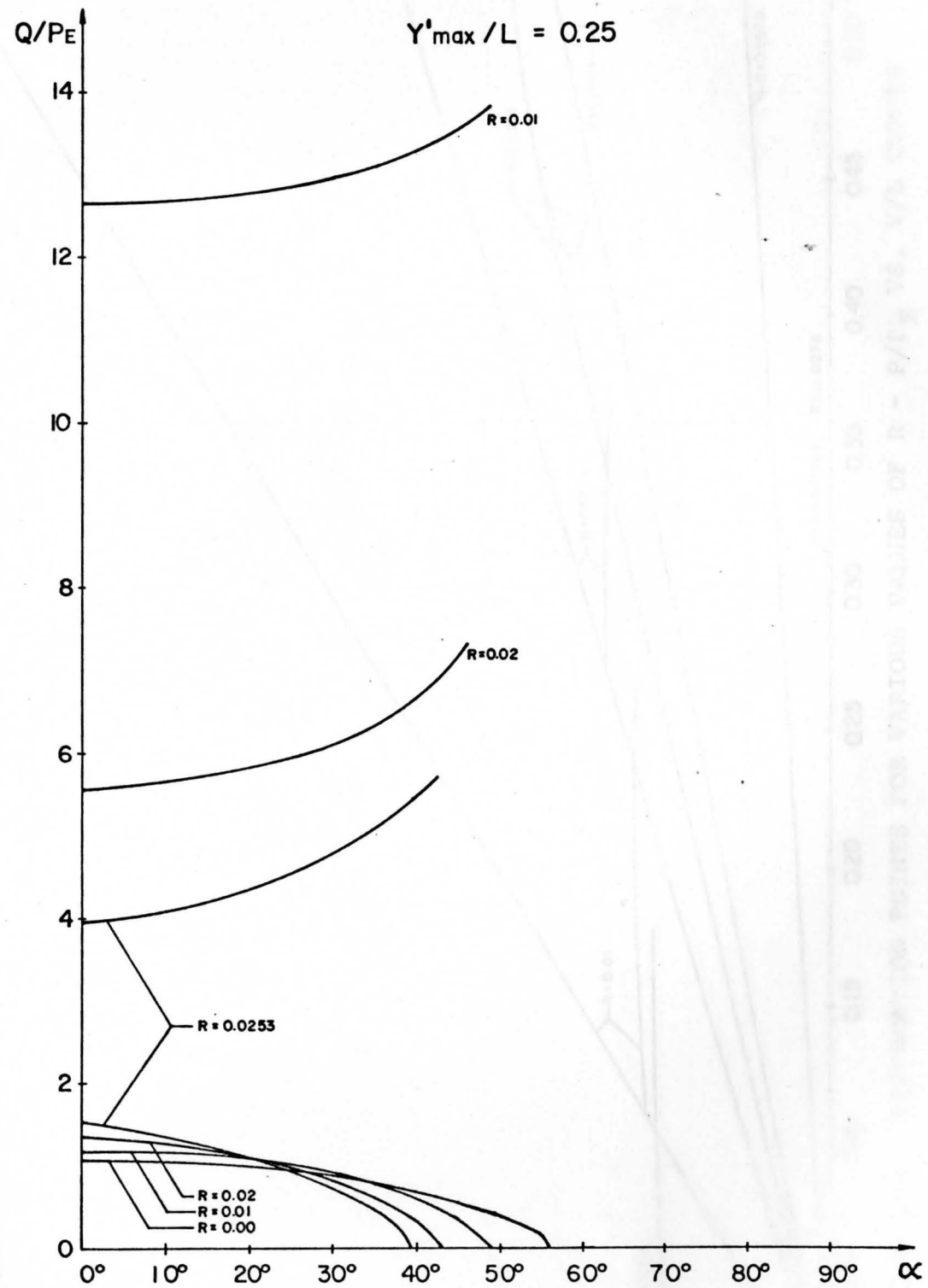

FIGURE 18f DIMENSIONLESS BUCKLING AND POSTBUCKLING LOADS VS. α, FOR VARIOUS VALUES OF R.

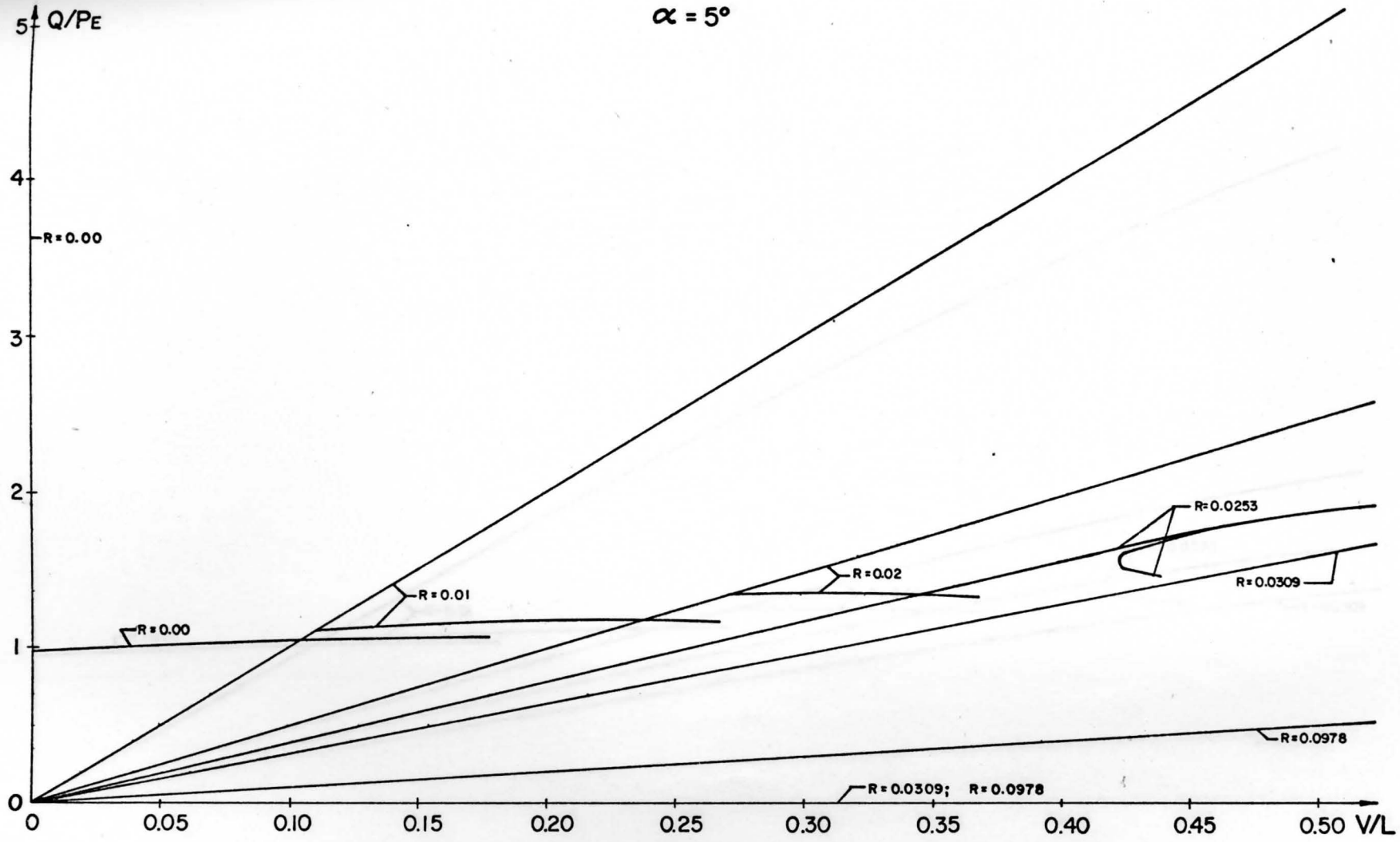

FIGURE 19a BIFURCATION POINTS FOR VARIOUS VALUES OF R - P/P_E VS. V/L CURVES

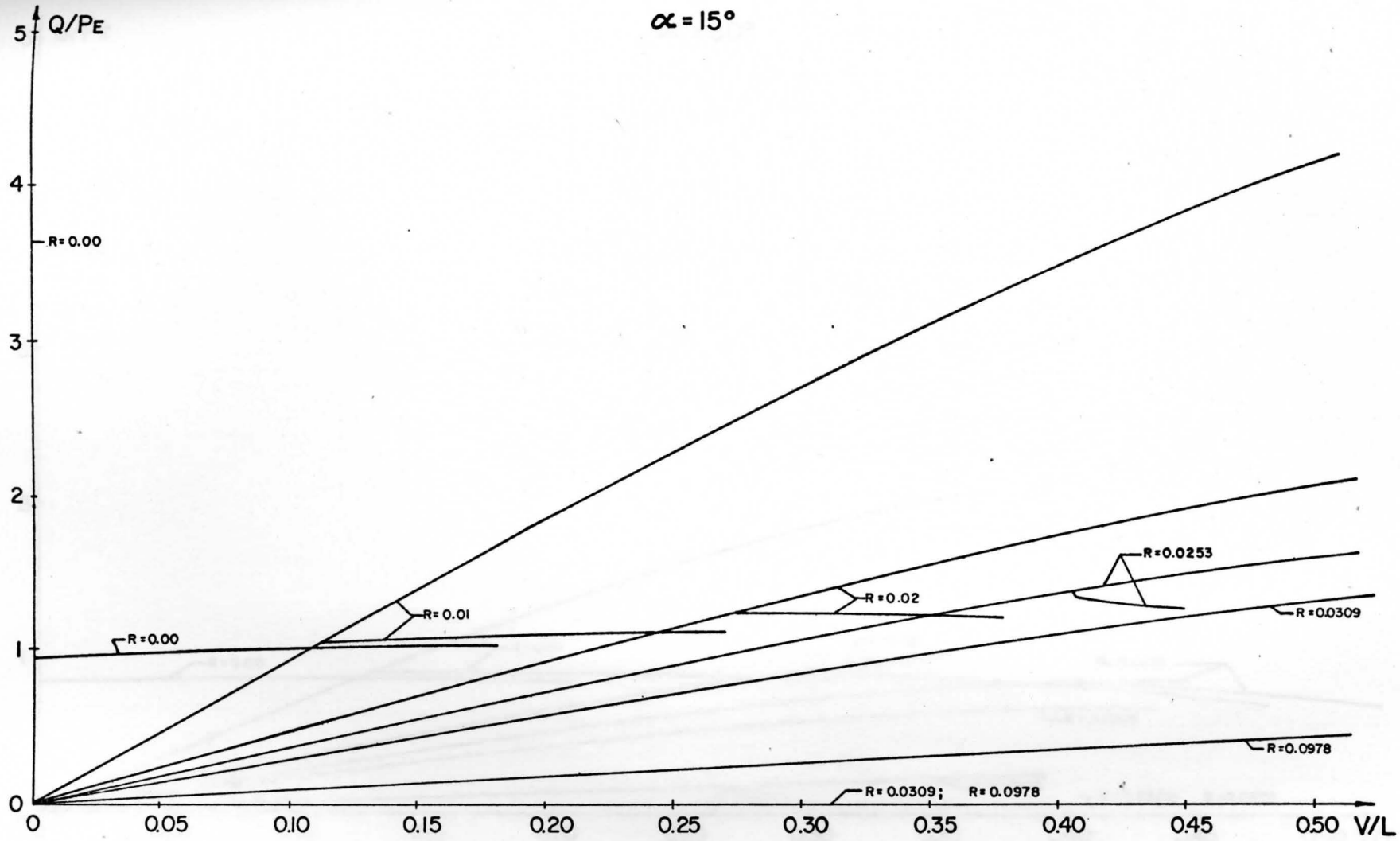

FIGURE 19b BIFURCATION POINTS FOR VARIOUS VALUES OF R - P/P_E VS. V/L CURVES

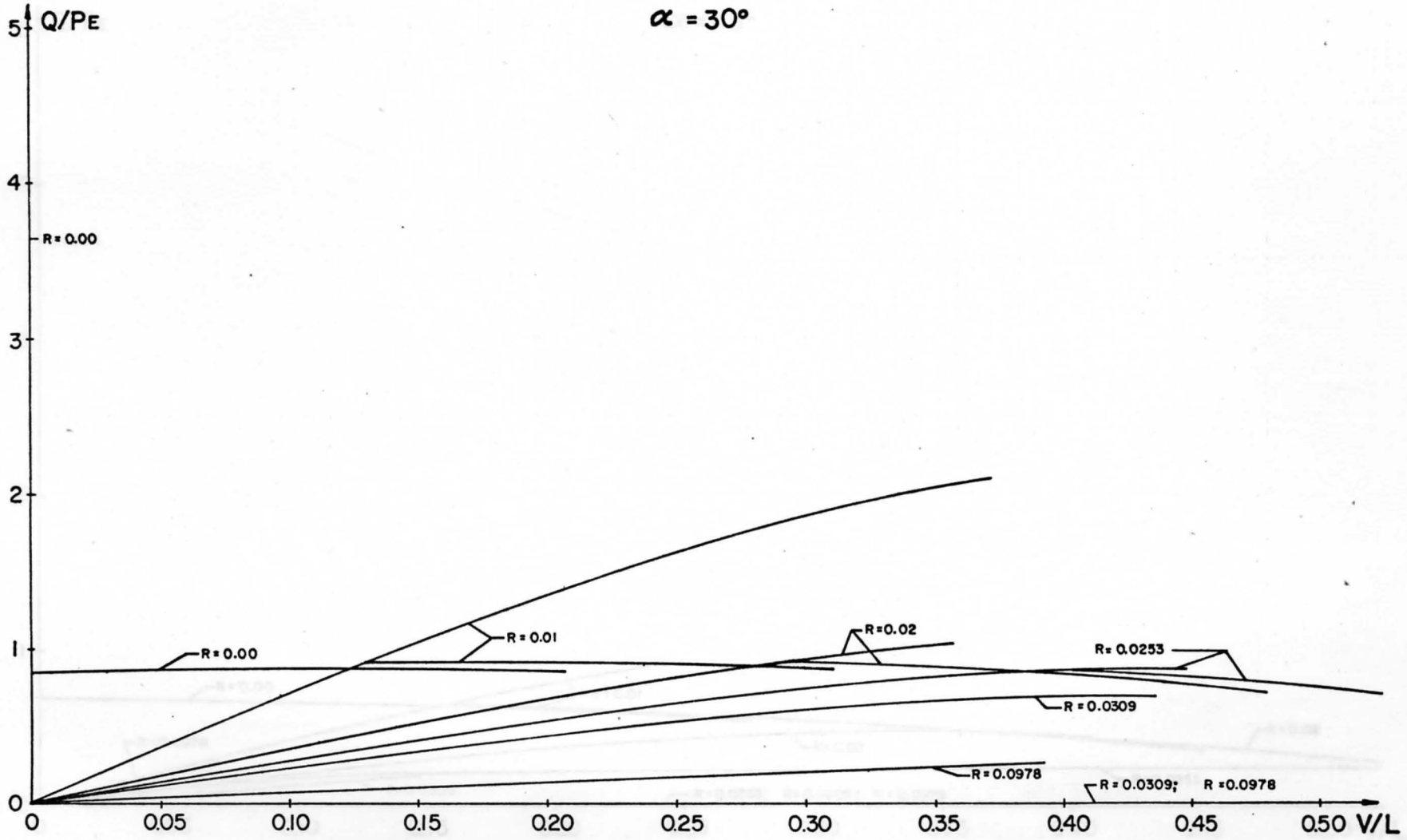

FIGURE 19c BIFURCATION POINTS FOR VARIOUS VALUES OF R - P/P_E VS. V/L CURVES

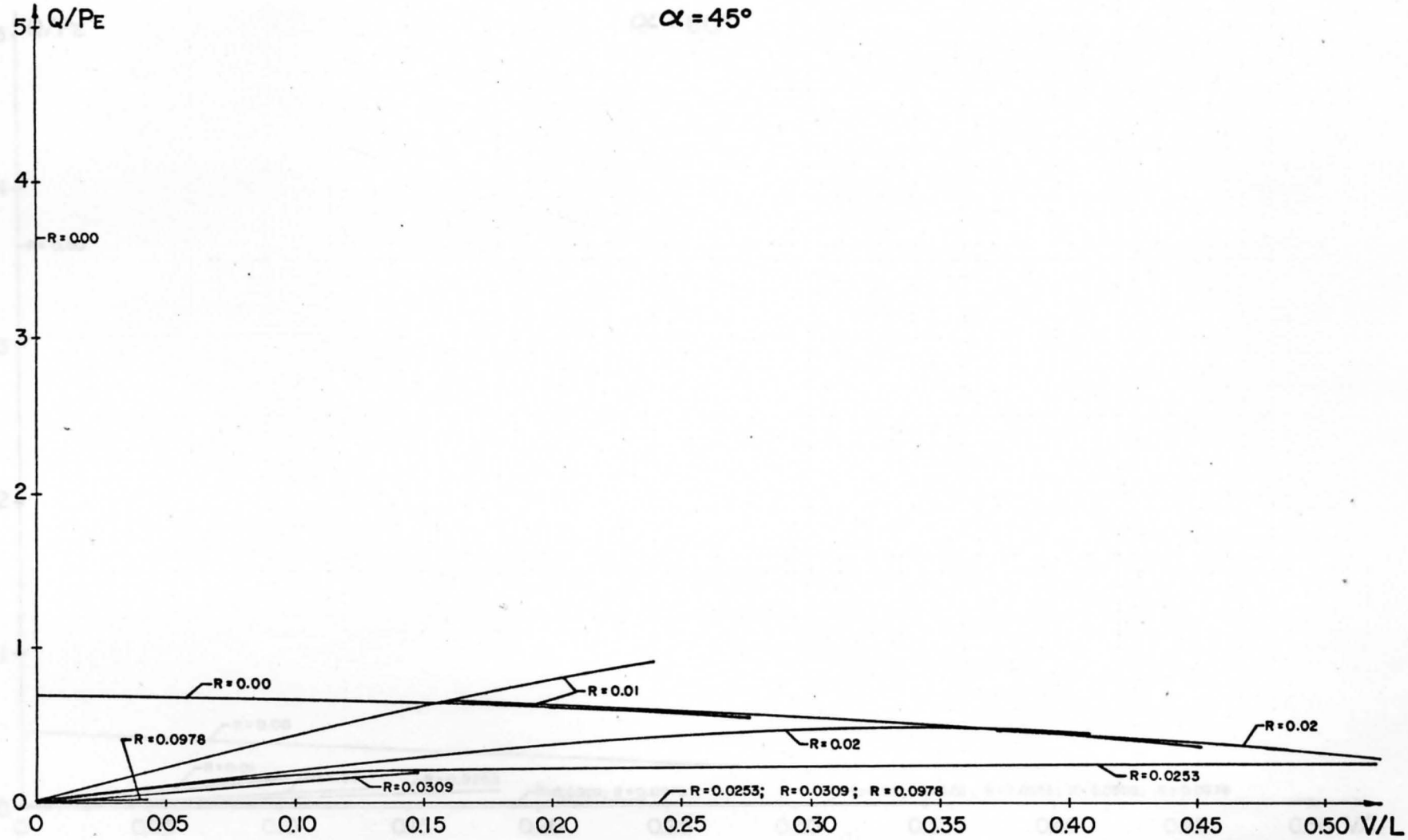

FIGURE 19d BIFURCATION POINTS FOR VARIOUS VALUES OF R - P/P_E VS. V/L CURVES

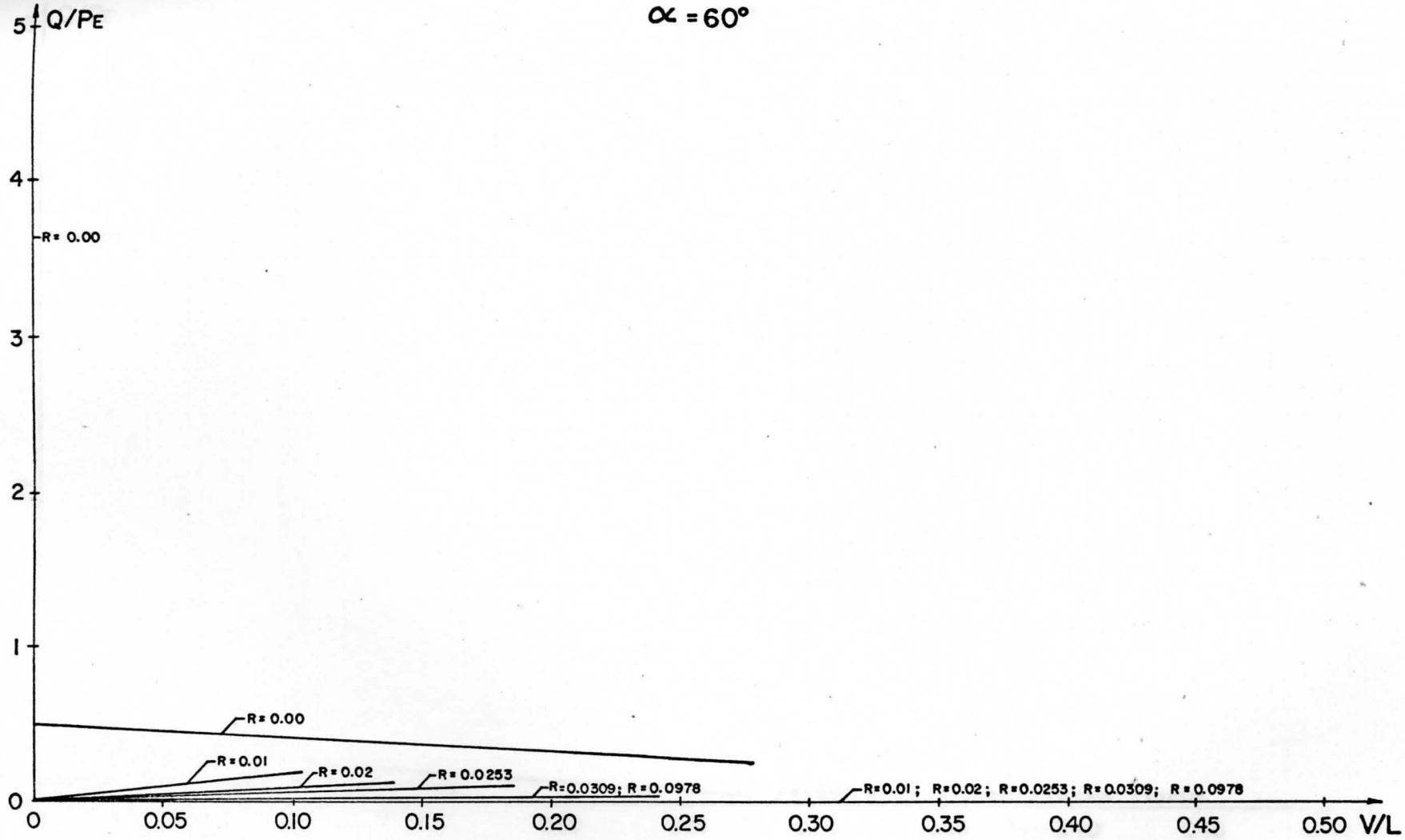

FIGURE 19e BIFURCATION POINTS FOR VARIOUS VALUES OF R - P/P_E VS. V/L CURVES

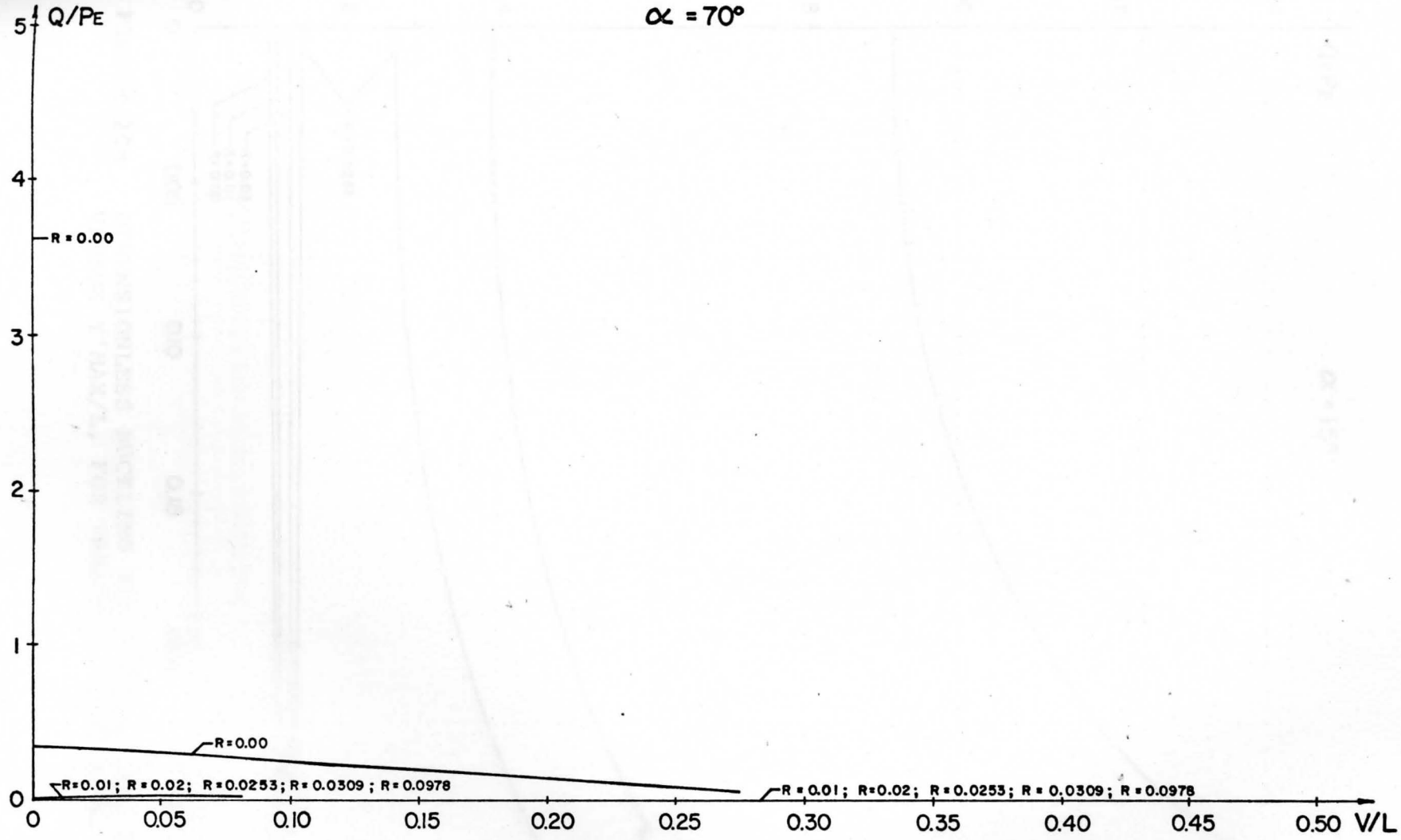

FIGURE 19f BIFURCATION POINTS FOR VARIOUS VALUES OF R - P/P_E VS. V/L CURVES

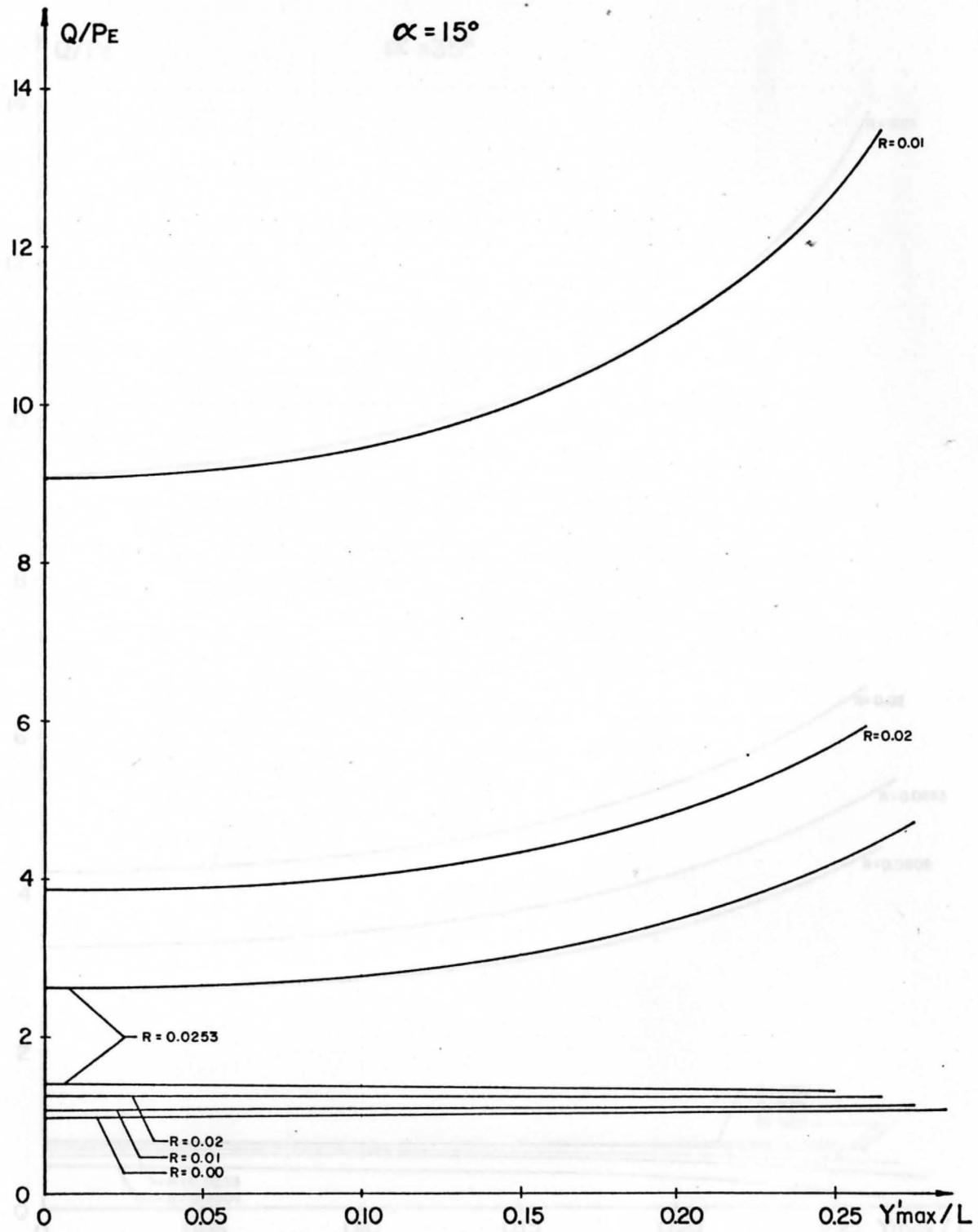

FIGURE 20a DIMENSIONLESS BUCKLING AND POSTBUCKLING LOADS VERSUS Y'MAX/L, FOR VARIOUS VALUES OF R.

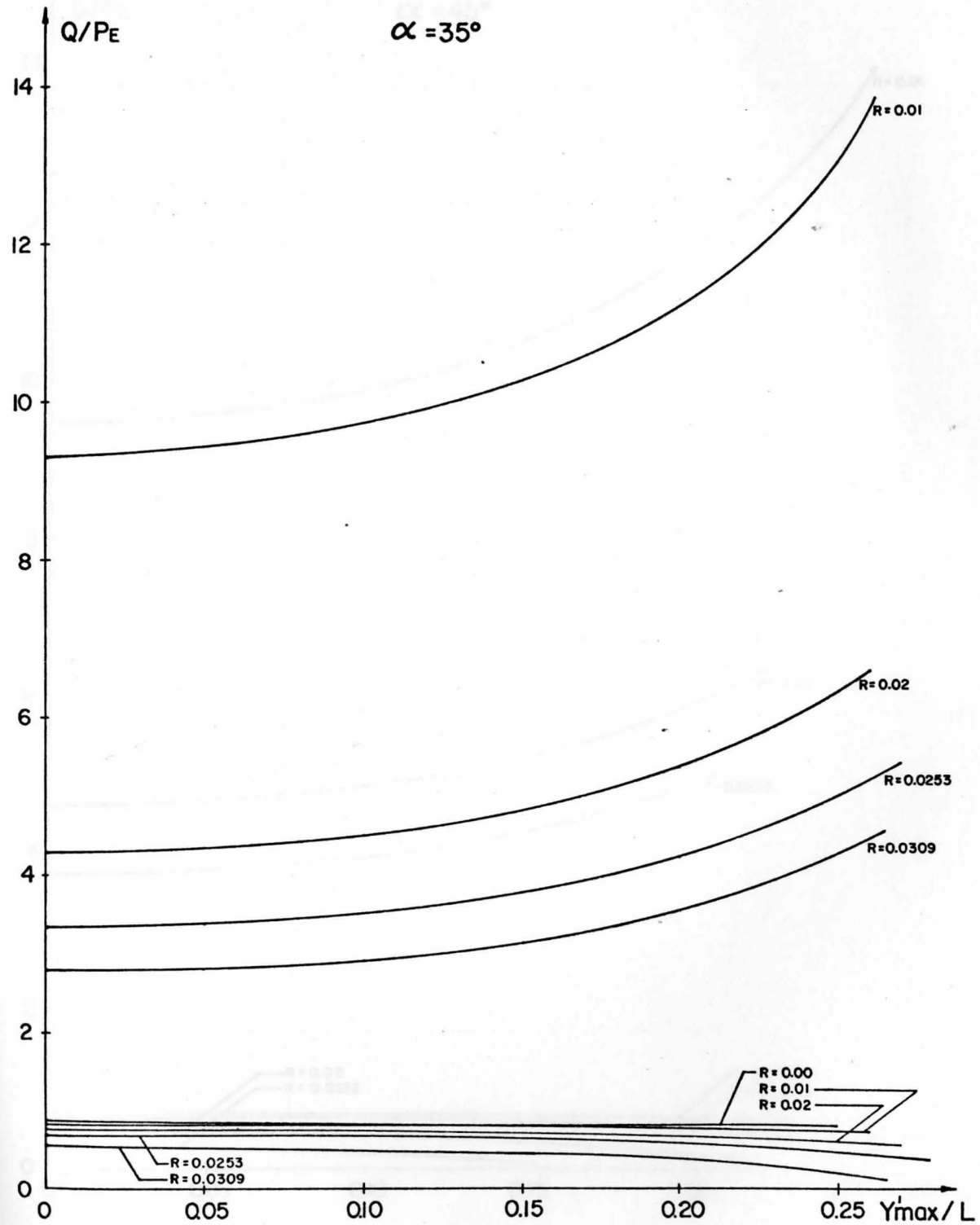

FIGURE 20b DIMENSIONLESS BUCKLING AND POSTBUCKLING LOADS VERSUS Y'MAX/L, FOR VARIOUS VALUES OF R.

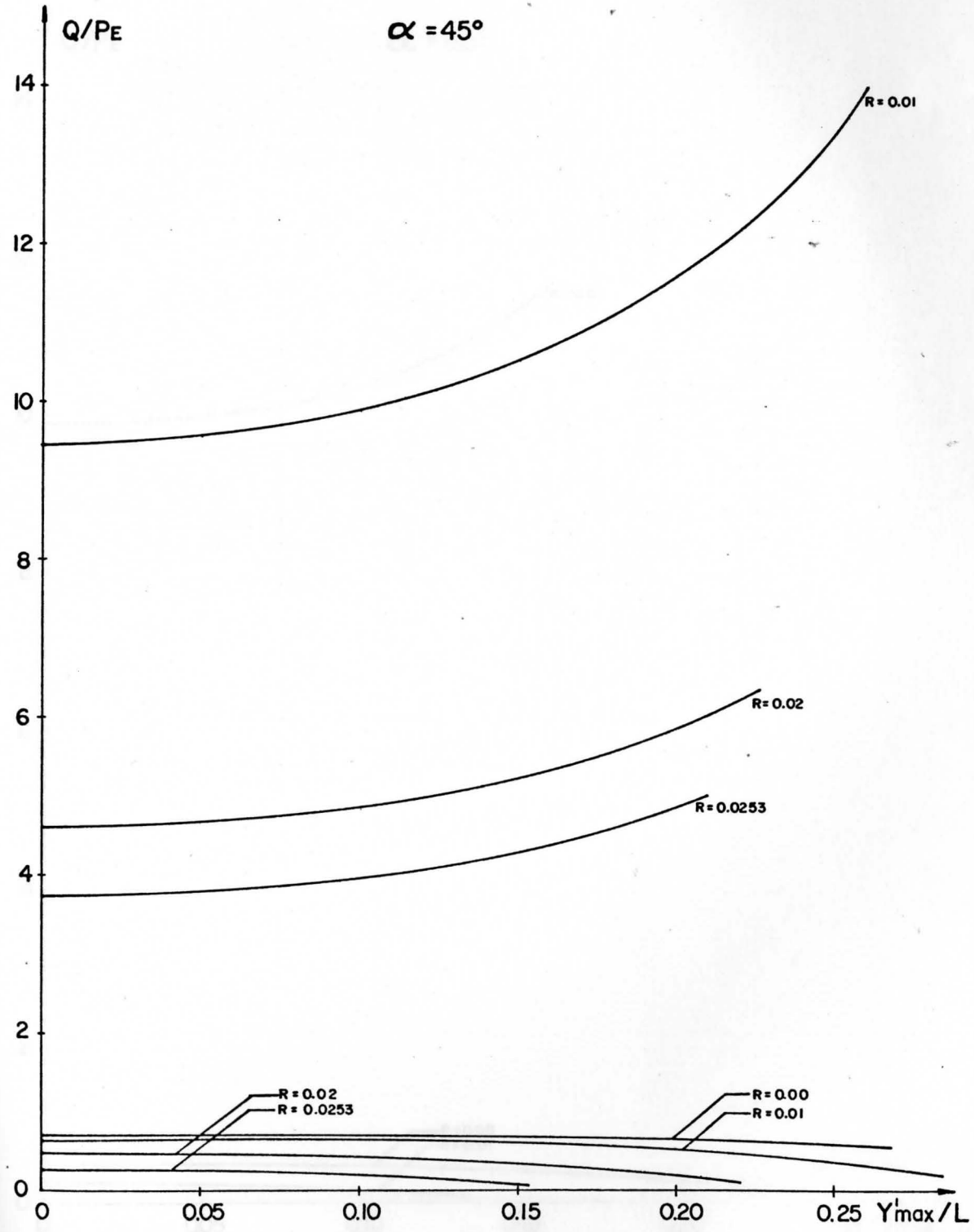

FIGURE 20c DIMENSIONLESS BUCKLING AND POSTBUCKLING LOADS VERSUS Y'MAX/L, FOR VARIOUS VALUES OF R.

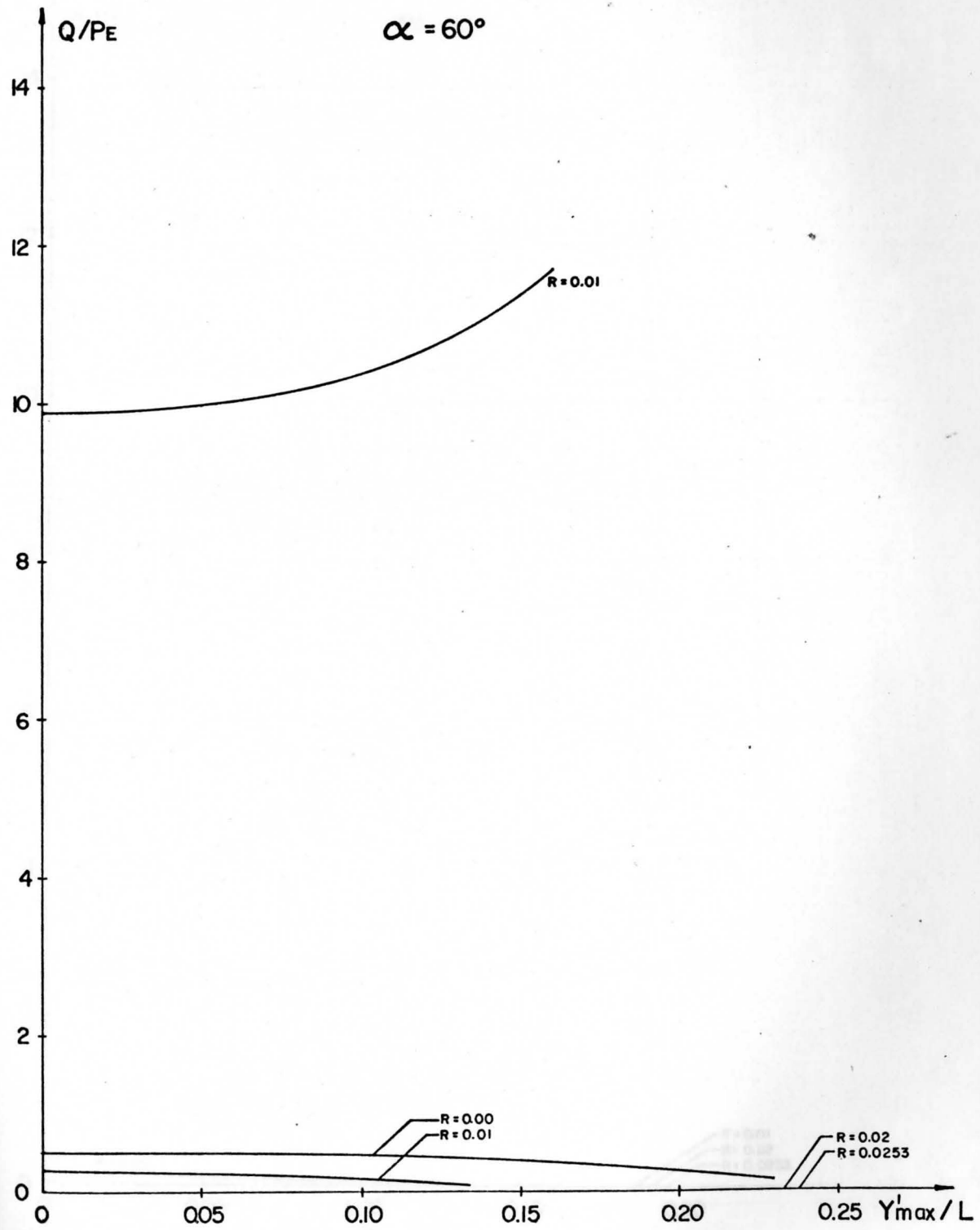

FIGURE 20d DIMENSIONLESS BUCKLING AND POSTBUCKLING LOADS VERSUS Y'MAX/L, FOR VARIOUS VALUES OF R.

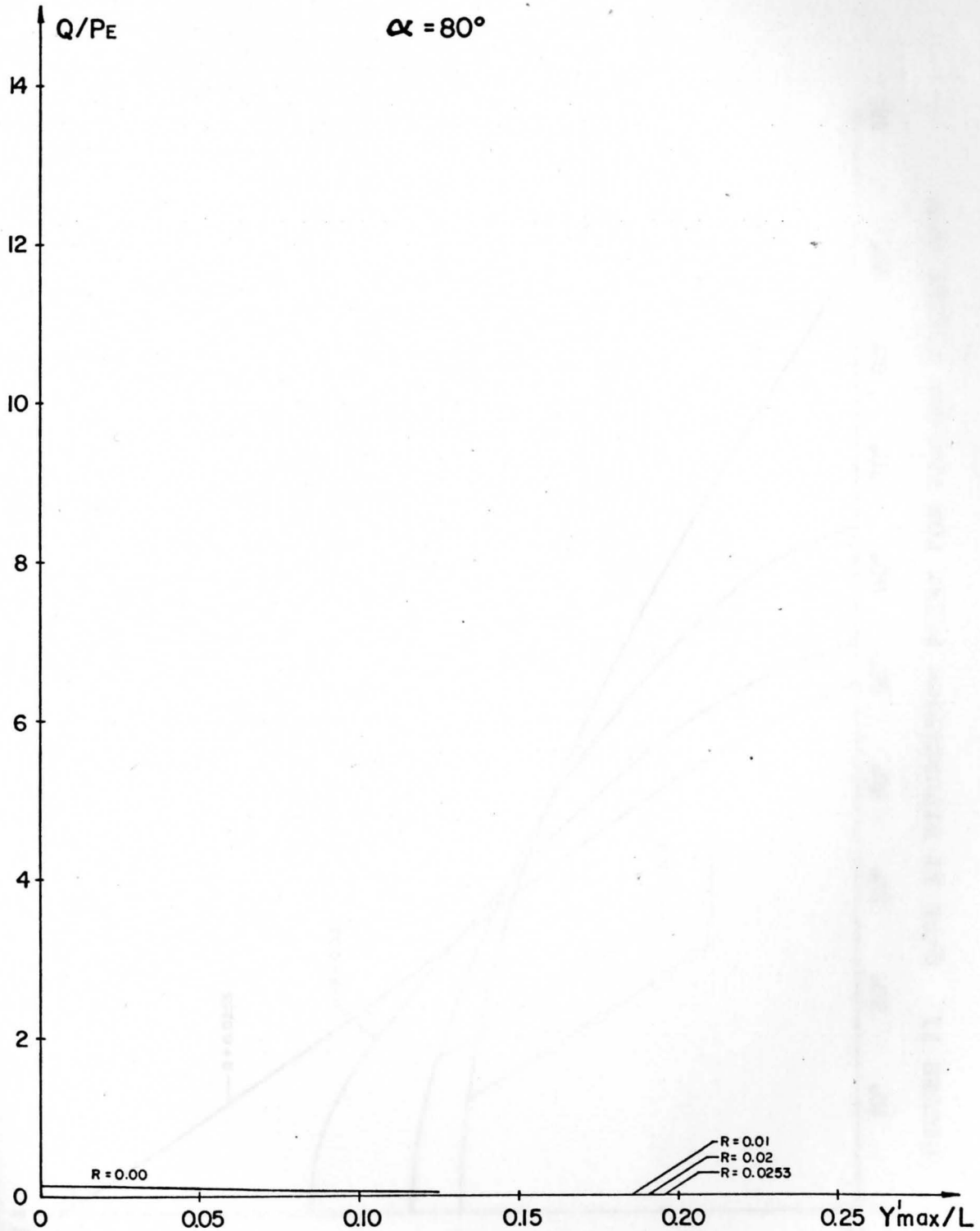

FIGURE 20e DIMENSIONLESS BUCKLING AND POSTBUCKLING LOADS VERSUS Y'MAX/L, FOR VARIOUS VALUES OF R.

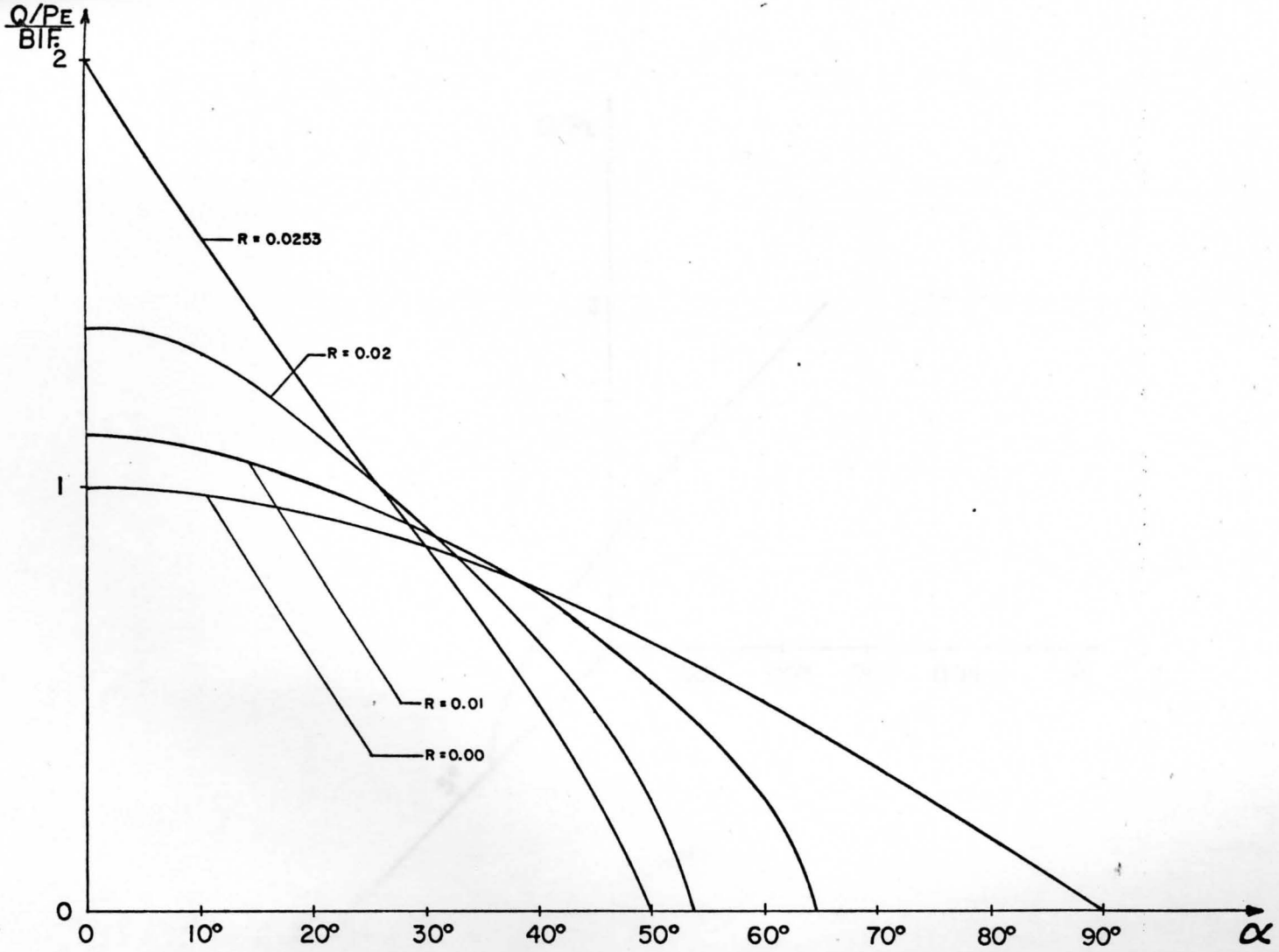

FIGURE 21 Q/PE AT BIFURCATION POINT FOR VARIOUS VALUES OF α

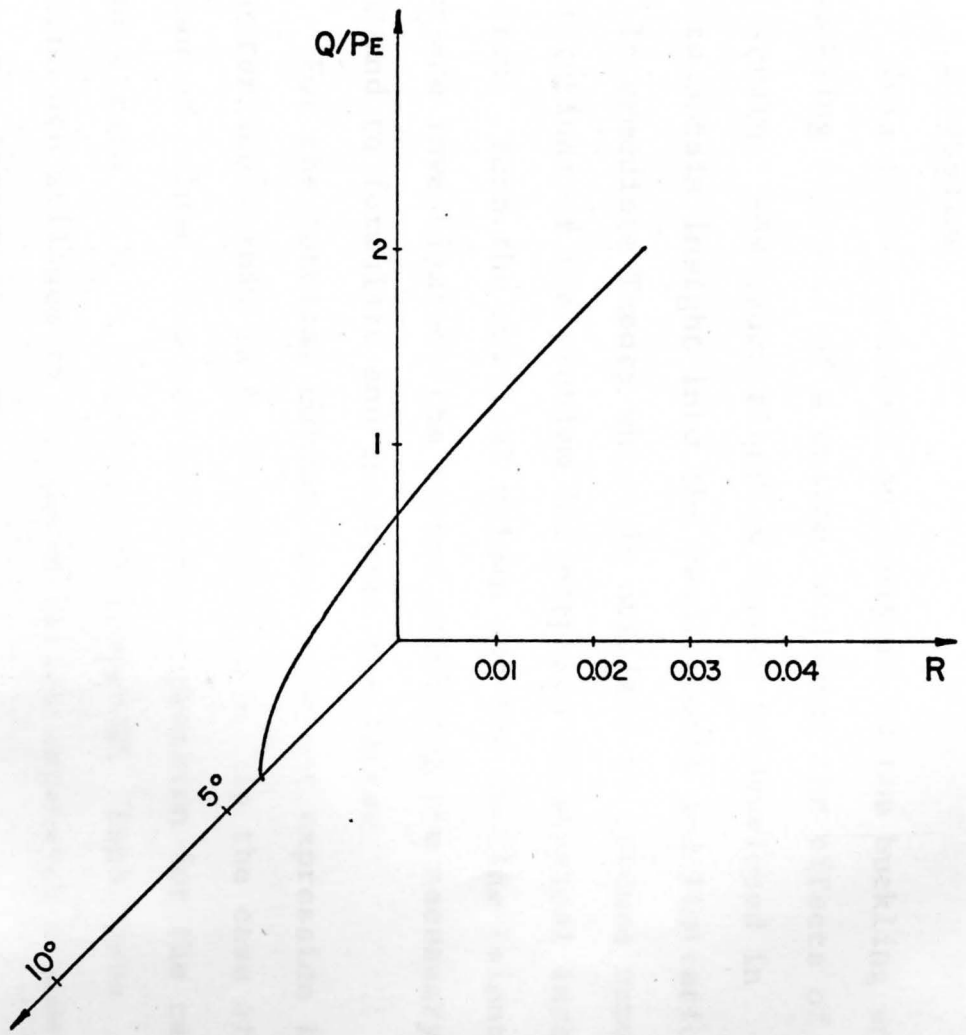

FIGURE 22 TRIFURCATION POINT FOR VARIOUS VALUES OF α

CHAPTER VI

DISCUSSION, CONCLUSIONS AND RECOMMENDATIONS

6.1 Discussion

This thesis presents an analysis of the buckling and postbuckling behavior of a column including the effects of axial strain. The exact elastica theory is developed in order to obtain insight into the requirements and limitations of an Intermediate Theory which is utilized to produce numerical solutions of the problem for purposes of physical interpretation. Both the vertical column and the incline (slanted) column are investigated, the former providing the necessary background to formulate and interpret the latter.

For the vertical column, the important expression for the centerline strain is $\epsilon_o = (P/EA) \cos \theta$. In the case of the slanted column, the corresponding expression for the centerline strain is $\epsilon_o = ((Q/EA)\cos\theta)/\cos(\alpha+\lambda))$. Both these functions are utilized in the power series expansion process used in the Intermediate Theory.

All numerical computations are carried out using a Hewlet Packard - 97 Programmable Calculator and checked by a set of Fortran IV programs run on an IBM computer and included in Appendix B.

For the vertical column, the following characteristic behavior exists as shown in Figure 10:

1. For R=0. The quadratic equation yields only one solution which is the "classical elastica solution." Consequently, only one bifurcation point exists.

2. For $0 < R < 0.02533$. A pair of bifurcation points corresponding to the two real roots of the quadratic equation, in P/P_E, are obtained. The curves themselves represent:
   a. For the lower values of P/P_E, shown the lower or primary mode of postbuckling behavior.
   b. For the upper values of P/P_E, shown the higher mode of postbuckling behavior.

3. R=0.02533. The quadratic equation yields two equal roots of P/P_E, which are 2. This solution is a trifurcation point which is the upper limit of the bending inestability mode.

4. R 0.02533. No bifurcation point exists corresponding to the complex roots of pipe obtained from the quadratic equation. The curves obtained show the pure axial instability defined as the condition where the column reduces to zero length without buckling and will remain stable unless subject to a perturbation.

Referring to Figure 11, the latter four geometrical observations are characterized in an alternate form. The inclined straight lines represent the pure axial mode of deformation. The intersection with the curved lines represent the

combined bending and axial mode. The three ranges of parameter R presented are interpreted as follows:

1. R = 0. Shows the case of the "classical elastica solution" with the bifurcation point located on the vertical axis ($P/P_E = 1$).

2. R = 0.02. Illustrates the two bifurcation points corresponding to the lower and higher modes of postbuckling.

3. R = 0.02533. Presents the trifurcation point and illustrates clearly the three paths that the column might follow in its postbuckling behavior.

It is observed from this graph that the column passes first through a state of pure axial compression reaching then a bifurcation point to finally follow the path of combined axial compression-bending mode with the least expenditure of energy.

Chapter V for the slanted column contains the geometrical and numerical results. The buckling characteristics of the inclined column are similar to that of the vertical column (i.e. bifurcation points, trifurcation points) for $0 < \alpha < 13.01^{o} \pm$. Beyond this value of α no trifurcation point exists as shown on Table 5, however, the three modes of postbuckling behavior still exists, but with no common boundary.

Referring to Figure 21, the graph illustrates the path that the bifurcation points follow for a range of the parameter α. The corresponding curves for R = 0, R = 0.01, R = 0.02 and R = 0.02533 interchange their path at approximately $\alpha = 31^{o}$. It is observed in this graph that for the larger value of R one obtains a smaller Q/P_E value for α more than 31^{o}.

6.2 Conclusions

The present study clearly shows that the Intermediate Theory produces reasonably accurate results for the case of the vertical column, with a technique that is relatibly simple. A comparison of the study performed by J. V. Huddleston[12] (see Appendix A, Figure A1 and Figure A2) shows that the curves of postbuckling loads versus the mid point displacements are in close agreement with that of the Intermediate Theory shown in Figure10. For Ymax/L $\leq$ 0.025, the Intermediate Theory produces identical results as the "exact" theory, for the lower deformation mode. This is of extreme importance since the lower mode controls in design, as well as the fact that the Intermediate Theory is relatively simple to apply. The mathematical technique of the Intermediate Theory yields a set of nonlinear algebraic equations which are simpler to solve numerically than the classical set of nonlinear differential equation.

The agreement between the Intermediate Theory and the "exact" solution for the higher bending mode of buckling is

reasonably good for Ymax/L smaller than 0.0025.

For the pure axial compression mode, the Intermediate Theory yields reasonably accurate results for $0.226 < Ymax/L < 0.35$.

Throughout the numerical computations, the value of ϵ_o is calculated and recorded to insure that it remains within the range of the nonlinear theory, that is, $\epsilon_o < 1.0$. For the lower bending mode with $Ymax/L < 0.025$ the value of ϵ_o always satisfied the latter inequality.

The Intermediate Theory is highly efficient because it exposes all the important phenomena involved in the post-buckling behavior of a column with a fairly simple process as well as accurate results for the range of parameters of practical engineering problems.

The results obtained by applying the Intermediate Theory to the slanted column, as expected, are quite encouraging. The classical solution for the elastica problem does not reveal the three basic modes of postbuckling behavior. The inclusion ofaxial strain eliminates the incompleteness of this theory.

The trifurcation is present only when the mathematical model that represents the column allows the axial strain to be an integral part of the solution. The primary observation inherent in the solutions is that the buckling load decreases as the inclination angle α increases.

Referring to Figure 21, a plot is shown in Figure 23 relating the limiting values of α when $Q/P_E = 0$ versus the

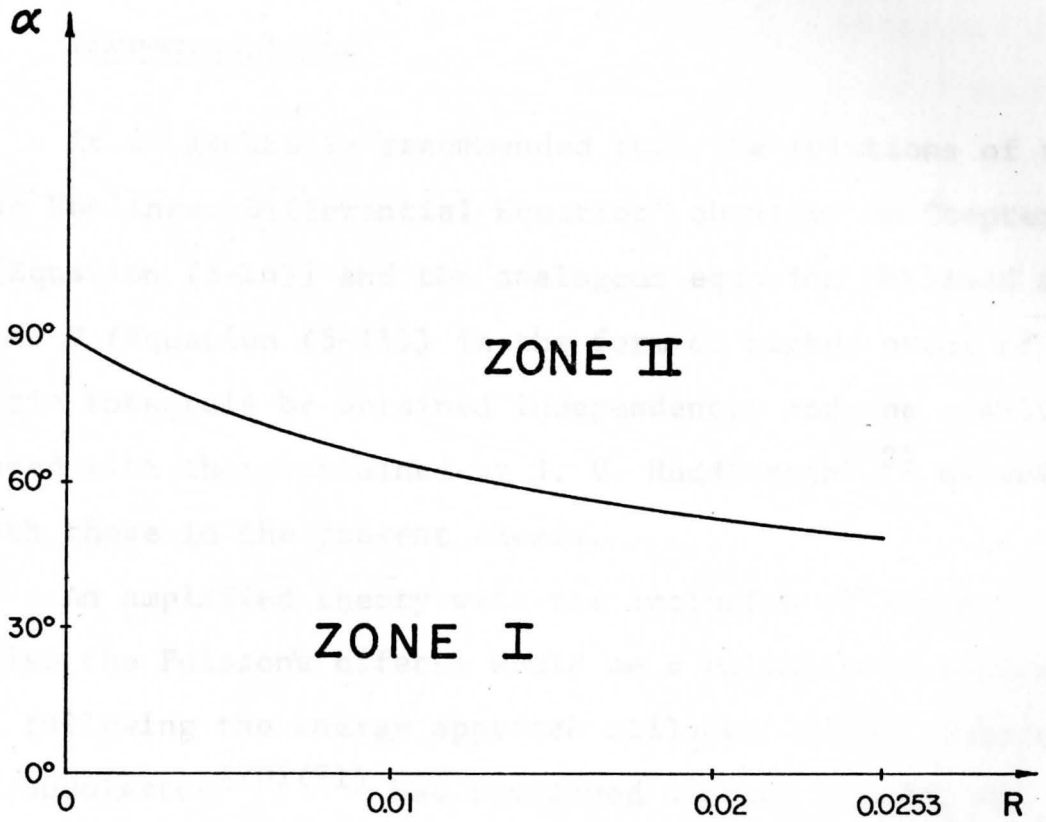

Figure 23 Limits of Bending Inestability for Slanted Column

associated values of R. The graph is divided into two zones. Zone I represents combinations of R & α where bending instability occurs after a finite amount of axial shortening. Zone II contains points where instability, if it exists, is most probably a pure axial phenomenon.

6.3 Recommendations

It is generally recommended that the solutions of the "Basic Nonlinear Differential Equation" obtained on Chapter III (Equation (3-16)) and the analogous equation obtained on Chapter V (Equation (5-11)) in the form of higher order of elliptic integrals be obtained independently and the results compared with those obtained by J. V. Huddleston[12] as well as with those in the present thesis.

An amplified theory with the inclusion of shear strains and also the Poisson's effects would be a valuable investigation, following the energy approach utilized in this thesis. J. V. Huddleston[20][21] has developed already a study in these areas by using the differential equation method.

An important investigation which is highly recommended is the reduction in the value of ϵ_o below unity based upon the number of terms used in the power series expansion process and in the number of terms taken in the assumed bending deflections function.

It is the observation of this author that future work on this problem should investigate the following areas:

1. A more precise geometrical interpretation of the P/P_E vs. V/L curves for the vertical column especially for the values $0.02 < R < 0.03$ although this thesis has already made significant contributions in this area.

2. An interpretation of the stability characteristics of the slanted column for value of R and α lying in Zone II of Figure 23 would be of significant value.

APPENDIX A

COMPARISON OF RESULTS WITH THE "EXACT" SOLUTION

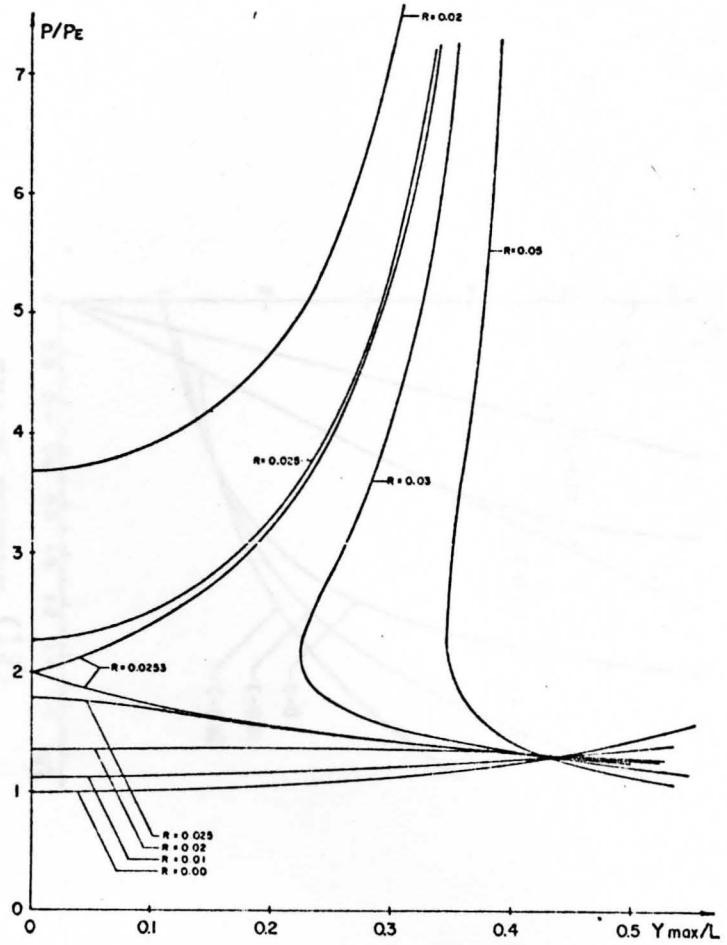

INTERMEDIATE THEORY

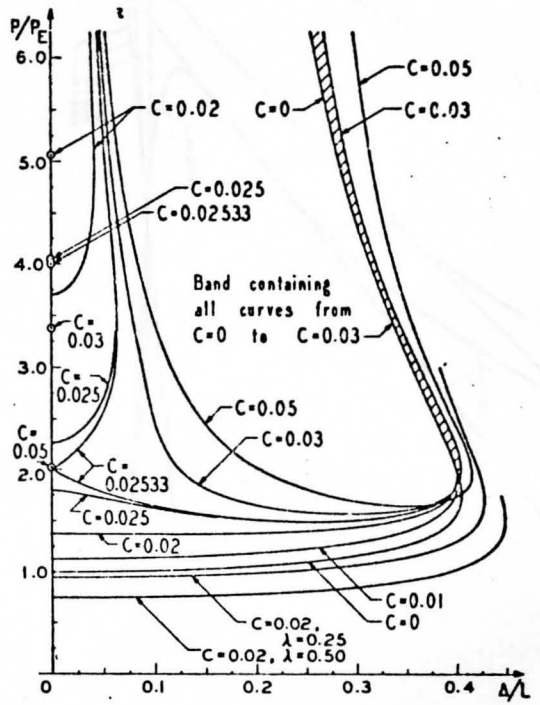

EXACT THEORY (12)

Figure A1

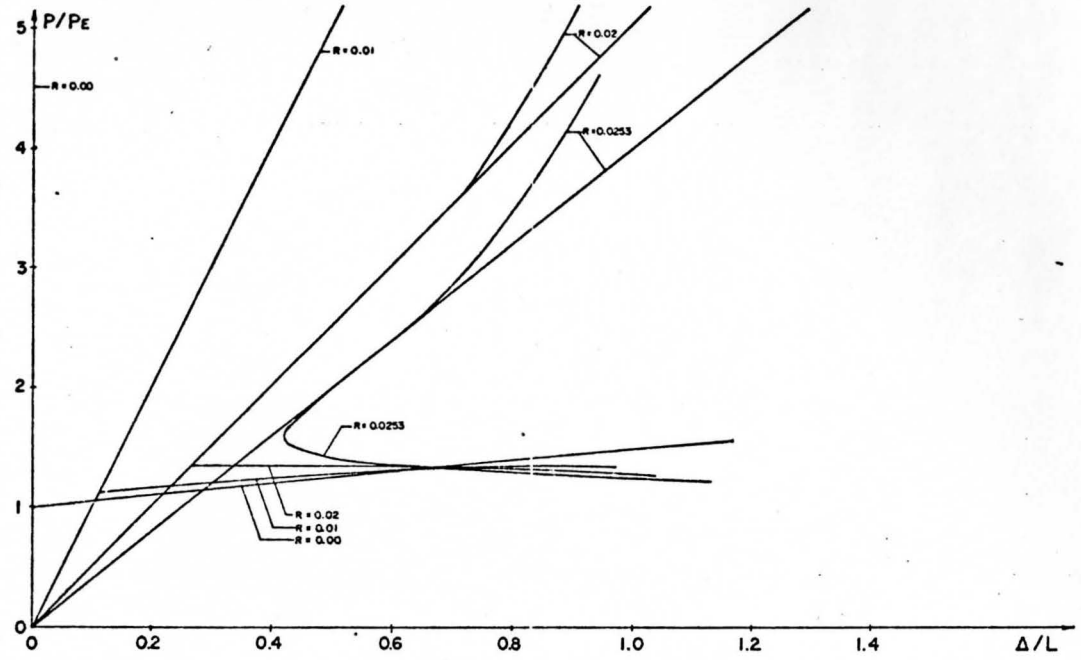

INTERMEDIATE THEORY

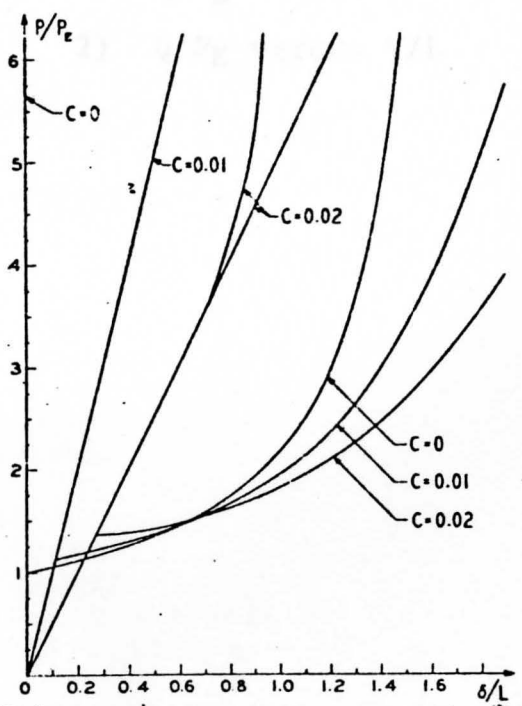

EXACT THEORY (12)

Figure A2

APPENDIX B

COMPUTER PROGRAMS FOR

1) Q/P_E versus Y'max/L

2) Q/P_E versus V/L

```
      IMPLICIT REAL*8(A-H,O-Z)
      DATA ERS/1.D-10/
      PI=3.14159265359D00
      BETHA=PI/9000.
      WRITE(3,400)PI,DELTA,BETHA
   50 FORMAT(2F10.0)
  250 FORMAT(6F20.8)
  350 FORMAT(' YMAX/L=',F10.2,'R=',F15.10)
  360 FORMAT(F20.8,'  *****IMAGINARY ROOTS FOR Q/PE*****')
  400 FORMAT(' PI= ',F20.15,'  DELTA= ',F20.17,'  BETHA=',F25.20//)
  270 FORMAT('ONOT ABLE TO FIND LAMDA AFTER 5000 TRIES',5X,'XLNEW=',
     +F20.8,'  XLOLD=',F20.8,'  JUMPING TO NEXT Y/L',///)
      CALL REREAD
   20 READ(7,50)R,YMAXL
      IF(YMAXL .LT. -999.)STOP
      WRITE(3,350) YMAXL,R
      IWRITE=1
      J=0
      IERROR=0
      DELTA=PI/36.
      A=YMAXL*PI
      A2=A*A
      A4=A2*A2
      A6=A4*A2
      A8=A4*A4
      AA=(2.-15.*A4/32.-35.*A6/512.)*R*PI*PI
      BB=2.+3.*A2/4.
      CC=2.+A2+3.*A4/16.
      ALPHA=0.-DELTA
   70 DO 300 I=1,19
      ALPHA=ALPHA+DELTA
   90 ICOUNT=0
      XLOLD=0.
  100 COSAL=DCOS(ALPHA+XLOLD)
      ICOUNT=ICOUNT+1
      IF(R.EQ.0.)QPE2=CC*COSAL/BB
      QPE1=QPE2
      IF(R.EQ.0.) GO TO 150
      SIGN=BB*BB-4.*AA*CC*COSAL
      IF(SIGN .GE. 0.) GO TO 130
      DALPHA=ALPHA*180./PI
      WRITE(3,360)DALPHA
      GO TO 300
  130 RR=DSQRT(SIGN)
      QPE1=(BB+RR)/(2.*AA)
      QPE2=(BB-RR)/(2.*AA)
  150 VOL=.25*(4.-(4.-A2-3.*A4/16.)*DCOS(XLOLD)+QPE2*PI*4*
     1PI*R*DCOS(XLOLD)/COSAL*(1.-A2/2.+5.*A6/128.+35.*A8
     2/8192.))
      TANAL=DTAN(ALPHA)/(1.-VOL/(DCOS(ALPHA)*DCOS(ALPHA)))
      XLNEW=DATAN(TANAL)-ALPHA
      IF(DABS(XLNEW-XLOLD) .LT. ERS) GO TO 200
      IF(ICOUNT .GT. 5000) GO TO 170
      IF(ALPHA+XLNEW .LE. PI/5.) XLOLD=XLNEW
      IF(ALPHA+XLNEW .GT. PI/5.)XLOLD=(XLOLD+XLNEW)/2
```

```
      GO TO 100
  170 DXLNEW=XLNEW*180./PI
      DXLOLD=XLOLD*180./PI
      WRITE(3,270) DXLNEW,DXLOLD
      GO TO 20
  200 UOL=VOL/DCOS(ALPHA)
      DALPHA=ALPHA*180./PI
      DXLOLD=XLOLD*180./PI
      IF(IWRITE .EQ. 1)
     +WRITE(3,250)DALPHA,QPE1,QPE2,DXLOLD,VOL,UOL
      IF(IERROR .EQ. 1) GO TO 20
      IF(DXLOLD .LT. 0.) GO TO 450
  300 CONTINUE
      GO TO 20
  450 CONTINUE
      ALPHA=ALPHA-DELTA
      DELTA=DELTA/10.
      IWRITE=0
      J=J+1
      IF(J .LT. 4) GO TO 70
      IWRITE=1
      IERROR=1
      ALPHA=ALPHA-DELTA*10.
      GO TO 90
      END
```

```
      IMPLICIT REAL*8(A-H,O-Z)
      DATA ERS/1.D-10/
      PI=3.14159265359D00
      DELTA=PI/36
   50 FORMAT(2F10.0)
  270 FORMAT('ONOT ABLE TO FIND LAMDA AFTER 5000 TRIES  ',' XLNEW
     +F20.8,'XLOLD= ',F20.8,'  JUMPING TO NEXT  R  ',///)
  350 FORMAT('OR = ',F10.2,5X,'QPEZ = ',F15.10)
      CALL REREAD
   20 READ(7,50)R
      IERROR=0
      IF(R .LT. 0)STOP
      DO 300 I=1,21
      READ(7,50)QPEZ
      IF(IERROR .EQ. 1) GO TO 300
      WRITE(3,350)R,QPEZ
      ALPHA=-DELTA
      DO 280 J=1,18
      ALPHA=ALPHA+DELTA
      XLOLD=0.
      ICOUNT=0
  100 COSAL=DCOS(ALPHA+XLOLD)
      ICOUNT=ICOUNT+1
      UOL=.25*(4.-4*DCOS(XLOLD)+QPEZ*4*PI*PI*R*DCOS(XLOLD)/COSAL)
      TANAL=DTAN(ALPHA)/(1.-UOL/DCOS(ALPHA)/DCOS(ALPHA))
      XLNEW=DATAN(TANAL)-ALPHA
      IF(DABS(XLNEW-XLOLD).LT.ERS) GO TO 200
      IF(ICOUNT .GT. 5000) GO TO 150
      IF(ALPHA+XLNEW .LE. PI/5.) XLOLD=XLNEW
      IF(ALPHA+XLNEW .GT. PI/5.) XLOLD=(XLOLD+XLNEW)/2
      GO TO 100
  150 DXLNEW=XLNEW*180./PI
      DXLOLD=XLOLD*180./PI
      WRITE(3,270)DXLNEW,DXLOLD
      IERROR=1
      GO TO 300
  200 VOL=UOL/DCOS (ALPHA)
      DALPHA=ALPHA*180./PI
      DXLOLD=XLOLD*180./PI
      WRITE(3,250)DALPHA,QPEZ,DXLOLD,UOL,VOL
  250 FORMAT(6F20.8)
      IF(DXLOLD .LT. 0.) GO TO 300
  280 CONTINUE
  300 CONTINUE
      GO TO 20
      END
```

BIBLIOGRAPHY

1. Koiter, W.T., On the "Stability of Elastic Equilibrium", Dissertation, Delft, Holland (1945). English translation, NASA, TT, FIO (1967).

2. Kirchhoff, G.R., J. Math, (Crelle Journal), vol. 56 (1859) or Vorlesungen uber Math. Physik, Mechanik.

3. Bernoulli, J., Collected Works (1744), vol. 2, p. 976.

4. Euler, L., The Addendum to "De Durvis Elasticis" in the Methodus Inveniendi Lineas Curvas Maximi Minimive Propietate Gaudentes, Lausanne, (1744)

5. Bernoulli, D., Correspondence Mathematique et Physique (1843), vol. 2.

6. Lagrange, J.L., Miscellanea Taurinensia, (1773)

7. Poincare, H., Acta Math. Stockh. 7 (1885)

8. Grammel, R., Z. Angew. Math. U. Mech., vol. 4 (1924)

9. Biezeno, C.B., and Koch, J.J., Z. Math. u. Mech., vol. 5 (1925)

10. Haringx, J.A., Philips Research Repts., vol. 3 (1948) and vol. 4, (1949)

11. Timoshenko, S.P. and Gere, J.M., Theory of Elastic Stability, 2nd. Edition, McGraw-Hill N.Y. (1961)

12. Huddleston, J.V., "Effect of Axial Strain on Buckling and Posbuckling Behavior of Elastic Columns." Developments in Theor. and Appl. Mech. vol. 4. Proc. 4th SE CONF. on TAM Mr. (1968).

13. Stoker, J.J., Nonlinear Elasticity, Gordon and Breach (1968)

14. von Mises, R., Z. Angew. Math. u. Mech., vol. 3 (1923)

15. von Mises, R., and Ratzersdorfer, J., Z. Angew. Math. u. Mech., vol. 5 (1925) and vol. 6 (1926).

16. Chang, C.H., "Buckling of Slanted Columns" Journal of the Engineering Mechanics Division, vol. 100 No. EM4, Aug. 1974

17. Dym, C.L., and Shames, I.H. Solid Mechanics: A Variational Approach

18. Sokolnikoff, I.S., Mathematical Theory of Elasticity, 2nd. Edition, McGraw-Hill N.Y. (1956)

19. Love, A.E.H., A Treatise on the Mathematical Theory of Elasticity, 4th. Edition, Dover Publications N.Y. (1944)

20. Huddleston, J.V., "Effect of Shear Deformation on the Elastica with Axial Strain" Int. Journal for Numerical Methods in Engineering Vol. 4, No. 3 May-June (1972)

21. Huddleston, J.V., "The Poisson Effect in a Column with Axial Strain" Journal of the Engineering Mechanic Division, Vol. 104. No. EM3 June (1978)